THE UNIVERSITY OF MICHIGAN

COLLEGE OF ENGINEERING

Department of Aerospace Engineering
Gas Dynamics Laboratories

Technical Report

THE STRUCTURE AND KINETICS OF THE H_2-CO-O_2 DETONATIONS

Pai-Lien Lu

E. K. Dabora and J. A. Nicholls, Research Advisors

ORA Project 06996

under contract with:

U. S. ARMY RESEARCH OFFICE (DURHAM)
CONTRACT NO. DA-31-124-ARO-D-299
DURHAM, NORTH CAROLINA

administered through:

OFFICE OF RESEARCH ADMINISTRATION ANN ARBOR

June 1968

This report was also a dissertation submitted in partial fulfillment of the requirements for the degree of Doctor of Philosophy in The University of Michigan, 1968.

ACKNOWLEDGMENTS

The author is grateful to the U.S. Army Research Office (Durham) for its financial support through Contract DA-31-124-ARO-D-299.

The author would like to thank the members of his doctoral committee for their interest and helpful suggestions. In particular he is indebted to Professor J.A. Nicholls and Dr. E.K. Dabora for their suggestions and personal encouragement throughout this study. The author is also grateful to Professor P. Sherman for her financial assistance and encouragement during the early phase of his graduate study.

The generosity of Professor C. Kikuchi of Nuclear Engineering in loaning the pulsed laser is gratefully acknowledged. The conscientious assistance of Mr. H.D. Radcliff in helping to set up the laser schlieren system and conducting the experiments, and the assistance of Mr. C.J. Iott with the electronic instrumentation are especially appreciated. Discussions with Professor S.W. Bowen on optics were very helpful. The difficult manuscript typing was performed ably by Mrs. E. Sherbrook.

TABLE OF CONTENTS

LIST OF FIGURES

LIST OF TABLES

NOMENCLATURE

$\mathring{A}$	Angstrom units = 10^{-8} cm
a	speed of sound
b	channel width
c_p	specific heat at constant pressure
d	channel depth
f	mole fraction
I	intensity of transmitted polarized light
I_o	intensity of incident polarized light
K	constant of polarizer
k_1, k_2	reaction rate constants
M	Mach number
[M]	third body concentration
p	pressure
R_o	universal gas constant
T	temperature
u	velocity in x direction
$\overline{X}$	reaction length
α, α'	angle of slit with the direction of motion of camera
β, β'	angles of detonation streak with direction of motion of film
γ	ratio of specific heats
θ	angle between the planes of polarization of a polarized light and a polarizer

δ	deflection angle of interface
ϵ	coefficient defined in Eq. (2.11)
ξ	fractional area increase defined by Eq. (2.9)
ρ	density

Subscripts

1	condition ahead of wave
2	condition behind wave
3	condition behind wave after expansion
c	critical
C-J	Chapman-Jouguet
e	explosive
f	thin film
i	inert
ion	ionization probe
th	theoretical
β	streak pictures

ABSTRACT

The characteristics of self-sustained detonation waves propagating in H_2-CO-O_2 mixtures was experimentally investigated. The main aspects of interest were the reaction zone thickness, the detailed structure, and the appropriate chemical kinetics. The concentration of carbon monoxide in the fuel ranged from zero to 97. 5% by volume; pure CO-O_2 mixtures did not detonate. Two major, independent techniques were employed; the side relief method and pulsed laser schlieren photography.

The experimental results from both techniques show that the reaction zone thickness increases slowly at first as CO replaces H_2 in H_2-O_2 mixtures. The laser schlieren data show that the reaction zone thickness increases exponentially with CO concentration after the CO exceeds about 75% of the total fuel. A simple relationship between the reaction zone thickness and the hydrogen concentration in the mixture was found.

The chemical kinetic scheme in H_2-CO-O_2 mixtures was investigated by studying the quenching of detonations by the side relief technique and with interpretation by an explosion limit criteria. The results rule out the kinetic scheme involving ozone as proposed by Lewis and von Elbe. The Minkoff and Tipper scheme, which involved the formation of HCO, shows slightly better agreement with the results than that proposed by Buckler and Norrish.

I. INTRODUCTION

Gaseous detonation waves have been studied quite extensively in the 70-80 years since their identification as a supersonic form of combustion. During that time much information has been gained as to propagation rates, pressure and mixture limits, influence of tube size, stability, local pressures, structure, etc. On the other hand the closer scrutiny of detonation with better instrumentation has opened up gaps in the understanding and appreciation of the process. One of these is the common presence of three dimensional effects. Another gap exists in the understanding of the chemical reaction mechanism which may be operative in a certain mixture under detonation conditions.

Many gaseous mixtures, such as hydrogen-oxygen, are relatively easy to detonate. The detonation can be initiated by a spark or glow plug if the tube has sufficient length for the detonation to fully develop. On the other hand, no self developed detonation has ever been observed in a dry hydrogen free $CO-O_2$ mixture. Kistiakowsky, Knight and Malin[1] used an energetic explosive to overdrive greatly a dry $CO-O_2$ mixture and they did achieve detonation. However, the detonation thus formed was not steady at all; its propagation velocity fluctuated by as much as 60%. Now the profound effect of trace amounts of H_2

(either in molecularly combined form or in free gaseous form) is well known but ill understood. Very small amounts of H_2 can cause $CO-O_2$ to detonate very readily and stably. It is this sensitivity to H_2 that motivated the major portion of the study described herein. The research seeks to determine experimentally the reaction zone thickness of $CO-O_2$ detonations with known trace additions of H_2. Also an attempt is made to investigate experimentally the quenching of such waves in order to test the validity of some of the reaction kinetic mechanisms that have been proposed.

At this point it is well to review briefly the pertinent literature. Dixon and Walls[2] and Campbell and Woodhead[3] were probably the first to discover the strong effect of a very small amount of hydrogen on the detonability of $CO-O_2$ mixtures. They found that the addition of about 1% (by volume) of hydrogen to the otherwise undetonable $CO-O_2$ mixture would make it detonable. Campbell and Woodhead also discovered the peculiar spinning propagation wave phenomena in such a mixture. Bone, Fraser and Wheeler[4] later noticed that the frequency of spin in such detonation waves is affected by the hydrogen concentration in the mixture. Since then, because of this hydrogen-sensitive spinning frequency property, the detonation waves in $CO-O_2$ mixtures, with small amounts of hydrogen added, have been used by various investigators, such as Dove and Wagner[5] and Voitsekhovsky et al[6], as a means for studying spinning detonation. However, with the

exception of Laffitte's[7] and Kistiakowsky and Kydd's[8] work, there was no information systematically describing the effect of H_2 concentration on the properties of detonation waves in H_2-CO-O_2 mixtures. Laffitte investigated the effect of hydrogen concentration on the detonation limits of H_2-CO-O_2 mixtures. He found that the first 2% of hydrogen, replacing the CO in a CO-O_2 mixture, lowered the lean fuel-oxygen limit of detonation from 38 to 28.4%; after this, further hydrogen replacement produced less and less effect. Kistiakowsky and Kydd studied the overall effect of hydrogen on the reaction time of the detonation in H_2-CO-O_2 mixtures in a shock tube. They concluded that the inverse reaction time was proportional to the square root of the ratio of the partial pressures of hydrogen and carbon monoxide, even though extrapolation of their experimental data did not agree with this trend very satisfactorily. Their experiments were conducted at low initial pressures (less than 90 mm Hg) and their mixtures were diluted with about 17% of Xenon which was used for the x-ray absorption measuring technique. The effect of Xe in the mixtures was not clear from their data.

More recently, Myers et al[9] investigated the influence of H_2 on the induction period preceding rapid CO_2 formation in shock heated H_2-CO-O_2-Ar mixtures. Their experimental range of H_2 concentration was rather small (0 - .43%) in reacting mixtures. They reported that at a temperature below about 2400°K the induction period was

generally decreased with increasing initial H_2 concentration. This decrease was not linear in hydrogen concentration and the effect of hydrogen addition on the decrease of the induction period diminishes with increasing amount of H_2. They further suggested that at temperatures lower than 2400°K and with hydrogen concentration larger than 0.43% by volume the induction periods of H_2-CO-O_2 systems and H_2-O_2 systems would be comparable and independent of H_2 concentration. Later Brokaw[10] suggested a chemical scheme to explain the data of Myers et al and estimated that their mixtures contained a mole fraction of 7×10^{-4} to 3×10^{-3}% water vapor for which they did not account.

In addition to the scarcity of information on the detonation wave in H_2-CO-O_2 mixtures, the absence of a generally accepted low temperature chemical kinetic scheme makes it further difficult to understand the role of hydrogen in H_2-CO-O_2 detonations. This lack is due largely to the extreme sensitivity of CO-O_2 mixtures to traces of hydrogeneous material. Thus, despite efforts to get rid of hydrogeneous material in the low temperature and pressure explosion limit studies, the results obtained varied drastically among various investigators. Accordingly, different chemical kinetics mechanisms were derived describing a supposedly hydrogeneous material free CO-O_2 reaction. Because of the uncertainty of CO-O_2 reactions, the relative importance of the role of H_2 also becomes uncertain.

The study of H_2 effects on $CO-O_2$ reaction in deflagrative combustion was started at the same time that investigators, such as Dixon and Campbell, studied the H_2 effects on detonations in $CO-O_2$ mixtures. Buckler and Norrish[11] were the first to systematically investigate the effects of hydrogen concentration (up to 10%) on the explosion limit in dry $CO-O_2$ mixtures. Their experiments were conducted at low temperature (lower than 565°C) and pressure (less than 125 mm Hg). They concluded that the catalytic effect of hydrogen in $CO-O_2$ reactions could be described by introducing two extra chain termination reactions of CO in addition to the reaction mechanism of hydrogen and oxygen; their complete reaction scheme will be stated in the next chapter. Their explosion limit, derived from their proposed kinetic schemes, accounted quantitatively for the experimental second explosion limit pressure variation with hydrogen concentration. Their kinetic schemes implied that the overall activation energy governing ignition in H_2-O_2 mixtures should be twice the overall activation energy in $CO-O_2$ mixtures with small amounts of H_2. This prediction was confirmed by comparing the experimental overall activation energy (13.3 Kcal/mole) of their low H_2 concentration (2 to 0.25%) mixtures to that of H_2-O_2 mixtures (26 Kcal/mole) obtained by Thompson and Hinshelwood[12].

Lewis and von Elbe[13] suggested a kinetic mechanism to explain the water vapor catalyzed $CO-O_2$ reaction experiment performed by Hadman et al[14]. They also suggested that the effects of water vapor and hydrogen on the $CO-O_2$ reaction were the same. Thus, with a small modification of their $H_2O-CO-O_2$ explosion limit mechanism, they derived a mechanism to describe Buckler and Norrish's experiment. Their mechanism was different from that of Buckler and Norrish's in that they included an ozone reaction which originated from their dry-H_2 free $CO-O_2$ reaction mechanism. However, the role of ozone in the latter case has been questioned by Gordon and Knipe[15] and Dickens et al[16] on the grounds that it is too slow a mechanism to be important.

Dixon-Lewis and Linnett[17] extended Buckler and Norrish's experimental range of H_2 concentration to a wider range (0% to 100% H_2 in the fuel). Their experiments were also conducted at low temperatures ($510^{o}C$ to $580^{o}C$). They proposed two families of reaction mechanisms. The differences between the two mechanisms emphasized various degrees of effects of ozone reactions. Their explosion limit expressions included, in addition to the identical terms proposed by Lewis and von Elbe, terms involving ozone reactions with H_2 and CO as well as a not satisfactorily explained reaction between O and CO. The inferred explosion limits generally described their experimental results well. Their experimental results indicated that replacing H_2

by CO did not have much effect on the overall activation energy as Buckler and Norrish's results showed. The activation energy changed from 21.4 to 19.3 Kcal/mole when the hydrogen concentration in the fuel was reduced from 100% to 0.5%.

Recently Baldwin et al[18] used a different approach to investigate the H_2-CO-O_2 mixture. They added small amounts of CO (up to 1%) into a slowly reacting hydrogen-oxygen mixture and measured the relative yield of CO_2 and H_2O from the reaction vessel. They compared their data with calculated values based on various reaction schemes. Since their experimental range was on the H_2 rich side, the validity of their chemical schemes on CO rich mixtures still remains to be tested.

From the above brief description, it can be seen that the kinetics of H_2-CO-O_2 mixtures are, unlike those of H_2-O_2 mixtures, far from being well understood. Accordingly an express aim of this research was to add to the understanding of H_2-CO-O_2 detonation. One specific purpose was to investigate the effect of hydrogen concentration on the reaction length of the detonation wave in H_2-CO-O_2 mixtures at one atmospheric pressure without an inert diluent. This information was not available. Also a comparison with the low pressure work of Kistiakowsky and Kydd was desired. Two independent techniques, namely Dabora's[19] indirect side relief technique and Q-switched pulse schlieren photography were used. The latter provided a direct check

on the accuracy of the side relief technique when applied to highly spinning detonation waves such as occur in low hydrogen content H_2-CO-O_2 mixtures.

A second aim of this investigation was to isolate the most likely chemical kinetic scheme from among the various schemes suggested. It was decided to study the quenching of detonations by the side relief technique with interpretation by Belles'[20] quenching criterion in order to make this comparison.

It should be added that the side relief method for determining the explosion limits is valid only when the induced shock is of the "attached" type. When the side relief gas sound speed is equal or higher than that of the explosive, a detached shock is realized and the flow structure becomes very complicated. A limited treatment of this phenomenon and its consequence on the continued propagation of the detonation wave is presented in Appendix I.

II. BACKGROUND

2.1 EXPLOSION LIMIT CRITERIA

A stable detonation involves the coupling of a shock front and a rapid chemical reaction which releases heat to sustain the detonation. The unburned mixture must be rapidly heated and compressed by the shock front to such a state that a very rapid reaction takes place close to the shock front. Belles[20] suggested that in hydrogen-oxygen mixtures and other chain-branching reacting mixtures, e.g., H_2-CO-O_2, the shocked but unreacted gases in the detonation wave front must be at a state which satisfies the explosion limit requirement, which is predicted by the chemical reaction scheme of a given mixture composition. The shocked gas state depends on the shock wave strength (Mach number), initial pressure, temperature, and composition and hence the explosion condition may be expressed in terms of these variables. Therefore, for a given composition mixture and initial conditions, there is a critical shock strength above which a propagating detonation wave is expected. Detonation waves propagating at a Mach number less than the critical wave strength will quench. It is the critical shock strength and mixture composition relationship which will be used later in this study to investigate the kinetic mechanism in the H_2-CO-O_2 mixtures.

Although Belles' criteria was criticized[21] for extending the second explosion limit condition to high pressure and temperature conditions as encountered behind detonations, recent studies by Brokaw[22] and Voevodsky and Soloukhin[23] and Dabora[19] proved the validity of Belles' assumption in hydrogen and oxygen mixtures. Brokaw calculated the ignition delay in the neighborhood of the lean limit of detonability of oxygen and hydrogen. His calculation indicated also that the second explosion limit condition must be satisfied for a stable detonation in the hydrogen-oxygen system. Voevodsky and Soloukhin's experimental study of shock ignition of hydrogen and oxygen also indicated that the second explosion limit predicted the explosive ignition condition of the shocked mixture well. Dabora verified experimentally in his study that the calculated critical Mach number at various compositions in hydrogen and oxygen agreed with his experimental data quite well.

In H_2-CO-O_2 mixtures, it is generally agreed that the reactions are chain-branching and the reactions are predominated by the well accepted hydrogen-oxygen chain-branching and termination reactions proposed by Lewis and von Elbe[13] when the CO concentration is small. In this case the CO behaves as an inert gas in the reactions. When the CO concentration increases in the mixture, the CO reactions begin to compete with the hydrogen reactions.

We shall now consider the reaction schemes proposed by Lewis and von Elbe[13], Buckler and Norrish[11] and Minkoff and Tipper[24]. Lewis and von Elbe's reaction scheme proposed a unique ozone reaction which has caused disagreement[15] for some time. The reaction schemes proposed by Buckler and Norrish, and Minkoff and Tipper are similar. However, the latter included some CO reactions which the former did not consider. The three proposed chemical schemes are briefly stated below. The original reaction numbers as used by the authors in their reference are listed along with new reaction numbers which are used in this study. For consistency, all equations in this report will be in terms of the new reaction numbers.

The reaction mechanism in H_2-CO-O_2 mixtures proposed by Lewis and von Elbe is as follows:

Reaction	New Number	Original Number
$H_2 + O_2 \rightarrow H_2O_2$		XXX
$H_2O_2 + M \rightarrow 2OH + M$		i
$H_2O_2 + CO \rightarrow CO_2 + H_2O$ (vessel surface)		XXXI
$H + O_2 \rightarrow OH + O$	II	II
$O + H_2 \rightarrow OH + H$	III	III
$O + O_2 + M \rightarrow O_3 + M$	XX	XX
$OH + CO \rightarrow CO_2 + H$		XXXII
$HO_2 + CO \rightarrow CO_2 + OH$		XXXIII
$H + O_2 + M \rightarrow HO_2 + M$	VI	VI
$HO_2 \rightarrow$ destruction (surface)		XII

(M = some third body)

The explosion limit as given in Ref. 13 is

$$\frac{2k_2}{k_6[M]} = 1 + \frac{k_{20}[O_2][M]}{k_3[H_2]} \qquad (2.1)$$

The scheme proposed by Buckler and Norrish is as follows:

Reaction	New Number	Original Number
$H + O_2 \rightarrow OH + O$	II	I
$O + H_2 \rightarrow OH + H$	III	II
$OH + H_2 \rightarrow H_2O + H$		III
$OH + CO \rightarrow CO_2 + H$		IV
$H + O_2 + M \rightarrow HO_2 + M$	VI	V
$O + CO + M \rightarrow CO_2 + M$	VII	VI

(M = some third body)

The explosion limit given in Ref. 11 is

$$\frac{2k_2}{k_6[M]} = 1 + \frac{k_7[CO][M]}{k_3[H_2]} \qquad (2.2)$$

The scheme proposed by Minkoff and Tipper is

Reaction	New Number	Original Number
$H + O_2 \rightarrow OH + O$	II	VIII
$O + H_2 \rightarrow OH + H$	III	XV
$OH + CO \rightarrow CO_2 + H$		IX
$H + O_2 + M \rightarrow HO_2 + M$	VI	XIa
$H + CO + M \rightarrow HCO + M$	VI''	XIb
$HCO + O_2 \rightarrow CO + HO_2$ (very fast)		
$CO + HO_2 \rightarrow CO_2 + OH$	XII	XII
$O + CO + M \rightarrow CO_2 + M$	VII	VII
$HO_2 \rightarrow$ destruction (wall)	XIII	XIII

(M = some third body)

The explosion limit given in Ref. 24 is

$$\frac{2k_2\, k_3[H_2][O_2]}{k_7[CO][M] + k_3[H_2]}$$

$$= \left\{1 - \frac{k_{12}[CO]}{k_{12}[CO] + k_{13}}\right\}(k_6[O_2][M] + k_6''[CO][M]) \qquad (2.3)$$

Minkoff and Tipper mention that reaction XII is not very important under the conditions of H_2-CO-O_2 ignition. Baldwin et al[18] recently estimated that reaction XII above is only about ten times faster than the reaction $H_2 + HO_2 \rightarrow H_2O_2 + H$, yet the latter is much slower than reaction XIII as suggested by Lewis and von Elbe[13]. Therefore, the above explosion limit (Eq. (2.3)) can be simplified by neglecting the term

$$\frac{k_{12}[CO]}{k_{12}[CO] + k_{13}}$$

on the right hand side, which after rearrangment becomes,

$$\frac{2k_2}{k_6[M]} = 1 + \frac{k_7[CO][M]}{k_3[H_2]} + \frac{k_6''[CO]}{k_6[O_2]}\left\{1 + \frac{k_7[CO][M]}{k_3[H_2]}\right\} \qquad (2.4)$$

The three proposed explosion limits, Eq. (2.1), (2.2), (2.4) and their related reactions are summarized in Table I. It is clear that all of the three explosion limits reduce to the well accepted explosion limit

Table I Summary of Pertinent Reactions and Explosion Limits

	COMMON REACTIONS	LEWIS & VON ELBE[13]	BUCKLER & NORRISH[11]	MINKOFF & TIPPER[24]
REACTIONS	$H + O_2 \xrightarrow{k_2} OH + O$ $O + H_2 \xrightarrow{k_3} OH + H$ $H + O_2 + M \xrightarrow{k_6} HO_2 + M$	$O + O_2 + M \xrightarrow{k_{20}} O_3 + M$	$O + CO + M \xrightarrow{k_7} CO_2 + M$	$\begin{cases} H + CO + M \xrightarrow{k_6''} HCO + M \\ HCO + O_2 \longrightarrow CO + HO_2 \end{cases}$ $O + CO + M \xrightarrow{k_7} CO_2 + M$
EXPLOSION LIMITS		$\frac{2k_2}{k_6[M]} = 1 + \frac{k_{20}[O_2][M]}{k_3[H_2]}$	$\frac{2k_2}{k_6[M]} = 1 + \frac{k_7[CO][M]}{k_3[H_2]}$	$\frac{2k_2}{k_6[M]} = 1 + \frac{k_7[CO][M]}{k_3[H_2]} + \frac{k_6''[CO]}{k_6[O_2]} \left\{ 1 + \frac{k_7[CO][M]}{k_3[H_2]} \right\}$
EQUATION NUMBER		$\frac{2.92}{f_M} = \frac{P}{T} \exp\left(\frac{17000}{RT}\right) \left[1 + 0.105 \exp\left(\frac{9100}{RT}\right) \frac{P}{T} \frac{f_{O_2} f_M}{f_{H_2}} \right]$ (2·6)	$\frac{2.92}{f_M} = \frac{P}{T} \exp\left(\frac{17000}{RT}\right) \left[1 + 3.84 \exp\left(\frac{4800}{RT}\right) \frac{P}{T} \frac{f_{CO} f_M}{f_{H_2}} \right]$ (2·7)	$\frac{2.92}{f_M} = \frac{P}{T} \exp\left(\frac{17000}{RT}\right) \left[1 + \exp\left(\frac{4800}{RT}\right) \frac{P}{T} \frac{f_{CO} f_M}{f_{H_2}} \left(3.84 + 0.654 \frac{f_{CO}}{f_{O_2}} \right) + 0.17 \frac{f_{CO}}{f_{O_2}} \right]$ (2·8)

$$\frac{2k_2}{k_6[M]} = 1$$

of the hydrogen-oxygen system when the CO concentration is low. The additional terms on the right hand side account for various CO reaction effects. The reactions which are relevant to the explosion limits are shown at the top in Table I. The values of the rate constants in the explosion limits are tabulated in Table II. If these values are substituted into the explosion limits shown in Table I, and the third body concentrations, [M], are expressed in terms of temperature and pressure by means of the perfect gas law, the explosion limits will be transformed into the forms shown in the last row in Table I. The expression f_M is the effective mole fraction of third bodies in reactions VI, XX, VII, and VI''. It is assumed that they all have the same efficiency as in reaction VI as given in Ref. 13. This assumption is necessary due to the unavailability of data of the third body efficiency in these reactions. Thus,

$$f_M = f_{H_2} + 0.35\, f_{O_2} + .77\, f_{CO} \qquad (2.5)$$

where f_{H_2}, f_{O_2}, f_{CO} are the mole fractions of hydrogen, oxygen and carbon monoxide in the mixture. This assumption may cause small errors in calculating the critical Mach number as the effective third

Table II. Values for the Reaction Rate Constant

Reaction No.	Value	Reference
2	$0.2 \times 10^{-18} \sqrt{\frac{T}{803}} \exp\left[-\left(\frac{803}{T} - 1\right) \frac{17000}{803R}\right] \text{cm}^3/\text{sec}$	13
3	$1.16 \times 10^{-11} \exp\left(-\frac{8500}{RT}\right) \text{cm}^6/\text{sec}$	25
6	$0.5 \times 10^{-35} \sqrt{\frac{T}{803}} \text{cm}^6/\text{sec}$	13
7	$9.65 \times 10^{-34} \exp\left(-\frac{1700}{RT}\right) \text{cm}^6/\text{sec}$	26
6''	$0.85 \times 10^{-36} \sqrt{\frac{T}{803}} \text{cm}^6/\text{sec}$ (as 6''/6 = 0.17)	18
20	$1.6555 \times 10^{-34} \exp\left(\frac{600}{RT}\right) \text{cm}^6/\text{sec}$	27

body efficiency in reactions VI, XX, VII, VI'' may not be identical. However the difference in effective third body efficiency among various gases is small and thus has only a small effect in comparison with that of the ratio of rate constants on the right hand side in Eqs. (2.6), (2.7), and (2.8). The T (in ^{o}K) and P (in atmospheres) are the temperature and pressure of the shocked but unreacted gas behind the shock front. In order to calculate the temperature and pressure reliably, it is necessary to know whether the shocked but unreacted gas is in a frozen or vibrational equilibrium state and whether the

dissociation of CO is important. Toennies and Greene[28] have shown that there is a negligible degree of dissociation (about 10^{-4}) of CO at $4000^{o}K$ (equivalent to $M \approx 8$) and 5 mm Hg initial pressure. Therefore, at a condition of about $1800^{o}K$ (behind the shock of $M \approx 5$) and 1 atmosphere initial pressure, the degree of CO dissociation is extremely small and its effect can be neglected. White and Moore[29] found that the shocked gas is in vibrational equilibrium preceding the exothermic reaction in the H_2-O_2 and CO-O_2 mixtures at subatmospheric initial pressure and one-dimensional flow condition. On the other hand, Patch[21] calculated the theoretical limit composition of H_2-O_2 mixtures, using Belles' explosion criterion, at both a frozen state and a rotational-vibrational equilibrium state. He found that the calculated limit composition assuming a frozen state agrees better with the observed limits composition. Recently, Urtiew and Oppenheim[3] used a frozen state in their calculation of shock induced detonative ignition and obtained satisfactory agreement between the theoretical and experimental results. Therefore, it is believed that a frozen state assumption is more appropriate to the self-sustained detonation. Thus, for a given composition mixture at an initial temperature of $300^{o}K$ and at a pressure of 1 atmosphere, it is possible, by trial and error, to use the standard shock wave equation to find a critical Mach number to satisfy an explosion limit expression. The critical Mach number is plotted in Fig. (36)for the three reaction schemes discussed.

2.2 COMPRESSIBLE BOUNDARY TECHNIQUE

Dabora, in studying the interaction process between a gaseous detonation wave and an inert boundary gas, demonstrated that the reaction length of a detonation wave can be inferred from the velocity decrease of the detonation wave. Since his technique will be used in this study, it will be briefly described.

Dabora's theoretical model of the interaction process is shown in Fig. 1. The coordinates are fixed with respect to the moving wave front. The detonation wave is assumed to be the classical one-dimensional model, except for relief and changing conditions, in which the reactions follow the shock wave and the C-J plane is separated from the shock front by a finite reaction length $\overline{X}$. It is further assumed that the explosive and inert gases are separated by some means so that no diffusion occurs between them. When the detonation wave is exposed to the inert boundary gas, the flow field behind the detonation wave expands due to the high pressure of the gas behind the wave. This expansion usually induces an "attached" oblique shock in the inert gas. By treating the gas behind the detonation wave as the driver gas and the inert gas as the driven gas, Dabora was able to calculate explicitly the inert-explosive interface deflection angle, δ, by using the standard shock-tube equation. He found that $\tan \delta$ is a function of a density parameter

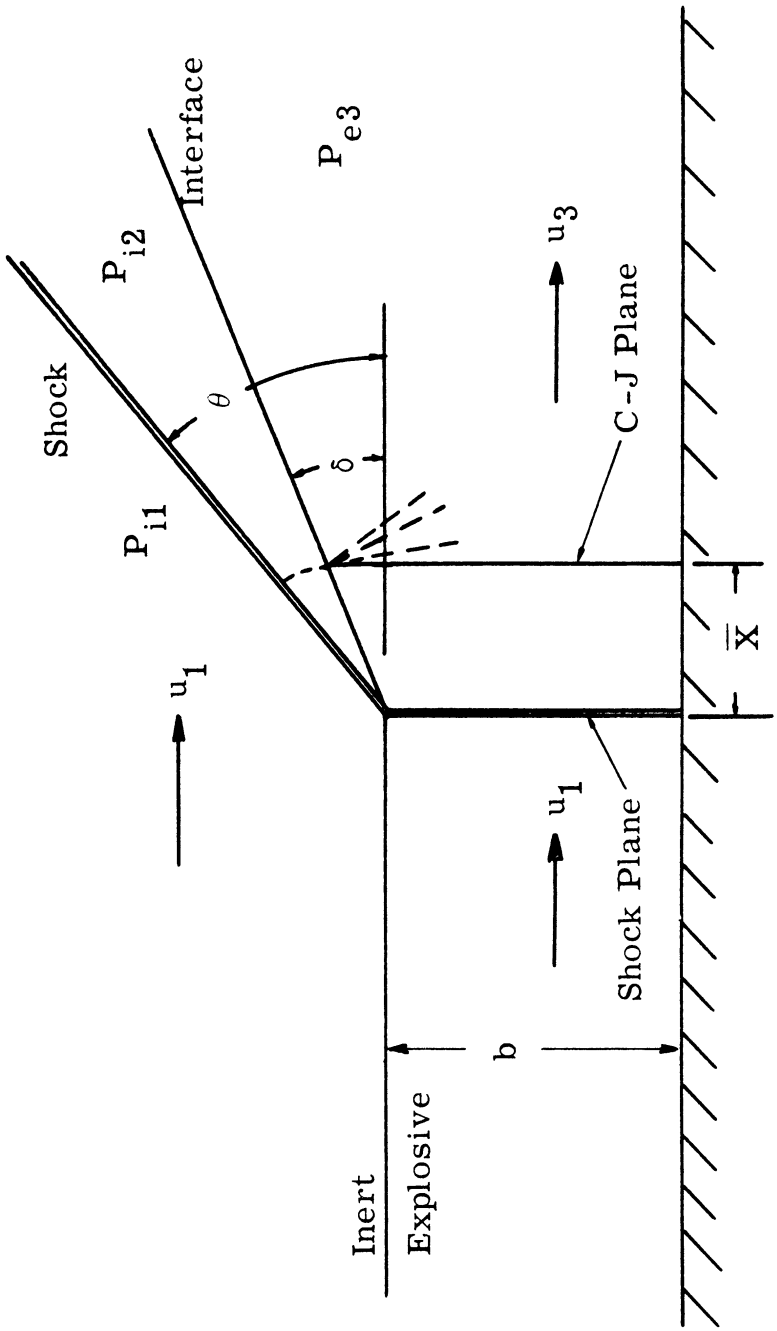

Fig. 1. Idealized Flow Model of Detonation Wave—Boundary Interaction with Finite Reaction Length. (Flow is assumed quasi one-dimensional within reaction zone but two dimensional behind C-J plane.)

$$\left[\frac{\rho_{e1}\,\gamma_{e1}}{\rho_{i1}\,\gamma_{i1}}\,\frac{\gamma_{i1}}{2(\gamma_{i1}+1)}\right]^{1/2}$$

Except for the factor

$$\left[\frac{\gamma_{i1}}{2(\gamma_{i1}+1)}\right]^{1/2}$$

the density parameter is equivalent to the acoustic impedance ratio $\rho_{e1}\,a_{e1}/\rho_{i1}\,a_{i1}$ for the experimentally possible case $p_{i1} = p_{e1}$. The variation of tan δ with the density parameter was calculated and experimentally verified by Dabora. The results are shown in Fig. 2.

The shock tube analogy was used also to derive the angle θ of the oblique shock induced in the inert gas. The angle θ is also a function of the density parameter and, again, good agreement between experiment and theory was obtained. The results showed that the denser the inert gas the better the confinement of the detonation wave.

In order to find the effect of the inert boundary gas on the propagation of the detonation wave, Dabora assumed that each stream tube, originating at the front of the detonation wave, would have an area increase at the C-J plane. The average fractional change in the area, ξ, of each stream tube is given by

$$\xi = \frac{\overline{X}\tan\delta}{b} \qquad (2.9)$$

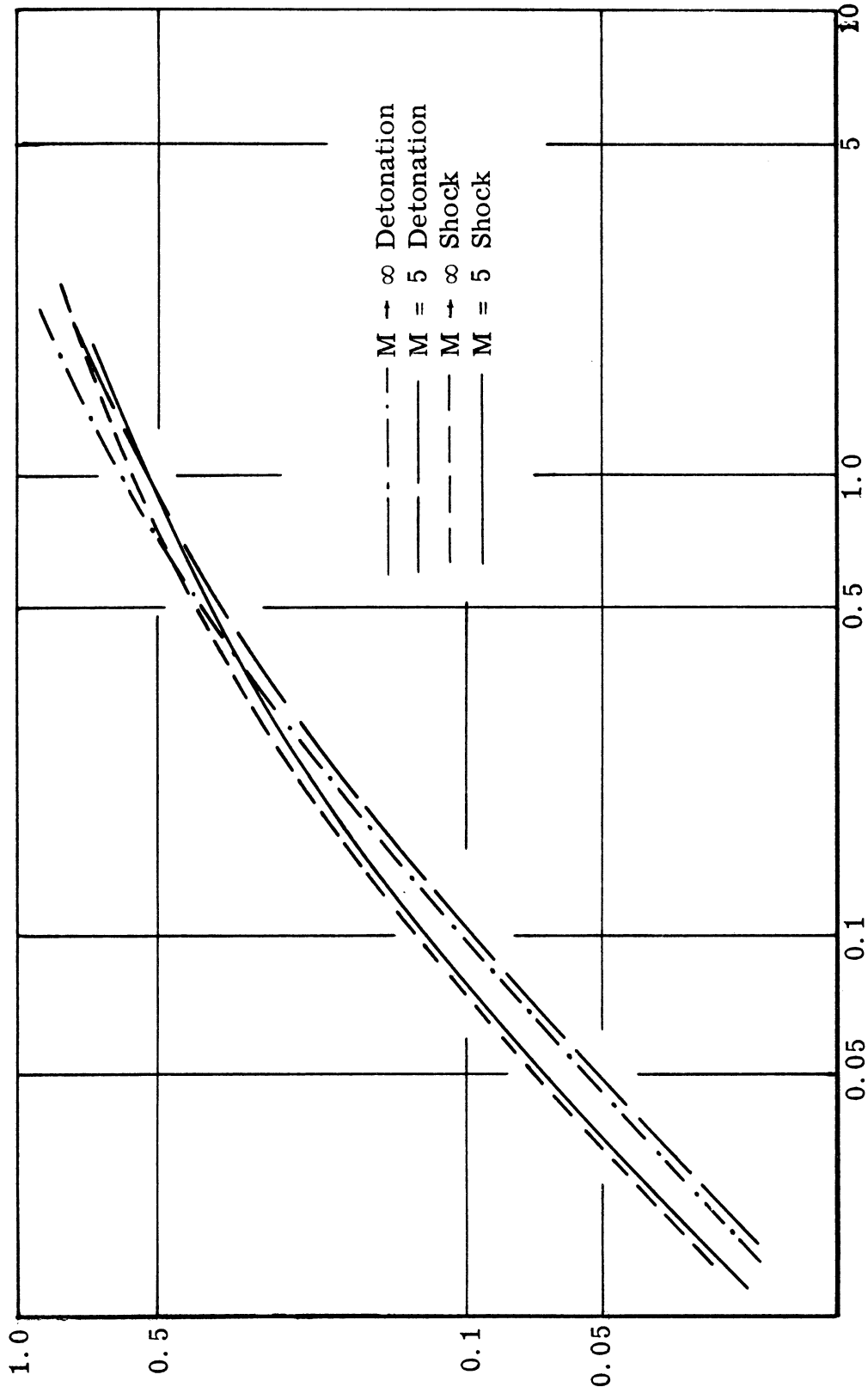

Fig. 2. Variation of Tangent of Interface Angle with the Density Parameter.

deduced from simple geometric consideration in Fig. 1 for a two-dimensional channel of width, b, exposed to the inert gas on one side normal to b. Using the conservation equations, the perfect gas law, the Chapman-Jouguet condition, and assuming

$$\int_0^{\xi} p_e \, d\xi = p_{e2} \epsilon \xi \tag{2.10}$$

Dabora obtained the following expression:

$$\frac{\Delta M_{e1}}{M_{e1}^{(\xi=0)}}$$

$$= 1 - \left\{ \frac{\left[1 - \frac{\epsilon}{1+\gamma_{e2}} \frac{\xi}{1+\xi}\right]^2}{\left[1 - \frac{\epsilon}{1+\gamma_{e2}} \frac{\xi}{1+\xi}\right]^2 + \gamma_e^2 \left[2 \frac{\epsilon}{1+\gamma_{e2}} \frac{\xi}{1+\xi} - \left(\frac{\epsilon}{1+\gamma_{e2}}\right)^2 \left(\frac{\xi}{1+\xi}\right)^2\right]} \right\}^{\frac{1}{2}} \tag{2.11}$$

where $\Delta M_{e1}/M_{e1}$ is the fractional decrement in Mach number or detonation wave propagation velocity. The variation of velocity decrement with ξ for the reasonable values $\epsilon = 1.13$ and $\gamma_2 = 1.2$ is shown in Fig. 3. Thus, it is possible to calculate the reaction length $\overline{X}$ (through ξ) of a given explosive mixture confined by a known inert gas if the wave propagation velocity decrement is measured.

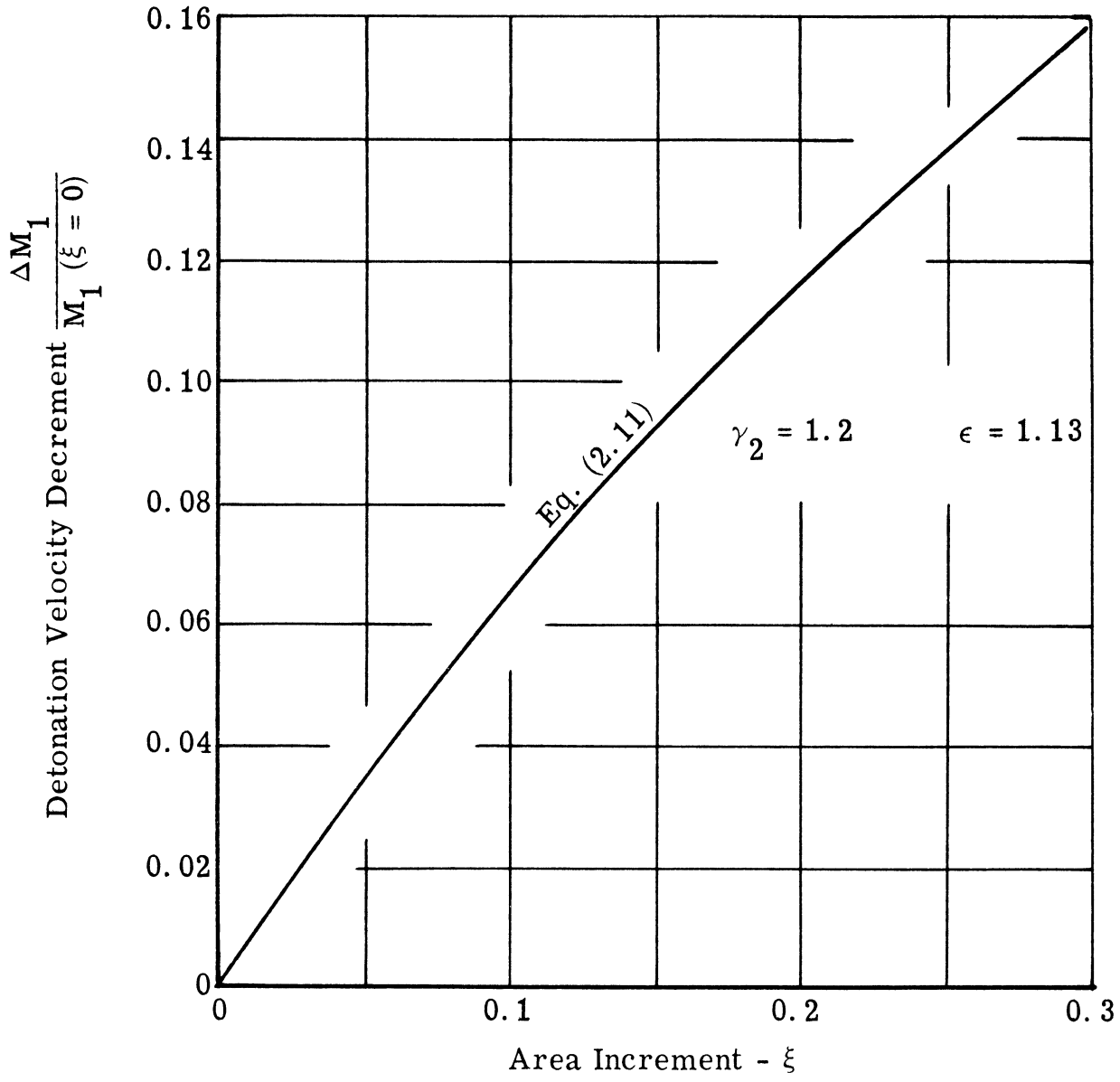

Fig. 3. Detonation Wave Velocity Decrement as a Function of the Area Increment.

The same problem was investigated theoretically by Sichel[31] who took into consideration the curvature of the wave and found a relationship between the explosive inert interface conditions and the velocity decrement. The velocity decrement and reaction length calculated based on Sichel's theory is close to the values found by Dabora's technique. In view of this agreement and the greater simplicity of Dabora's analysis, the latter was used in reducing the experimental data in this research.

It was mentioned previously that the deflection angle of the inert-explosive interface and the induced oblique shock angle in the inert gas are a function of the density parameter

$$\left[\frac{\rho_{e1}\,\gamma_{e1}}{\rho_{i1}\,\gamma_{i1}}\,\frac{\gamma_{i1}}{2(\gamma_{i1}+1)}\right]^{1/2}$$

When the density of the inert gas is much lower than that of the explosive, the induced shock angle in the inert gas becomes so large that the flow deflection downstream of it becomes impossible and a detached shock is realized. This case will be discussed in Appendix I.

III. EXPERIMENTAL SETUP AND PROCEDURE

The three experimental techniques used in this study will be described in this section. The first is the side relief technique, the second is the pulsed laser schlieren photography, and the third is the soot track technique.

3.1 SIDE RELIEF TECHNIQUE SETUP

3.1.1 Mixing and Charging System

The mixture preparation and charging system was designed to prepare and charge the pre-mix explosive in a simple and safe manner. Interlock safety devices were installed to prevent accidental misfire of explosives. Figure 4 is a schematic diagram of the system. With the exception of the flame tube and the transition tube, 1/4 in. stainless steel tubing was used throughout the whole system. The pre-mix explosive storage tank was a 1-A steel cylinder used for commercial high pressure nitrogen. The explosive storage tank and its related tube system were vacuum leak checked by means of an Alphatron*. It could be evacuated down to 10 micron vacuum in one hour and could hold this pressure for an hour without pumping; thus the possible contamination by air in the prepared mixture was negligibly small

*Model 530, NRC Equipment Co., Newton, Mass.

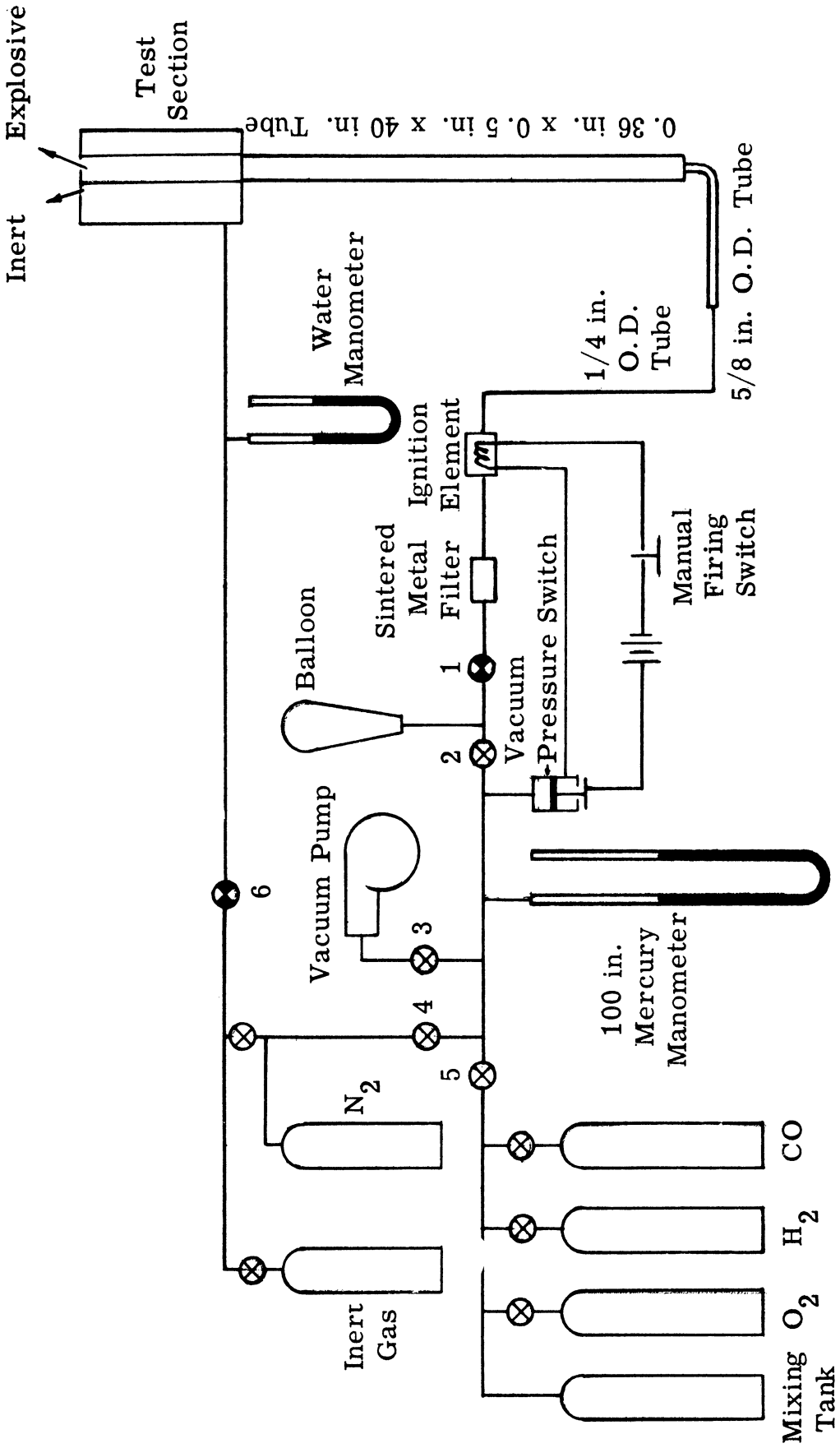

Fig. 4. Schematic Diagram of Mixing and Charging System.

since the mixture preparation pressure was usually about 80 in. Hg. The explosive was prepared by the partial pressure method. When a fresh mixture was prepared, the mixing tank and tube system was first evacuated for an hour, then flushed with nitrogen at room pressure, and then evacuated again for another hour and a half. This was done to prevent any possible contamination from a previous stored mixture. The gases were filled in the order of successive larger molecular weight, e.g. hydrogen, carbon monoxide, oxygen. The partial pressure of each gas was measured by a 100 in. long mercury manometer which could be read with an accuracy of 0.05 in. To insure that the gases were mixed thoroughly in the tank before any runs, a heat lamp was placed at the bottom end of the mixing tank for at least two hours to accelerate the mixing process by convective flow; the mixture was then left at room temperature for at least ten hours before it was used. High pressure commercial bottled gas was used in preparing the mixtures. The hydrogen and oxygen were extra dry grade; and the carbon monoxide was C.P. grade. The small amount of impurity of water vapor (less than .002% as checked by a mass spectrometer) in carbon monoxide was assumed to have negligible effect since the hydrogen content in the mixture was rather high.

The vertically mounted steel flame tube had a channel dimension of 0.36 x 0.5 x 40 in. Its interior wall was smoothed and cadmium

plated to minimize disturbances from the wall irregularities and to avoid the possibility of rust formation. A 13 in. long 5/8 O.D. stainless steel tube connected the lower end of the flame tube to the 1/4 in. charging tube. In some preliminary experiments, it was found that in high CO content mixtures, due to the large area change from the 1/4 in. tube to the flame tube, the detonation re-establishment distance was longer than 40 in. and resulted in a nonsteady wave in the test section. The installation of the 5/8 in. O.D. transition tube eliminated this problem completely for all mixtures used in the experiments.

The glow plug which initiated the detonation was placed 15 ft ahead of the entrance of the transition tube to insure that a fully developed wave was formed before entering the flame tube.

The explosive charging system was a flowing system, i. e. the explosive was flowing in the test section at low velocity while the detonation was formed. The purpose was to minimize the diffusion effect between the explosive and the boundary gas in the test section. Dabora used a balloon as a temporary explosive reservoir to provide the flow. This balloon burst as the detonation flashed back upstream from the glow plug. It worked well except that it was not very safe if the explosive in the balloon was not quite exhausted. It was found that a commercial sintered metal filter used to entrap foreign particles in gaseous systems could also quench a fully developed detonation. Therefore,

a 5 to 9 micron stainless steel sintered filter manufactured by Hoke Co.*, was installed in the line between the balloon and the glow plug. After this was installed, not a single flash back occurred during all of the experiments.

Another positive safety device was installed in the system to prevent a detonation from accidentally starting and flashing back into the explosive storage tank (which was in the same room where the experiments were performed). The device was a vacuum pressure switch as shown in Fig. 5. It was placed between valves 2 and 5 as shown in Fig. 4. The section of the tube between valves 2 and 5 had to be evacuated before the power circuit for the glow plug could be energized and ignite the explosive. The evacuated section served as a buffer zone to stop any accidental detonation wave from flashing back to the mixing tank.

3.1.2 Thin Film and Test Section

Dabora used a thin collodion film to separate the inert boundary gas and the explosive. From some preliminary tests, it was found that the thin collodion film was porous to Freons (which were required to confine a detonation in high carbon monoxide content mixtures). The diffusion of Freon into the explosive caused the detonation to quench prematurely. Attempts were made to find a suitable material

*Micron filter with 2232 element, Hoke Co., Tenakill Park, Cresskill, N. J.

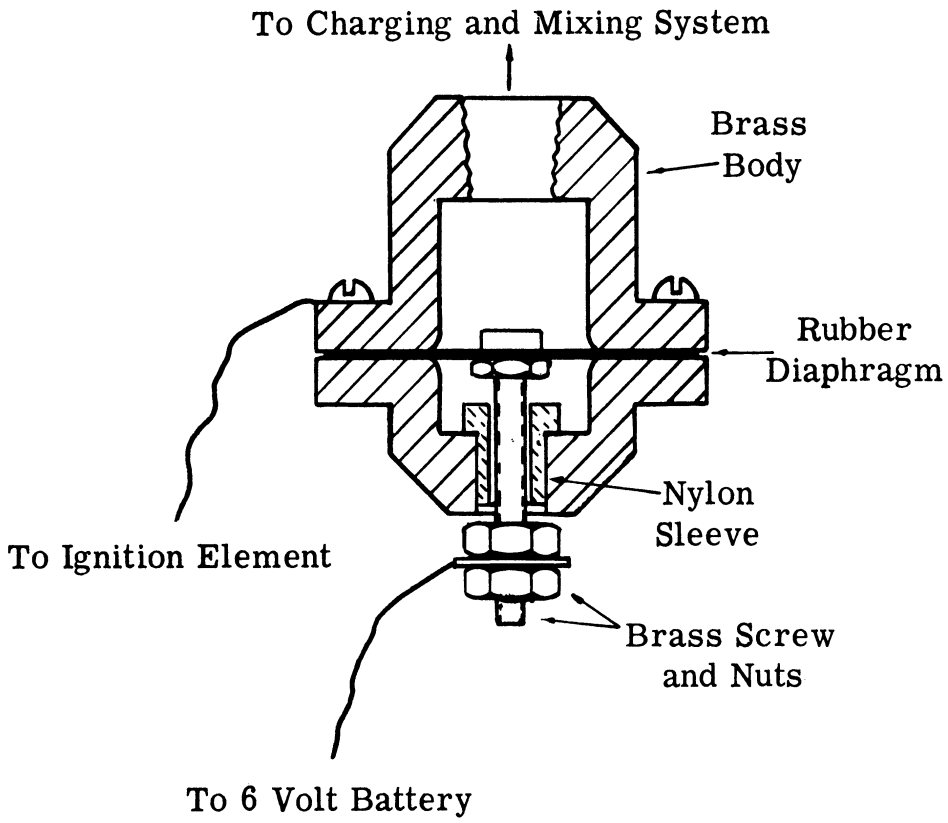

Fig. 5. Vacuum Switch

for a thin film which was not porous to Freons. Diluted Duco cement, clear lacquer, and diluted nail polish were tried. The first two materials were given up as it was impossible to make a thin film from them. It was found that a properly diluted clear nail polish produced a thin film comparable to the one made of collodion. The concentration was one part Revlon clear nail polish No. 65 in four parts of Revlon nail polish solvent. The thin film was made by the same method used in making collodion film, i.e. by casting one drop (about .019 cc) of this solution on a clean water surface. It spread out evenly on the water surface and after the solvent was evaporated a thin film was formed. A crude measurement was made and it was found that the non-volatile material concentration in the nail polish was 0.32 gm/cc nail polish, and the density of the non-volatile residue was 1.51 gm/cm^3, which is very close to the density of nitrocellulose in collodion (1.58 gm/cm^3). Thus the film thickness for one drop of diluted solution distributed over about a 14 cm diameter area was calculated to be 530 $\mathring{A}$.

Dabora estimated that the effect of the film in confining the detonation would be negligible when the film thickness, t_f, is

$$t_f \leq 0.1 \frac{\rho_e}{\rho_f} \bar{x}$$

Thus, for a nail polish density = 1.51 gm/cc and for an explosive ($1/3\ CO + 1/3\ H_2 + 1/3\ O_2$) density = 9.2×10^{-4} gm/cc at N. T. P. and a reaction length of about 2 mm, the critical film thickness is 1220 Å, which is larger than the 530 Å thick film used.

The effectiveness of the nail polish thin film in preventing the diffusion of Freon into the explosive was confirmed by taking schlieren photographs. However, the nail polish film was much more brittle and easier to crack than the collodion thin film, so that it was used only for runs with 30% or more CO in the mixture when Freon was used as the boundary gas. Collodion film was used for all low CO content mixture runs. Usually several thin films were made and mounted on film holders before a series of runs. The film holder configuration is shown in Fig. 6.

The test section used was that used by Dabora and is shown in Fig. 7. The test section was mounted vertically at the top end of the flame tube. There was a 0.035 in. wide by 0.135 in. deep groove cut in each of the two 1/2 in. thick plate glass windows for the thin film holder to slide in. The depth of the explosive section was the same as the flame tube, 0.36 in. The width of the explosive channel could be changed from 0.5 in. to 0.1 in. with 0.05 in. intervals by suitable spacers and a wedge piece.

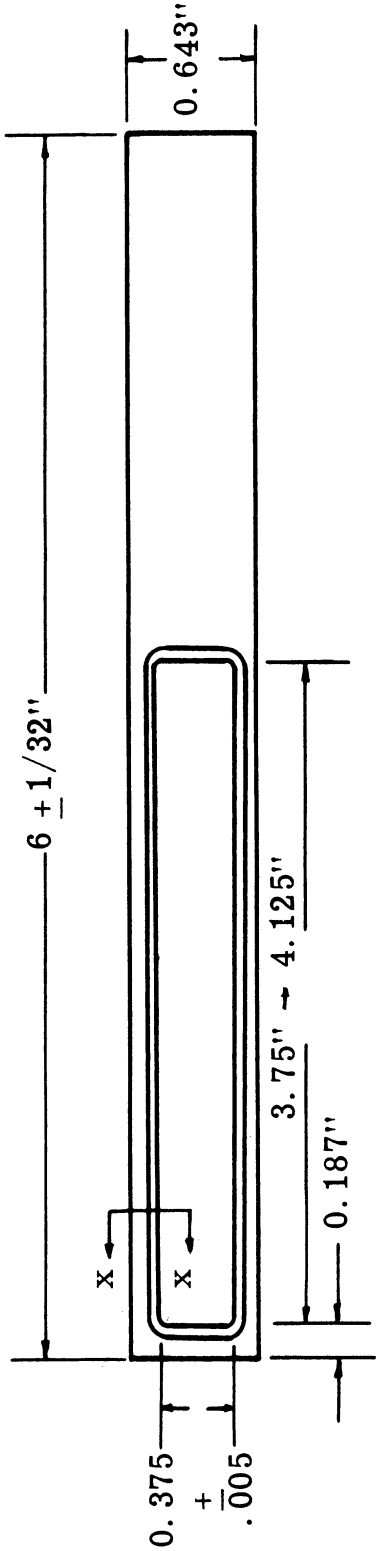

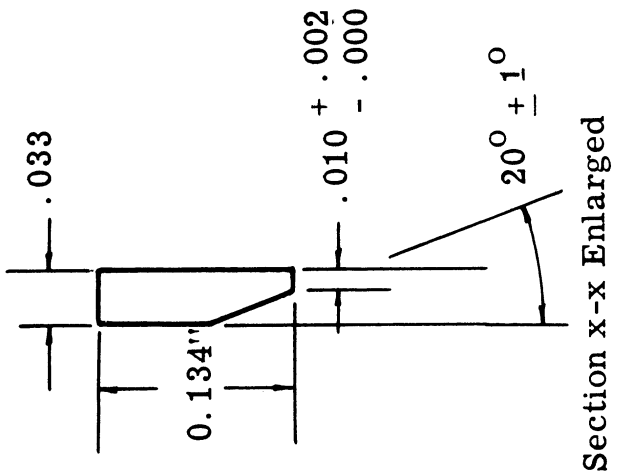

Section x-x Enlarged

Fig. 6. Thin Film Holder.

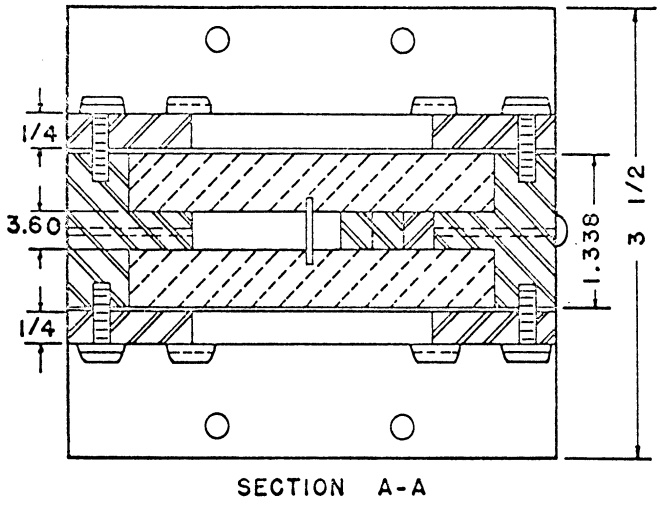

SECTION A-A

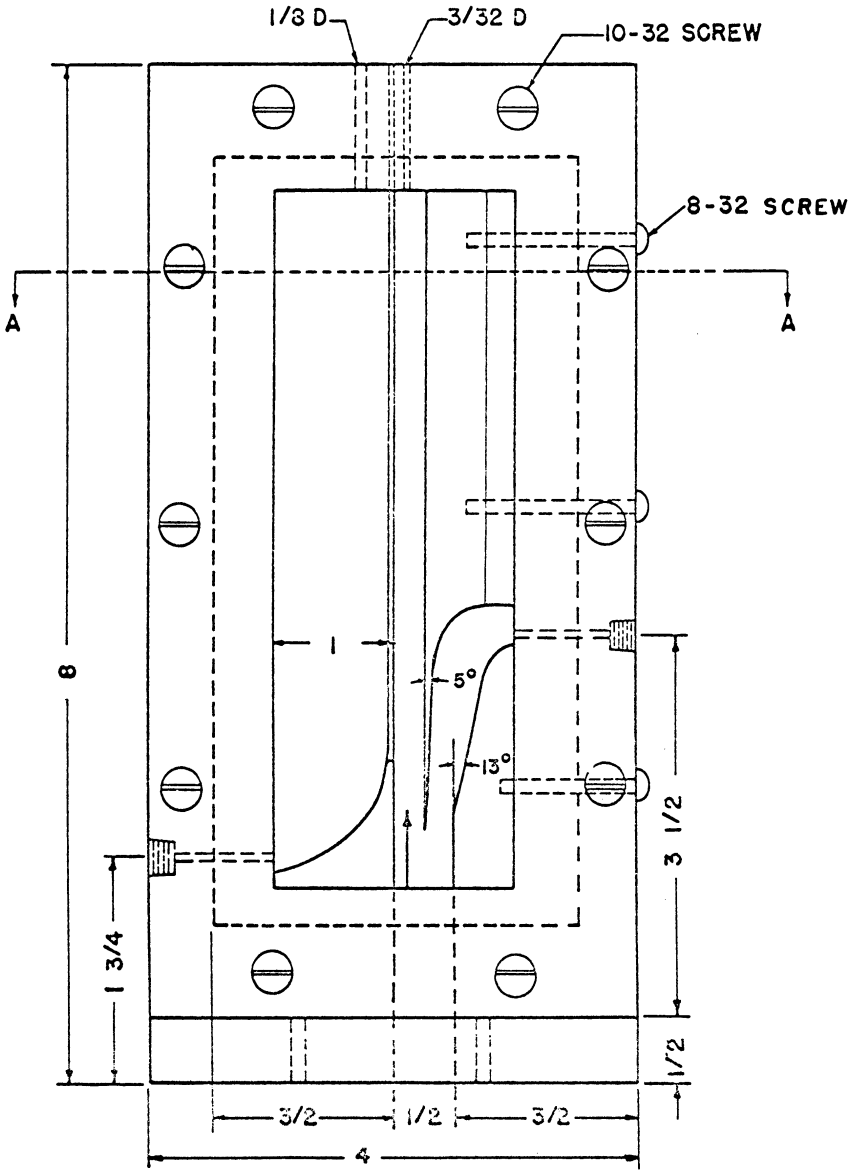

Fig. 7. Test Section Assembly.

Different boundary gases were used in the H_2-CO-O_2 experiments; namely, nitrogen, argon, Freon 14 (CF_4), Freon 116 (C_2F_6), and Freon C-318 (C_4F_8). In general, heavier boundary gases were used in high CO content mixture runs; however, sometimes heavier boundary gas along with a narrower channel were used to achieve a desired velocity decrement. The use of Freons not only caused diffusion problems when collodion film was used but also greatly shortened the useful life of the test section glass windows. The Freons generally decompose above 1000 C. This temperature was easily attained behind the induced oblique shock in Freon. The decomposition products tended to etch the glass. As an example, a pair of new glass windows lasted only four runs. They became frosty and lost their transparency.

3.1.3 Streak Schlieren Photographic System

The streak schlieren photographic system and its related controls are shown schematically in Fig. 8. Four ionization probes were installed in the flame tube to detect the passage of the detonation wave and to achieve certain synchronization functions which will be described later. The ionization probe is shown in Fig. 9. It has a smooth surface to minimize any disturbance to the detonation wave.

Referring to Fig. 8, in probes 1, 2, and 3 one wire was grounded and the other was connected to the grid of an 884 thyratron in a thyratron unit described by Morrison[32]. When the ionized detonation

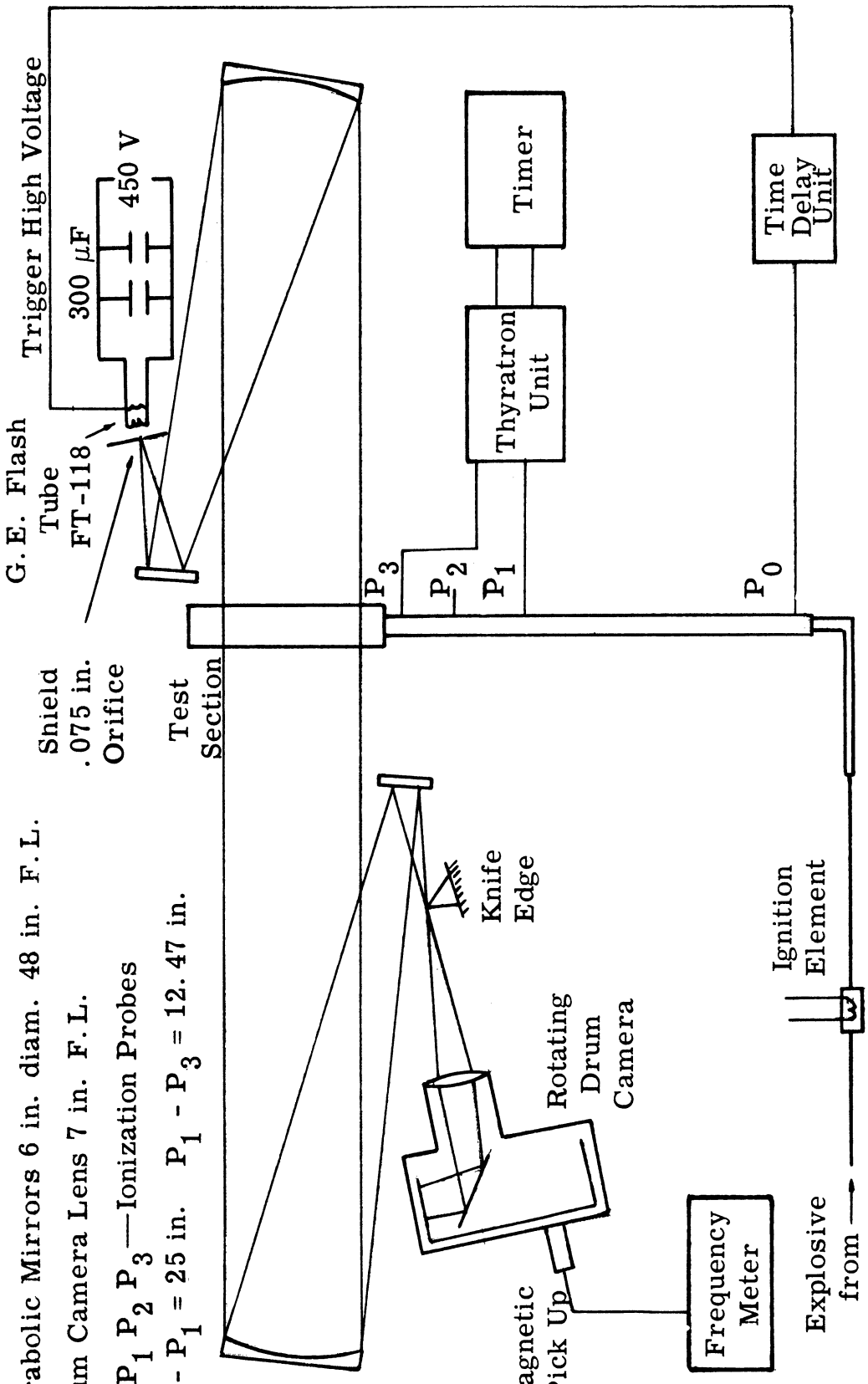

Fig. 8. Schlieren System and Block Diagram of Instrumentation for Streak Pictures.

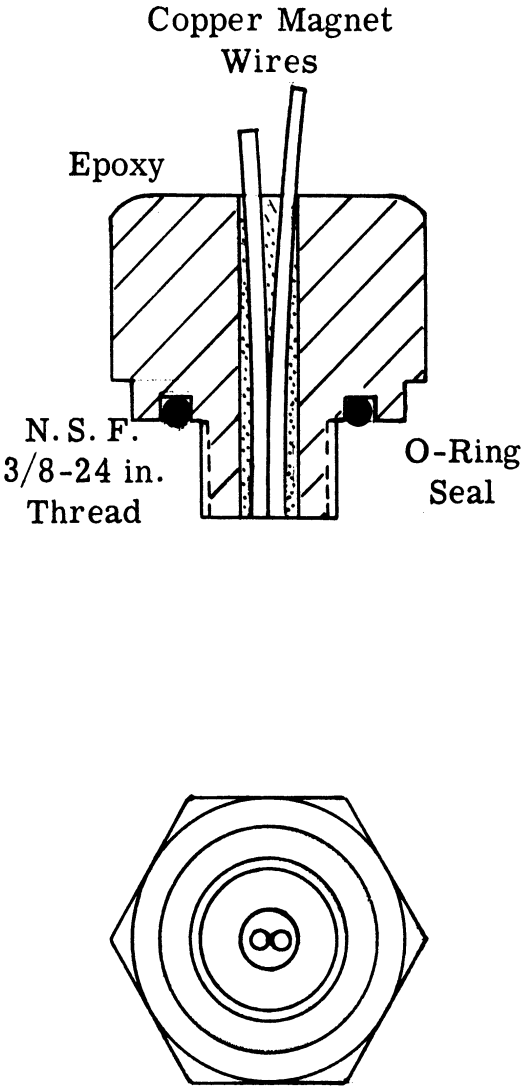

Fig. 9. Ionization Probe

wave passed over the probe it shorted the probe, thus firing the thyratron and producing a voltage signal. The voltage signal was fed into a start or stop channel of a microsecond timer to provide the wave speed. The wave speed steadiness was checked by comparing the wave velocity between probes 1 to 2 and probes 2 to 3. The timers used were two TSI megacycle counters* with an accuracy of 1 μsec.

The probe 0 was used to command the firing of a Xenon flash tube or a spark light source for streak or spark schlieren photography. The ungrounded wire was connected to the grid of a 2050 thyratron in the time delay unit described by Morrison[32]. The firing of this thyratron triggered, after a predetermined time delay set by a potentiometer adjustment in the unit, a second 2050 thyratron. The voltage spike from the firing of the second 2050 thyratron was amplified to about 15 KV by means of a pulse transformer arrangement. This high voltage pulse was used to trigger the G.E. FT-118 Xenon flash tube.

The FT-118 flash tube was mounted in a box with a 0.075 in. hole on one wall serving as the point light source. The duration of the flash was about 1 msec which was much longer than the time required for a detonation wave to travel the whole test section.

---

*Model 361, Transistor Specialties Inc., Plainview, L.I., N.Y.

The schlieren system was a simple, conventional, single pass, folded Z configuration, system. In taking streak schlieren pictures the test section was blanked off except for a 0.011 in. wide slit which was close to the solid wall in the explosive channel. One side of the slit had notches to provide excess exposure on the film to establish the vertical spatial scale. The straight knife edge was set horizontally, parallel to the detonation wave front, in the schlieren system.

A drum camera similar to the one used by Wilkerson[33] was used to obtain streak pictures. The drum diameter was 8.371 in. and standard unperforated 35 mm film was used. It was driven by a Dumore grinder motor through pulleys resulting in a maximum rotational speed of the drum of about 240 rev/sec, which corresponds to a writing speed of 0.16 mm/μsec. A magnetic pick up with its signal fed into a TSI counter was used to measure the drum speed and to insure that the speed was steady before a run was made. The reduction of the image in the camera was about 0.2.

Regular unperforated 35 mm Kodak Tri X film was used for all runs. The temperature of the developer, fixer, and washing water was maintained at the same level to minimize possible dimensional change in the emulsion caused by temperature change.

3.1.4 Experimental Procedure

Before each run the flame tube and test section were flushed with dry nitrogen for at least five minutes to drive out residual moisture from the previous run. Then a film holder, on which a dry thin film had been previously mounted and with its edge lightly coated with a layer of vacuum grease to provide a seal with the slots in the window glass, was inserted into the test section. With valve 1 (Fig. 4) closed, the balloon was first evacuated and then filled with the explosive mixture. Usually, the balloon was charged until the pressure was about 4 in. Hg gauge and its volume at this pressure was more than twenty times the total internal volume of the charging tube and flame tube. After the balloon had been fully charged, valves 2 and 5 were closed and the section of tube in between was evacuated. Then the vacuum pressure switch was automatically closed and the ignition power circuit was closed; so that the glow plug was ready to be fired whenever the manual firing switch was closed.

The drum camera was then turned on and brought up to speed by adjusting the Variac connected to its motor. At the same time valves 1 and 6 were opened slowly and simultaneously in such a way as to keep the pressures of the boundary gas and explosive gas the same all the time. The pressure fluctuation was indicated by the reflection of a focused filament image from a small light bulb on the thin film. The

explosive and boundary gas were usually kept at a pressure of 4 to 5 cm of water above atmospheric pressure. This provides a flow velocity of about 40 in/sec in the test section. The diffusion between the explosive and the boundary gas through the film is negligible at this flowing velocity.

When the balloon was almost exhausted and the drum camera had reached a steady speed, the glow plug manual switch was momentarily closed to start the detonation. As the detonation passed the ionization probe, 0, a sequence of events was initiated, as described in the previous section, that resulted in a schlieren photograph.

3.2 LASER SCHLIEREN PHOTOGRAPHIC TECHNIQUE SETUP

The conventional schlieren photographic technique was used successfully to measure the reaction zone thickness of a detonation in low initial pressure mixtures by Opel[34] and Jost et al[35]. However, Opel found at higher initial pressure conditions, e.g. 1 atmosphere, the smear of the wave front due to the spark source duration was comparable to the reaction zone thickness so that no reliable data could be obtained. The Q-switched pulse laser appeared to be very attractive because of its very short duration yet intense light pulse. The pulse time is about 20 nanosecond vs. 200 nanosecond for conventional spark sources, hence a sharper image can be obtained. Its parallel and monochromatic

light will also theoretically increase the sensitivity of a schlieren system. However, in practice, the noisy background of diffraction patterns is so severe that the event to be studied is sometimes masked off. Some of the noisy background is caused by the optical component imperfection[36], but the major factor is due to the diffraction patterns which are caused by the sharp knife edge[37]. Oppenheim et al[37] devised a technique to avoid the latter difficulty by using a quartz prism-polarizing filter combination in place of a knife edge (its principle is explained in Appendix III). This is the technique used in this experiment and is described in the following sections.

3.2.1 Optical System

The basic schlieren system was the same as the one used in the streak schlieren photograph work described previously. Additional optics, as shown in Fig. 10, were installed to modify the system for laser schlieren use. The pulse laser was a modified Lear Siegler Model H-150*. Its performance and properties will be discussed in detail in the next section. A small continuous He-Ne laser† was also built into the system. The gas laser light was in alignment with the pulsed laser light by means of a beam splitter. Thus with the aid of

---

*Lear Siegler Inc., 313 N. First St., Ann Arbor, Michigan.

†Model LAS201, Electro Optics Assoc., 981 Commercial St., Palo Alto, Calif. 94303.

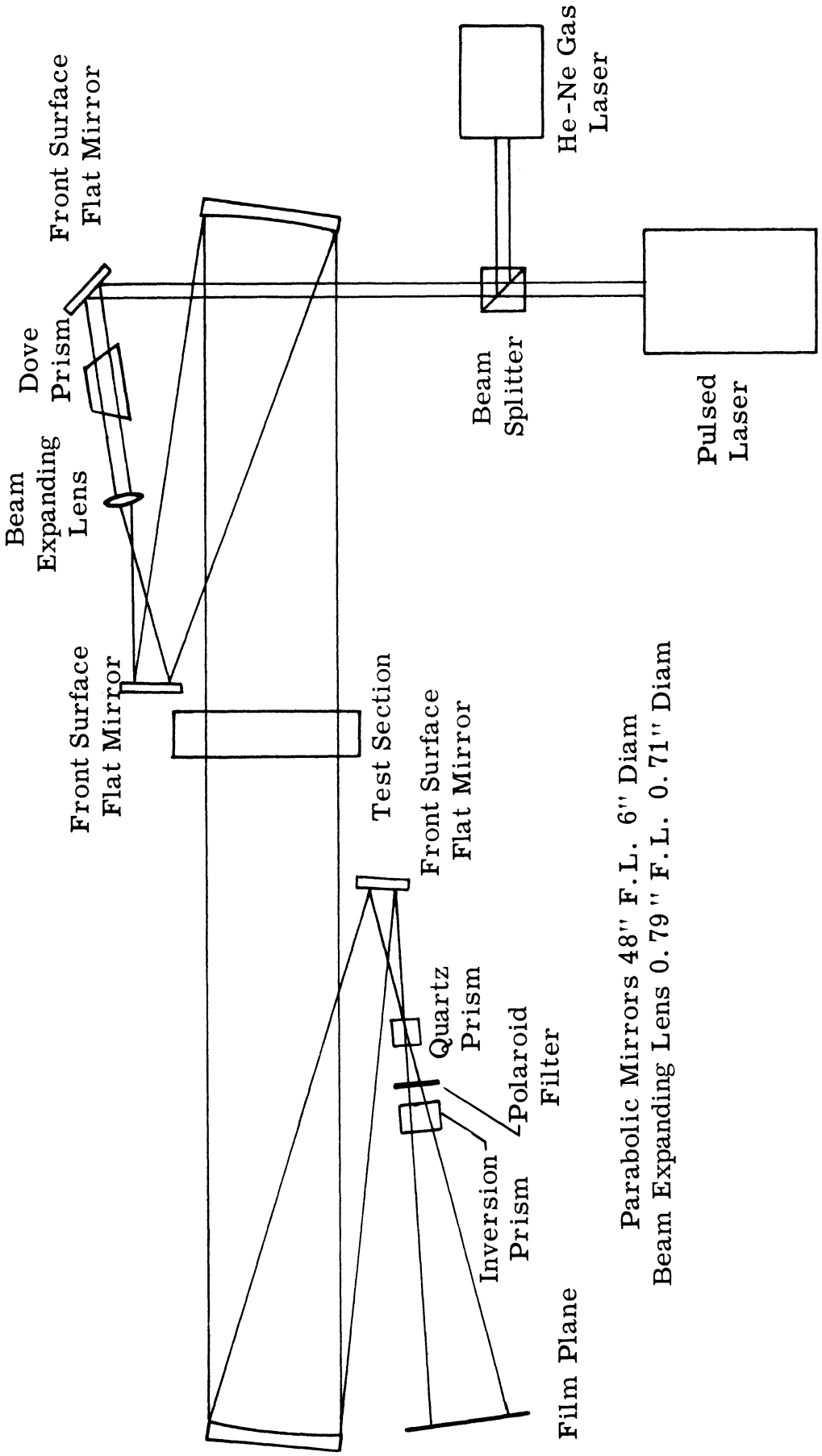

Fig. 10. Laser Schlieren System.

the continuous gas laser, the optics in the schlieren system could be aligned preliminarily. The final alignment was made with the pulse laser.

A simple double convex lens was used to expand the light beam. Since the aperture ratio of the expanding lens and the schlieren mirror did not quite match, only 20% of the expanded light was captured by the schlieren mirror. The pulse laser light was not uniform across its beam as there were two bright horizontal bands which caused uneven illumination on the vertical test section. A Dove prism was installed in the light path to rotate the light beam 90^{o} along its path so that one of the bright bands fell on the vertical test section.

The crystal quartz prism* had angles of $30\text{-}60\text{-}90^{o}$ and the optic axis was parallel to the smaller base. A conventional photographic Edenlite polarizer filter was used. An inversion prism was used to bring the bent light beam emerging from the quartz prism into its original path. The second schlieren mirror was used for focusing an image in the lensless Graphex press camera. The image reduction factor was about 0.93 of the object. Polaroid P/N (ASA50) 4 x 5 in. film was used in all the runs. This film was chosen for its convenience in producing instant results and a negative.

---

*Karl Lambrecht Co., 3959 N. Lincoln Ave., Chicago, Ill. 60613.

In setting up the schlieren system several unique problems arose due to the coherent and monochromatic properties of the laser light. It was necessary to avoid two parallel reflecting surfaces too close to each other, e.g. the slanting surfaces of the quartz prism and the inversion prism, or the test section windows. The parallel surfaces acted as a crude Fabry-Perot interferometer and caused interference fringes. This annoying effect was corrected by either destroying the parallelism of the reflecting surfaces or by inserting other optics in between to disrupt the reflection (such as placing the polaroid filter in between the quartz and inversion prisms).

The optical quality of all optics, with the exception of the quartz-prism, was unknown but it was noticed that the optical quality requirement of all optics was more stringent in this kind of system than in a system using a conventional light source. Any imperfection in the optics caused diffraction patterns which greatly deteriorated the image quality.

3.2.2 Pulse Laser and Its Control System

The pulse laser was a modified Lear Siegler Model H-150†. The laser head was equipped with an air cooled 1/4 in. diameter neodymium doped glass rod. The Q-switching mode was achieved by means of a

---

†Loaned to us by Professor Kikuchi of the Nuclear Engineering Department, University of Michigan.

rotating roof prism which reflected totally in the laser cavity. The threshold output from the neodymium glass rod was about 20 megawatts at 10600 Å. By passing the infrared light through a KDP (potassium-dihydrogen-phosphate) crystal, about 2 megawatts output at 5300 Å, the second harmonic of 10600 Å, was obtained. With the use of a suitable filter the infrared portion was blanked off and therefore the green (5300 Å) light was used in the experiments.

The rotating prism type Q-switched laser was not designed for synchronization with any given event. Since the detonation wave remained in the test section for only about 60 μsec, means of synchronization had to be found. To achieve synchronization the emission of the laser light and the initiation of the detonation were controlled as will be described below.

The principle of the operation of the rotating prism Q-switching is illustrated schematically in Fig. 11. The roof prism is mounted on a spinning platform on which there is a slit. Whenever the slit passes the small light bulb and photo sensor assembly and the manual switch is in a closed position, the photo sensor will be energized and sends a signal pulse to the trigger circuit which fires the flash lamp that energizes the laser rod. After a time lapse, determined by the relative position of the slit and prism and the rotational speed of the platform the prism moves into the critical alignment position in the cavity and

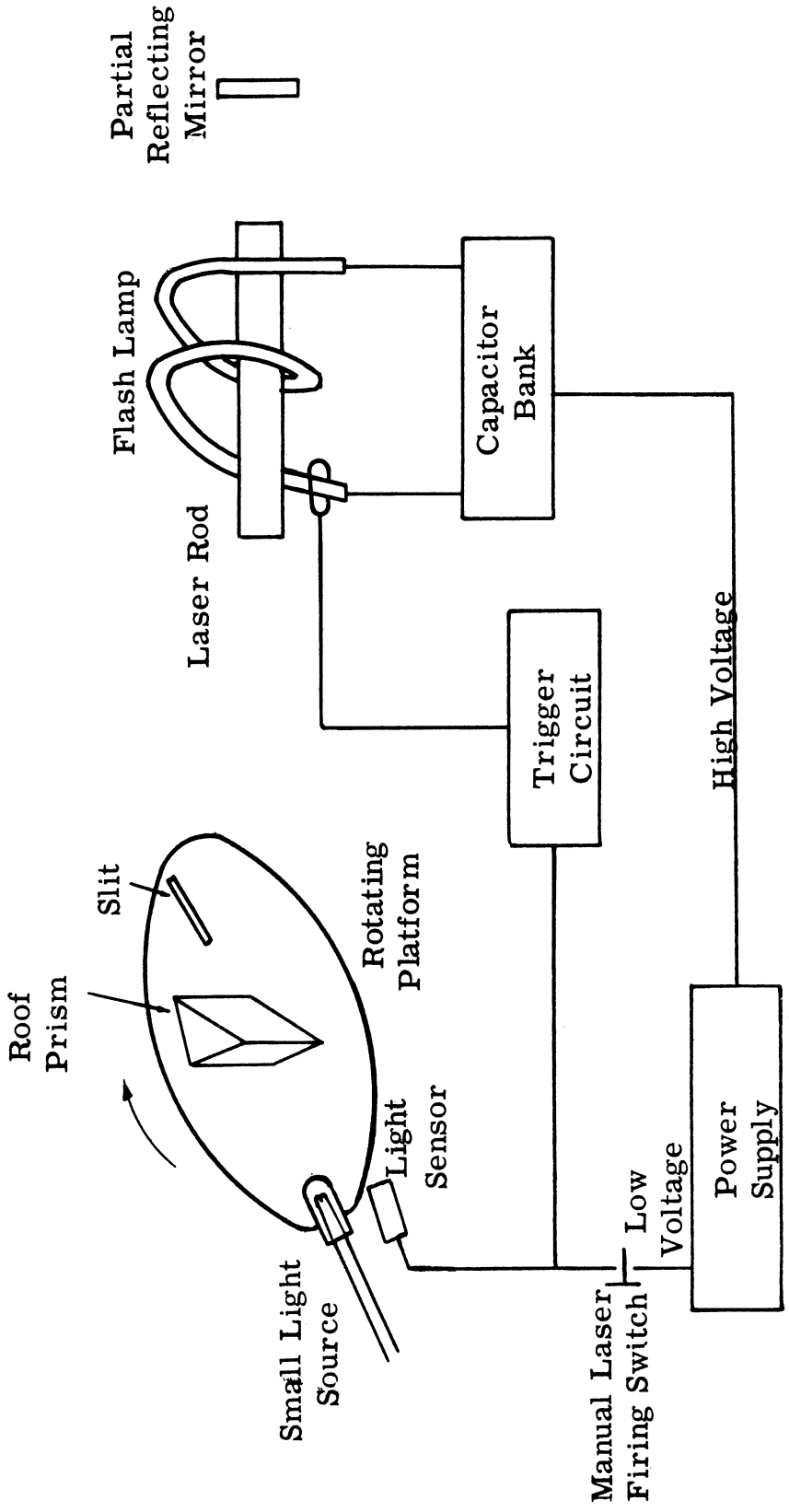

Fig. 11. Rotating Prism Q-Switching Laser.

the light amplification occurs to emit the laser light. The time lapse was 250 μsec. Since the flash lamp discharges in about one millisecond and the period of the rotating prism is 3.8 msec in this unit, only one light pulse is obtained.

From the above paragraph, it can be seen that there is a minimum time requirement (250 μsec) to energize the laser rod. On the other hand, it was known, from some preliminary experiments, that the time required to develop a detonation and its arrival to the test section varied from 700 μsec to 3600 μsec in various H_2-CO-O_2 mixtures, with mixtures richer in CO having longer development time. It was figured that the synchronization might be achieved by using the same signal to trigger the two events, discharging the spark in the explosive and firing the flash lamp, at different times which were compensated by using independent time delays. The triggering signal had to be taken out from the rotating platform because of the relationship between the rotating prism and the laser rod axis. The laser head was then modified in the following manner. The old light sensor unit was disconnected from the circuit because it did not respond reliably. A new light bulb and light sensor assembly was installed at the location which was 2.5 msec ahead of the laser rod axis as shown in Fig. 12. The circuit diagram of the new light sensor* is as shown in Fig. 13. The time

---

*Light Sensor LS 400, Texas Instrument Inc., 13500 N. Central Expressway, Dallas, Texas.

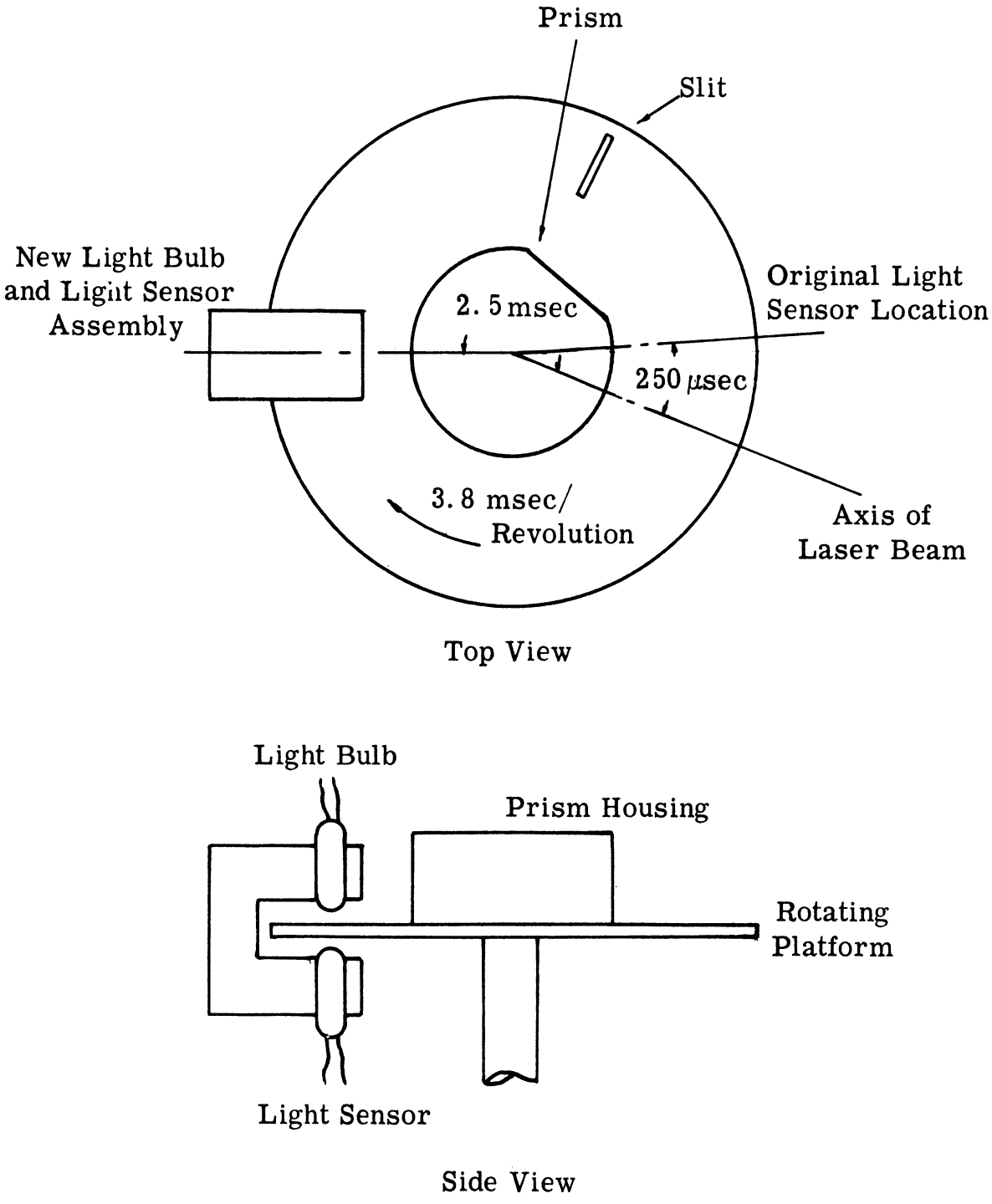

Fig. 12. Rotating Prism Assembly and Related Critical Positions.

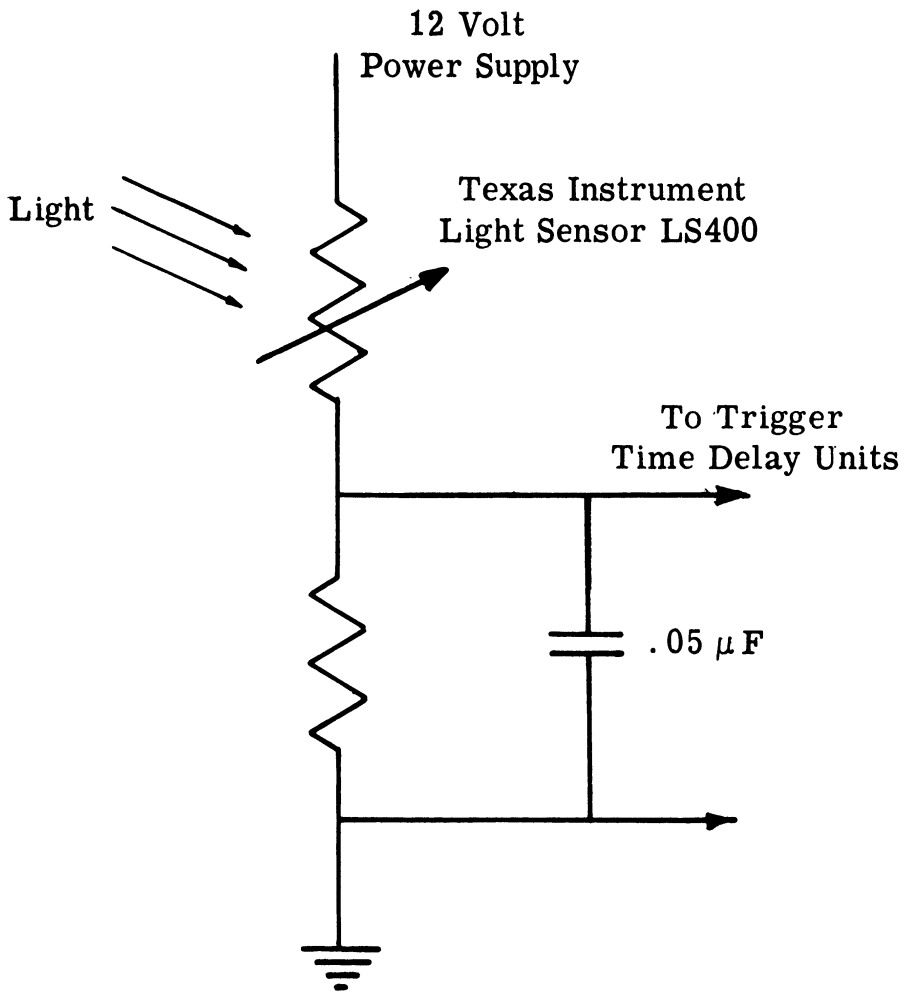

Fig. 13. Light Sensor Circuit in Laser Head.

sequence of the occurrence of various events to achieve the synchronization is as shown in Fig. 14. The signal from the light sensor, upon seeing the passage of the slit on the rotating platform, triggered two time delay units 1 and 2. The time delay unit 1, after a predetermined delay, triggered the firing circuit of the flash lamp to energize the laser rod so that 250 msec later when the rotating prism arrived at the critical alignment position, the laser light emitted. This delay was 2.25 msec in most cases. In very rich CO content mixtures, when the time lapse between the spark discharge and the arrival of the detonation in the test section was longer than 2.5 msec, the delay was set at 2.25 msec plus any multiple of 3.8 msec—the period of the rotating prism. The time delay unit 2 was used to trigger a thyratron unit—the same one used to trigger the flash tube in the streak photography work—to produce a high voltage pulse (1 μf at 15 kv) to be discharged through a spark gap in the explosive to initiate a detonation. This time delay was set to compensate the variation of the time lapse between the spark discharge and the arrival of the detonation in the test section. The synchronization arrangement worked well when the prism rotational speed and the time lapse of the initiation of a detonation were reproducible. Unfortunately there was $\pm$ 1.5% variation of the prism rotating speed, and the time lapse of detonation initiation was less stable as the CO content increased in the mixtures. Therefore, additional auxiliary

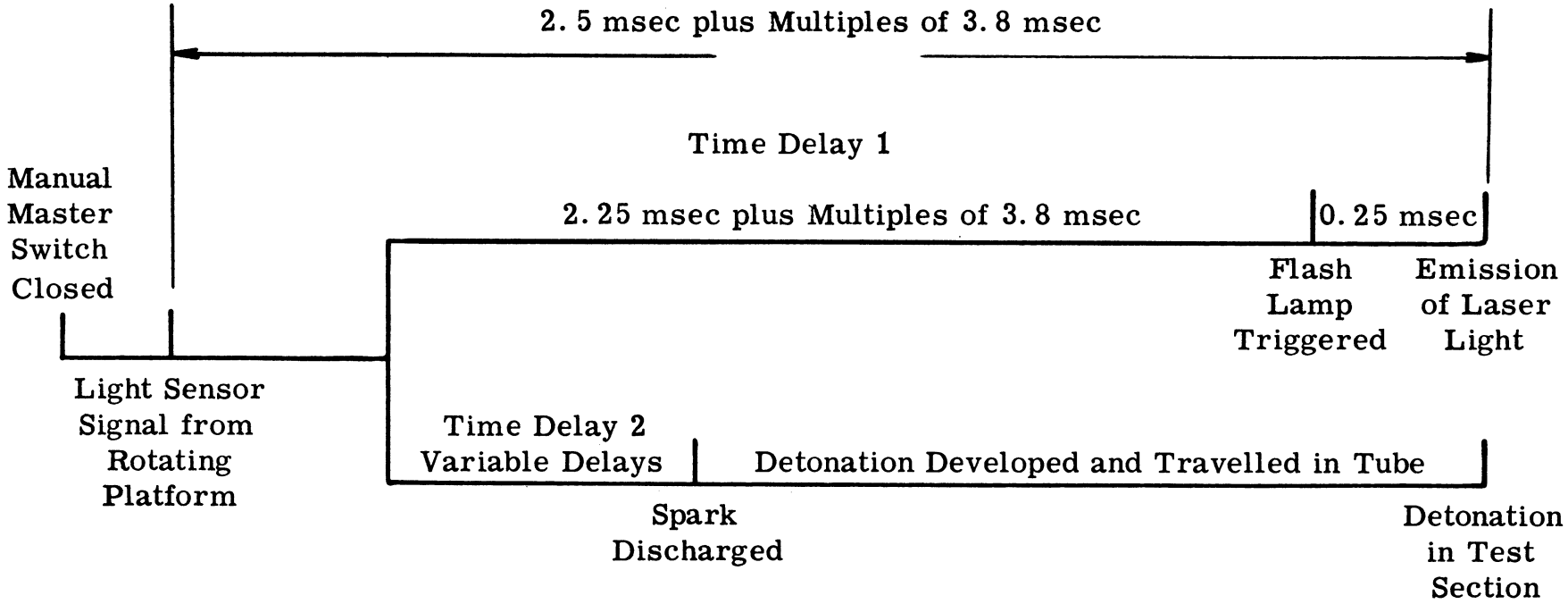

Fig. 14. Time Sequence of Occurrence of Events in the Synchronization Process.

instruments were installed to monitor the system more closely. The block diagram of the complete laser firing control system is shown in Fig. 15.

In Fig. 15, the function of the laser head, time delay units 1 and 2, and thyratron unit 1 were as described in the last paragraph. The timer 1 was used to measure the prism rotational period from the light sensor signal registering the passage of the slit, just before making a run, so that the time delay unit 2 could be adjusted accordingly. The timer 1 was also used to calibrate the time delay unit 2. The timer 2 was used to measure the time lapse between the spark discharge and the arrival of the detonation wave at the ionization probe 3 which triggered the thyratron unit 2. The same signal, which stopped the timer 2 from the thyratron unit 2 was fed into an oscilloscope*. A light sensor†, upon seeing the laser light which was partially diverted by the beam spitter, sent a signal to the oscilloscope also. Thus after a run, it was possible to tell, from the relative time lapse between the two signals of the oscilloscope trace, whether proper synchronization was achieved and if not, the time delay unit 2 could be corrected accordingly for the next run.

---

*Model 565, Tektronix Co., Beaverton, Ore.

†Photodiode Model 100, EG and G Inc., 160 Brookline Ave., Boston 15, Mass.

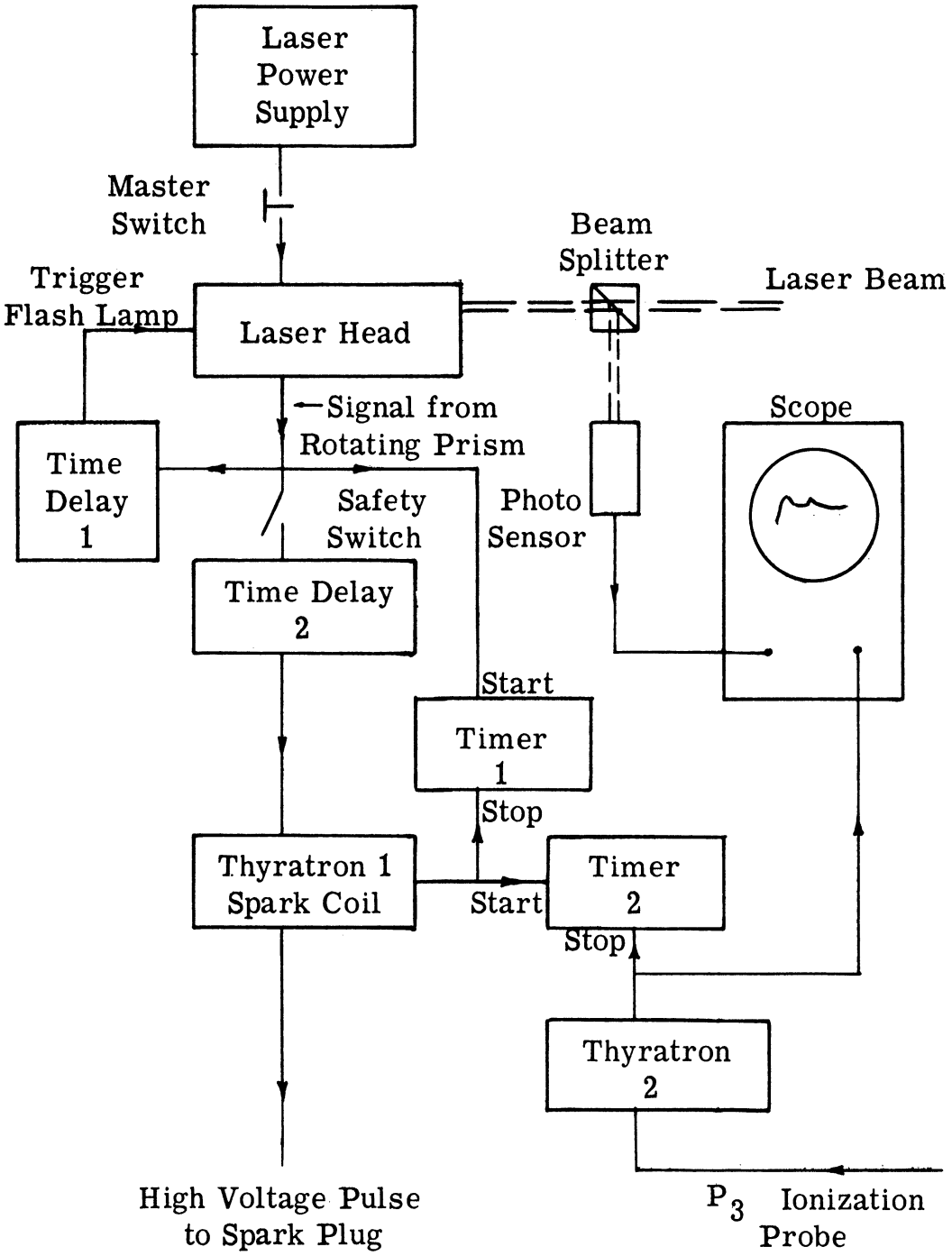

Fig. 15. Schematic Diagram of Instruments Controlling Time Sequence of Events.

It must be mentioned that the control problem of the laser light can be greatly simplified and perfect synchronization with the detonation wave can be achieved if a very expensive Kerr cell or Pockel cell type Q-switching laser is used.

3.2.3 Mixing, Charging, and Ignition System

The same mixing and charging system as was used in the side relief work was used here. However, the ignition system was modified to give better control and shorter induction times for the detonation to minimize the synchronization problem. It is the induction time of detonation which fluctuates and causes synchronization problems as discussed before.

To shorten the induction time, a spark discharge was used to ignite the explosive instead of a glow plug. The spark ignition arrangement is as shown in Fig. 16. The high voltage pulse (1 μf at 15 KV) from the thyratron unit 1 described in the last section was applied to an automobile spark plug. The spark plug was installed in a steel housing and two coil springs were silver soldered in the housing to further reduce the induction time. The spark plug housing arrangement was placed in between the 1/4 in. charging tube and the entrance of the 5/8 in. transition tube (refer to Fig. 4) in most mixtures. For high CO content mixtures, the spark plug had to be placed at least 48 in. upstream of the entrance of the 5/8 in. transition tube. This

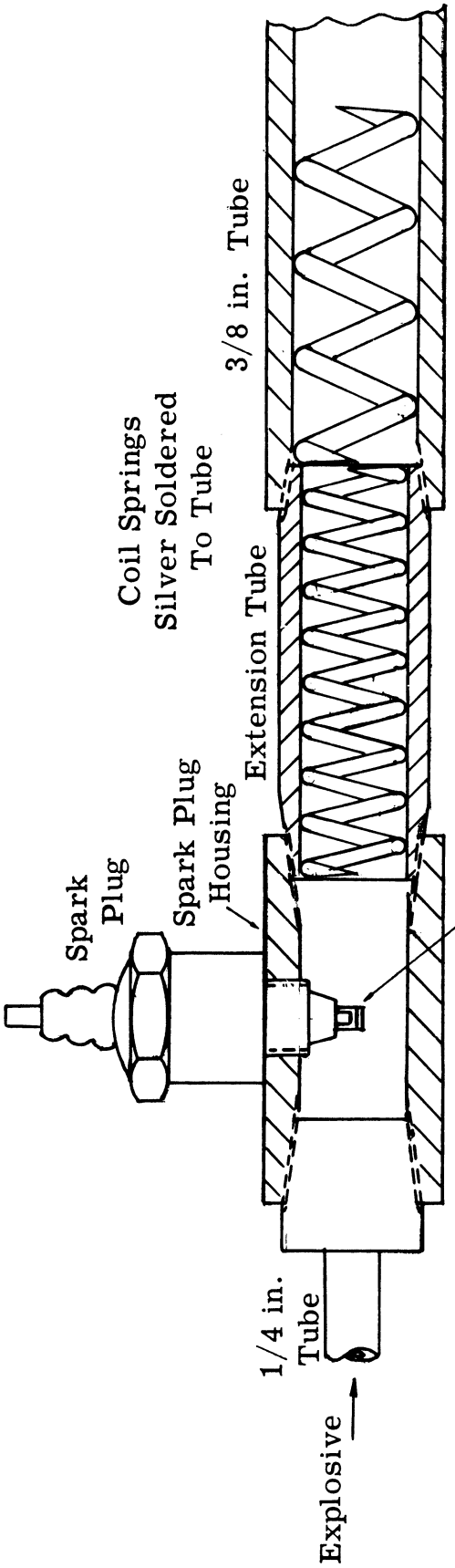

Fig. 16. Spark Ignition Arrangement

was done when the detonation wave appeared unsteady when measured between ionization probes 1, 2, and 3 on the flame tube. The steadiness of the detonation wave was always checked before photographic runs were made.

The test section was the same one used in the side relief work, except that the inert boundary gas side was replaced by a steel block and a non-grooved plate glass window was used.

3.2.4 Experimental Procedure

The flame tube and test section was flushed with dry nitrogen to get rid of the residue moisture from the previous run. The balloon reservoir (refer to Fig. 4) was first evacuated and then charged with the premixed explosive. The section of the tube in between valves 2 and 5 (after closing them) was evacuated for safety reasons as discussed earlier. Valve 1 was then opened and the explosive flowed through the flame tube and the test section was ready for the run. During the time of discharging the balloon reservoir, the laser was fired three or four times to warm up the laser rod whose output was sensitive to the temperature. The safety switch was in an open position (refer to Fig. 15) so that there were no spark discharges in the laser rod warm up process. The period of the rotating prism was measured and if it showed appreciable drift, the time delay unit 2 was readjusted accordingly. When the balloon was almost exhausted the

safety switch was closed. The room was darkened and the photographic film cover was opened. By closing the master manual switch momentarily, the initiation of explosion and triggering of the laser light followed the sequence automatically as described previously. After the run, the schlieren photograph and the oscilloscope trace were developed immediately and studied. Noting the relative time differences of occurrence of the wave and laser light, the time delay 2 was adjusted accordingly for the next run.

3.3 SOOT TRACK TECHNIQUE

The soot track technique was first used by Denisov and Troshin[38] to demonstrate that a steady, one-dimensional detonation wave did not exist in a self-sustained gaseous detonation. The technique is to coat the side of a tube with a thin layer of soot. When a detonation passes over the soot, a characteristic diamond pattern cell structure is inscribed in it. The cell structure is inscribed by the triple points of interacting transverse waves in the detonation wave front as reported by Duff[39], Denisov and Troshin[40]. Voitsekhovsky et al[6] suggested that the combustion zone thickness is determined by the dimension of the cell in a detonation. Although no reliable theory is available to predict the relationship between the reaction length and the "cell" size, it was nevertheless decided to obtain soot track prints of all the mixtures used in the laser schlieren work.

The window glass was easily coated with a layer of soot by passing it through a coverless kerosene lamp several times. After the window glass was properly coated with soot, it was installed in the test section and a detonation passed over it. The window glass was then removed from the test section and covered with a layer of clear lacquer for preservation.

The soot track technique was also used in some side relief runs. Instead of coating the window glass itself with soot, a 0.006 in. thick clear mylar was used. The mylar was cut to a suitable size to fit the interior wall of the explosive channel in the test section, then it was attached to a metal plate which served as a heat sink to prevent the mylar from burning and the soot was applied to the mylar in the same manner as on the window glass. The soot coated mylar was stuck to the interior wall of the test section, then the experiment was performed as in the side relief work described before. After the run, the mylar was carefully removed from the wall and also preserved with a coating of clear lacquer.

IV. EXPERIMENTAL RESULTS AND DISCUSSION

4.1 REACTION ZONE IN H_2-CO-O_2 MIXTURES

4.1.1 General Description of the Influence of the H_2 on the Wave Front Structure, and the Influence of the Side Relief on the Wave Front.

The photographic results from the laser schlieren and streak schlieren techniques reveal interesting information on the wave front structure which is influenced by the hydrogen concentration in the mixtures. Three different fuel-oxygen ratio mixtures, lean fuel (1 fuel + 1 oxygen), stoichiometric fuel (2 fuel + 1 oxygen), and rich fuel (3 fuel + 1 oxygen), were used. Typical laser schlieren photographs of detonation waves in H_2-CO-O_2 mixtures in a solid channel are shown in Fig. 17,18,20 and 21. In all these pictures the regions next to the main shock fronts have the characteristic "turbulent" structure observed by White[41] in his interferograms of self-sustained detonation waves. This "turbulent" region is recognized as the reaction zone by White because after the sharp decrease in density through the "turbulent" region, the density decrease is small, which indicates that chemical equilibrium is approached. The characteristic transverse waves which accompany all self-sustained detonation waves also show up clearly in the photographs. Some general conclusions as to the influence of hydrogen concentration on the wave structure of the detonation in H_2-CO-O_2 mixtures can be made from the schlieren photographs.

It is necessary to explain briefly the "sense" of the schlieren effect in these pictures, so that it will be easier to interpret the events in the pictures. In all laser schlieren and streak schlieren photographs, a horizontal schlieren aperture was used so that only density gradients normal to the wave front are subjected to schlieren effects. The schlieren effect was set in such a way that an increase of density (such as a shock) towards the burned mixture produced a dark shadow in the picture. A vertical disturbance in the photographs shows up due to shadowgraph effects. Thus a transverse wave, which is nearly vertical with respect to the horizontal schlieren aperture, is shown as a dark line followed by a white line; the latter is at the downstream side of the transverse wave. In laser schlieren photographs, there are fine fringes next to the test section channel walls and downstream of the transverse waves. These fringes are caused by the effects of diffraction of laser light at sharp boundaries and steep density gradient regions, and they should be ignored.

Figure 17 shows typical schlieren pictures of a detonation wave in H_2-O_2 mixtures. Invariably the main shock front is smooth and is slightly convex to the fresh mixture. The turbulent reaction zone is very thin and is uniform in thickness. The reaction zone does not have a clear cellular structure as those shown in Urtiew and Oppenheim's[42] work at sub-atmospheric initial pressures. The cellular structure

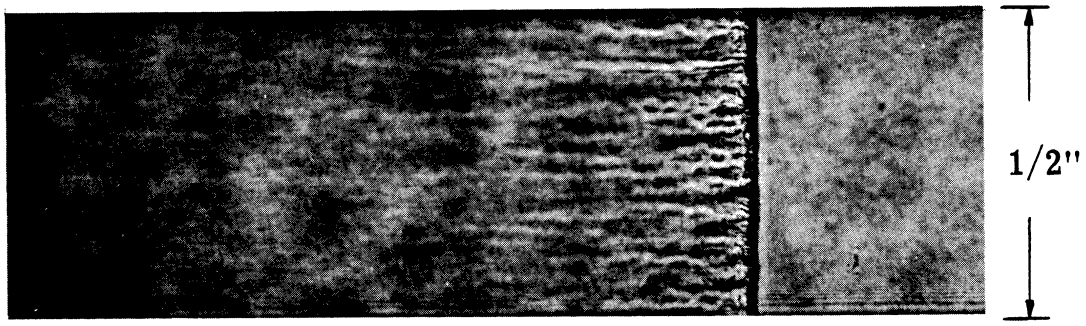

a. Run 1180 75% H_2 + 25% O_2

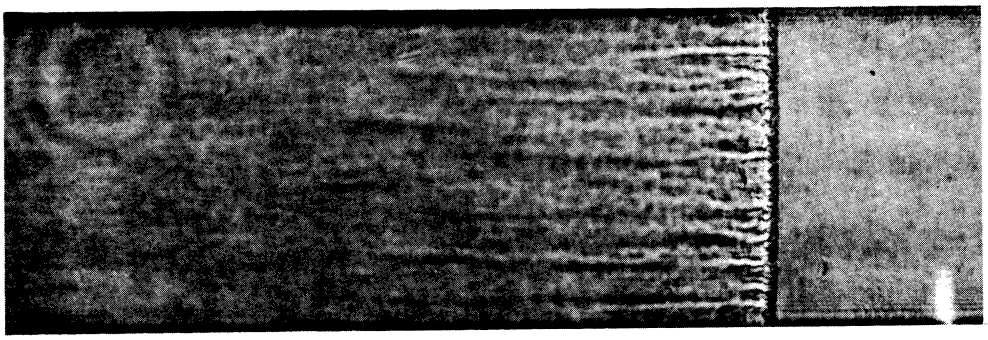

b. Run 1130 66.7% H_2 + 33.3% O_2

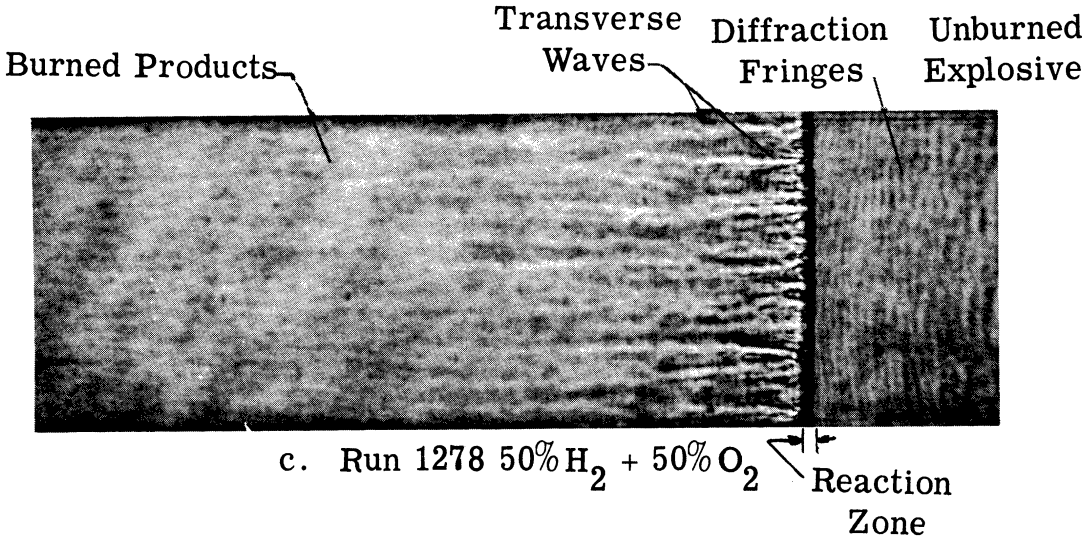

c. Run 1278 50% H_2 + 50% O_2

(Detonation Wave Propagates to Right)

Fig. 17. Laser Schlieren Photographs of H_2-O_2 Detonations.

may exist but due to the high initial pressure, it could be too fine to be resolved in the picture. The straight transverse waves, which are perpendicular to the main front, are short with small spacing.

When hydrogen is gradually replaced by carbon monoxide, the main shock front gradually becomes non-planar, and the reaction zone becomes thicker and non-uniform in thickness, as shown in Fig. 18. Generally, the reaction zones in lean fuel mixtures are thicker than those in rich fuel mixtures, as can be seen in Fig. 18c and 18a. When the reaction zone becomes thick, some orderly wavelets still appear in the reaction zone despite the overall turbulent structure. The schlieren effect indicates a negative density gradient across the wavelets which may be interpreted as due to the exothermic reaction occurring there. The straight transverse waves, which are still perpendicular to the main shock front, become very long and extend deep into the burned products, and their spacing becomes larger. The transverse wave spacing, like the reaction zone, is larger in lean fuel mixtures than in rich fuel mixtures. Some weak shock waves appear behind the reaction zone. They interact with the transverse waves and move into the on-coming burned gas as shown in Fig.18c. The origin and characteristics of these shock waves show up more clearly in very rich CO mixtures and are discussed in the following paragraphs.

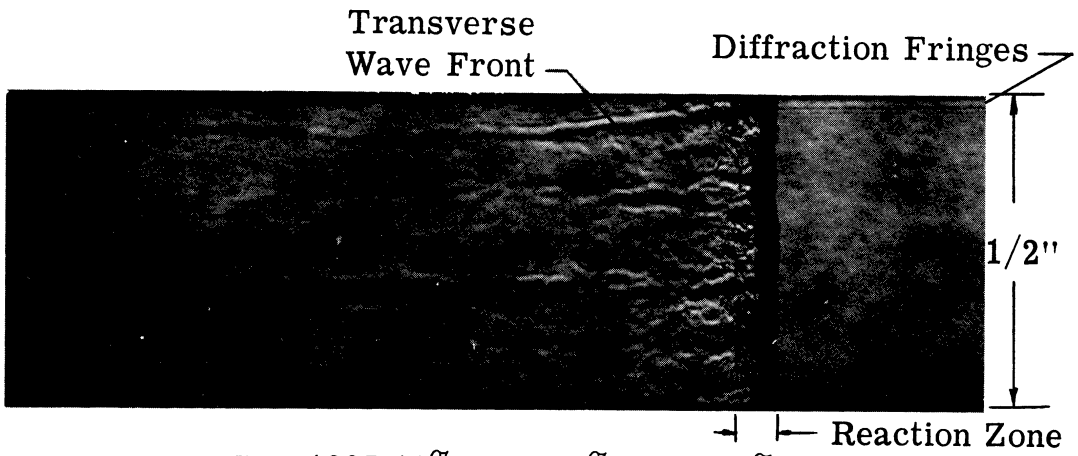

a. Run 1225 12% H_2 + 63% CO + 25% O_2

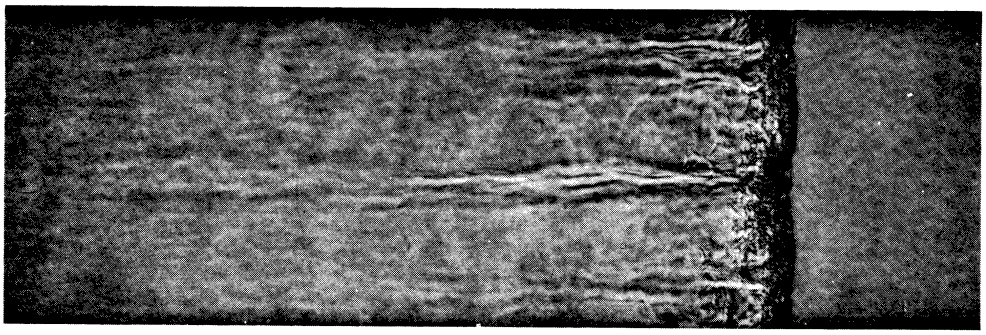

b. Run 1072 10.7% H_2 + 56% CO + 33.3% O_2

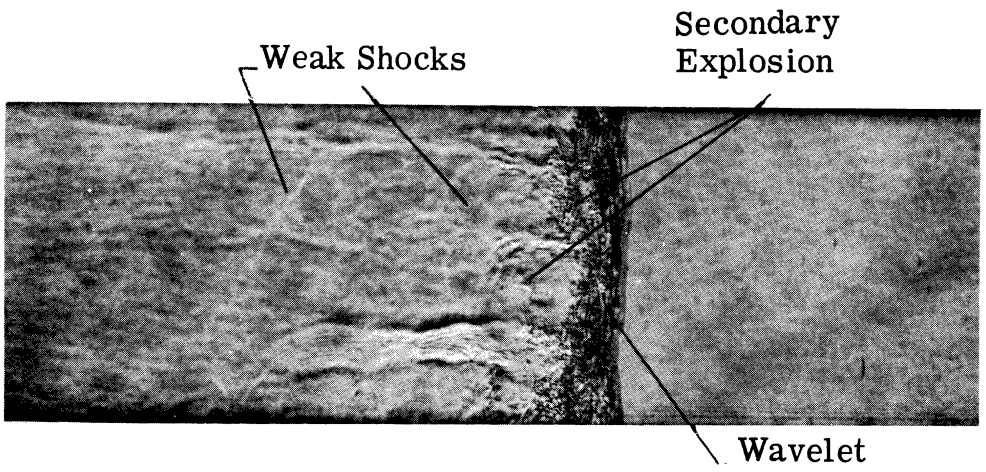

c. Run 1308 8% H_2 + 42% CO + 50% O_2

(Detonation Wave Propagates to Right)

Fig. 18. Laser Schlieren Photographs of H_2-CO-O_2 Detonations.

When the CO concentration is very high, the detonation wave does not propagate steadily any more. It becomes a "single headed" or "double headed" spinning wave. The term "head" refers to the transverse wave. A "single headed" spinning wave is shown in the streak schlieren photographs in Fig. 19a and b. The wave speed, which is represented by the slope of the streak trace of the wave front, is apparently strongly pulsating. There is only one wave which oscillates transversely that is attached to the main wave front. In Fig. 19a the slit is at the centerline of the channel and the transverse wave appears at almost equal time intervals. In Fig. 19b, the image slit is near one side of the channel, thus the time interval is small between the appearance of the incident wave and the reflected wave from the wall; but the total time interval between two incident waves is the same as in Fig. 19a. Therefore there is only one transverse wave in the system. The main wave front, as shown in the laser schlieren photographs in Fig.20 and 21, is not planar anymore and tilts with the channel axis severely. The reaction zone is very uneven in thickness; the thicker portion is two or three times that of the thinnest part. The wavelets, which are observed in the reaction zone of lower CO content detonations, become more distinguishable. The nonuniformity of the reaction zone is not stationary but oscillating transversely with respect to the main wave

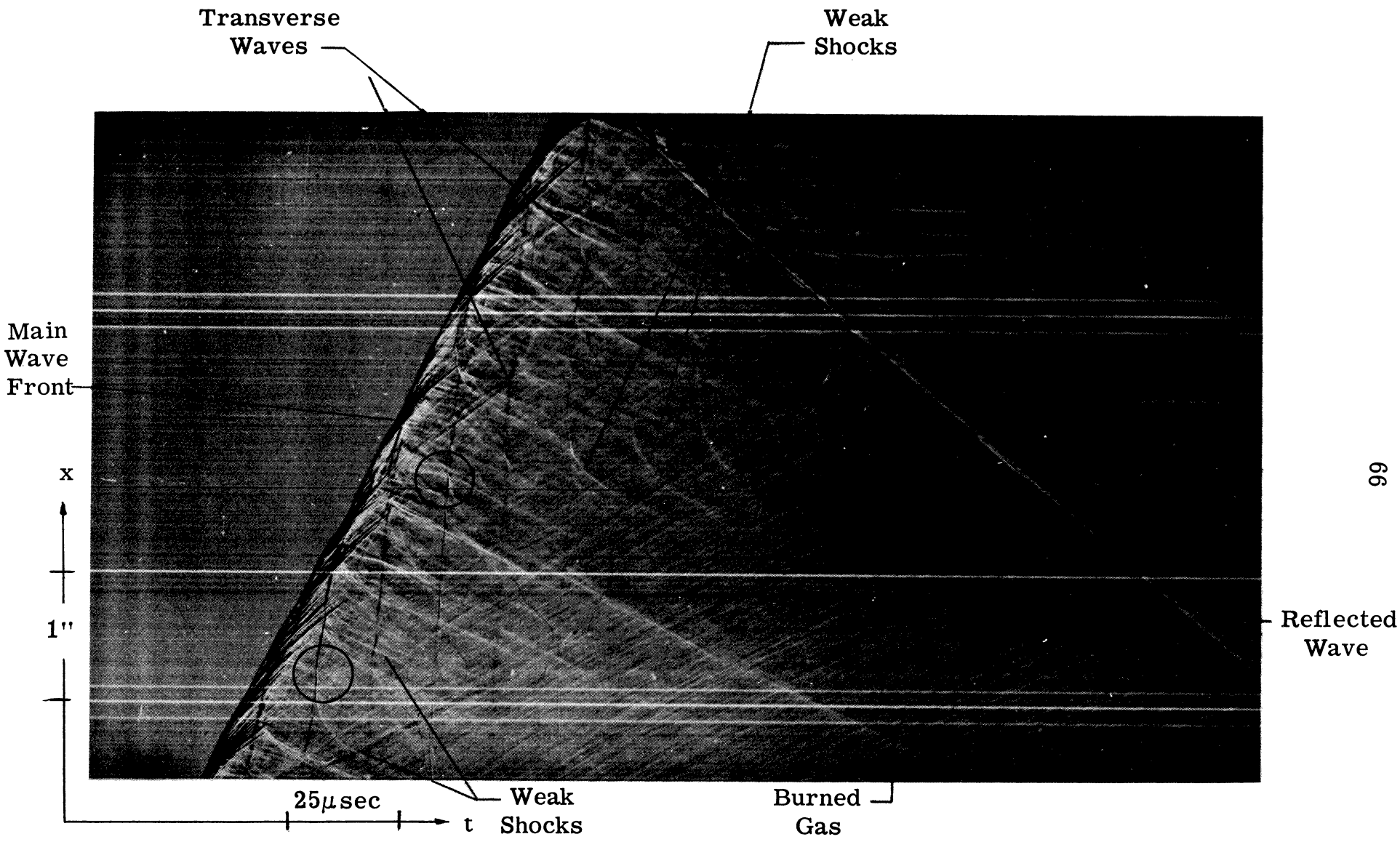

Fig. 19a. Streak Schlieren Photograph of a Detonation in 1.7% H_2 + 65% CO + 33.3% O_2 Mixture (slit at center line of channel) Run 1426.

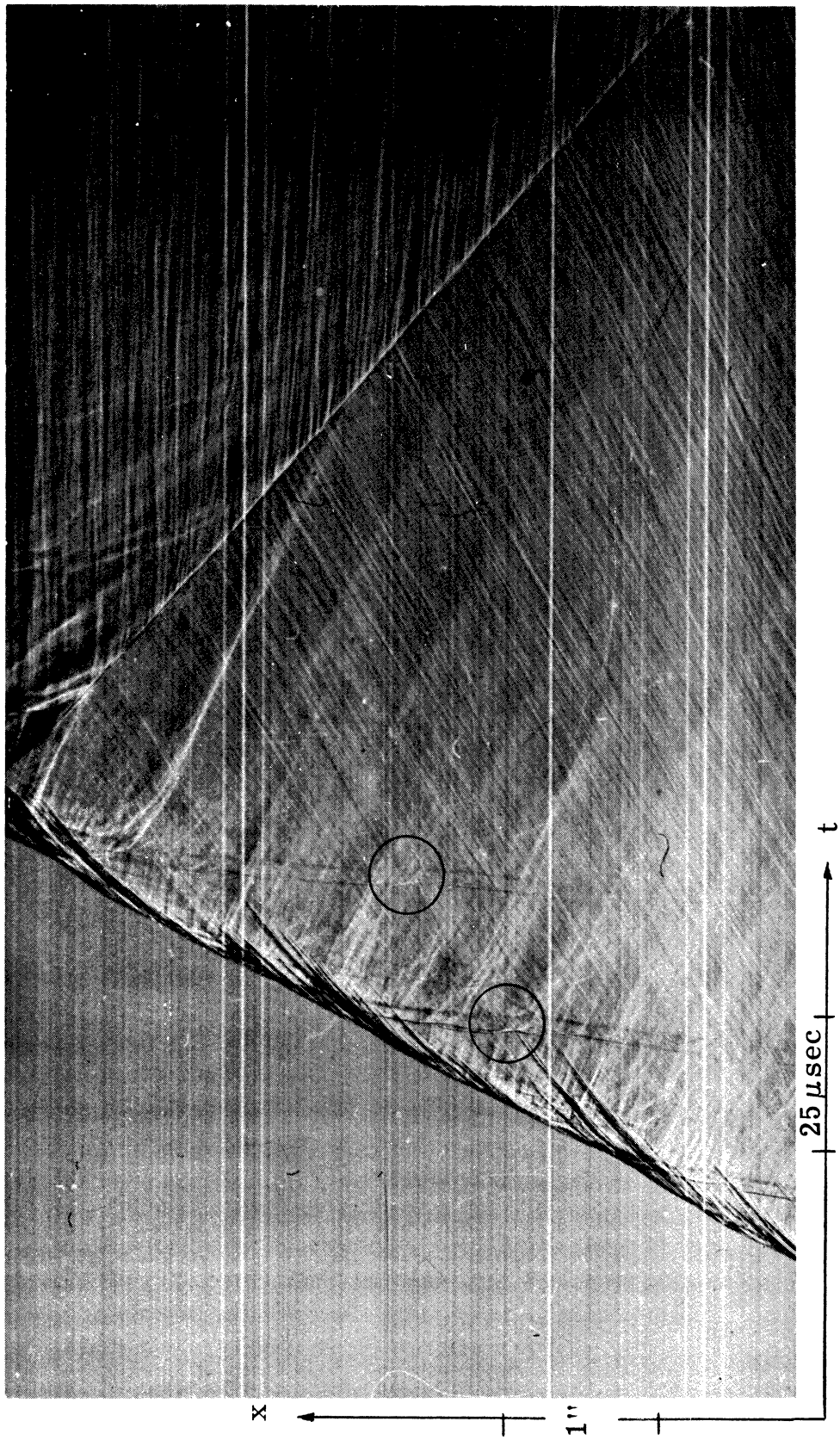

Fig. 19b. Streak Schlieren Photograph of a Detonation in 1.7% H_2 + 65% CO + 33.3% O_2
Mixture (slit close to one side wall) Run 1425.

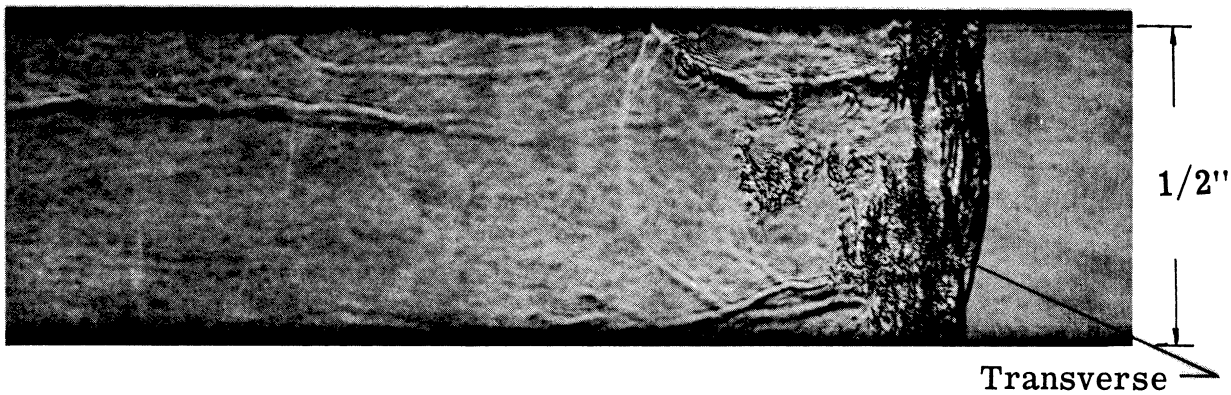

a. Run 1268 2% H_2 + 73% CO + 25% O_2

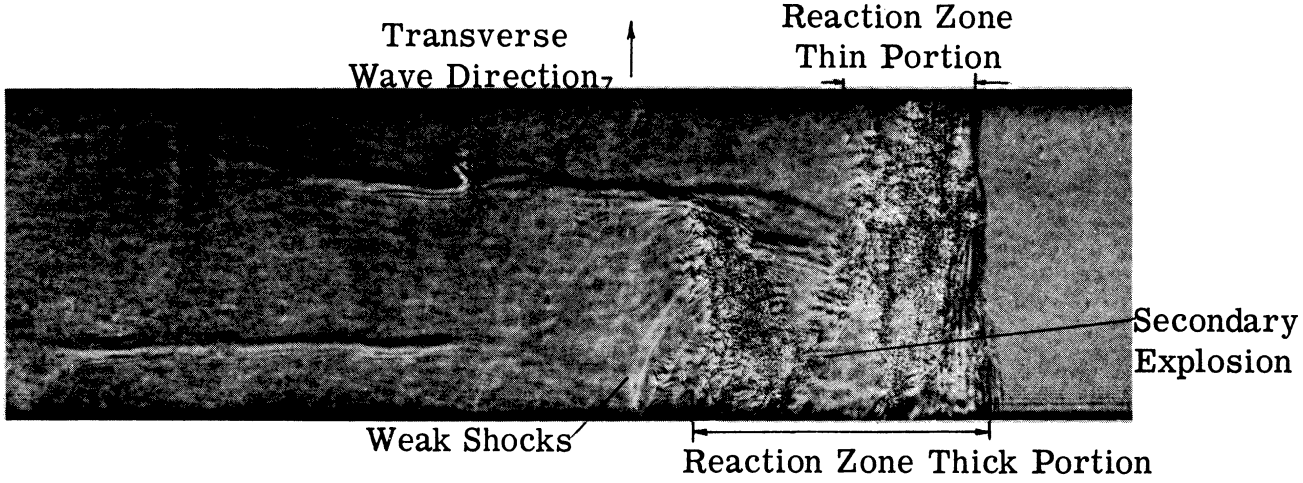

b. Run 1108 1.7% H_2 + 65% CO + 33.3% O_2

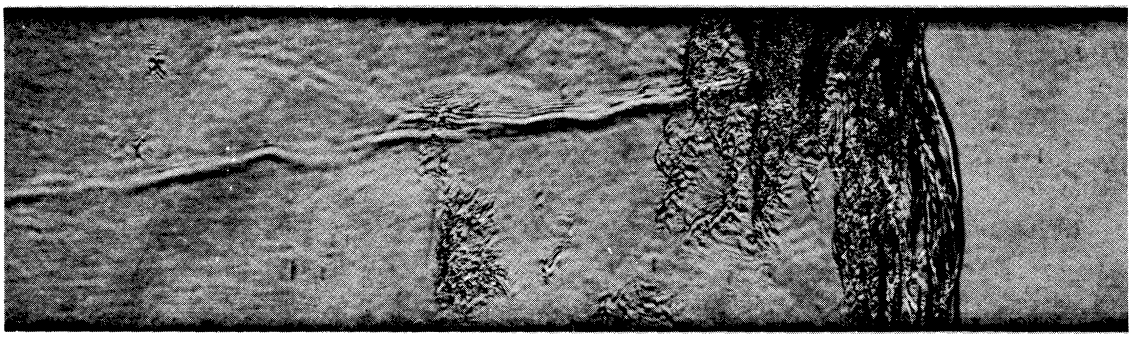

c. Run 1340 2.6% H_2 + 47.4% CO + 50% O_2

(Detonation Wave Propagates to Right)

Fig. 20. Laser Schlieren Photographs of H_2-CO-O_2 Detonations.

a. Run 1256 2% H_2 + 73% CO + 25% O_2

b. Run 1100 1.7% H_2 + 65% CO + 33.3% O_2

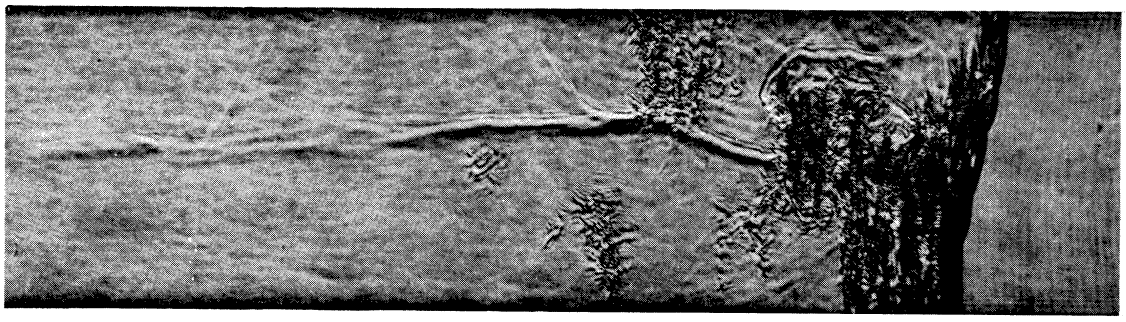

c. Run 1336 2.6% H_2 + 47.4% CO + 50% O_2

(Detonation Wave Propagates to Right)

Fig. 21. Laser Schlieren Photographs of H_2-CO-O_2 Detonations.

direction as shown in Fig. 19a and b. Some secondary explosions occur behind the main reaction zone and make the reaction zone very thick.

Only one or two transverse waves appear in the very rich CO mixtures laser schlieren photographs. There is an indication that the portion of the transverse waves immediately behind the main shock front has a narrow reaction zone behind it, as shown in Fig. 20 and 21. This reaction may provide the source of energy which supports the propagation of the transverse waves. The average velocity of the transverse wave in the stoichiometric mixture (CO/fuel = 97. 5%) is measured from the streak photographs (Fig. 19b) and is 4000 ft/sec relative to the burned gas. This velocity is obtained from the known distance the transverse wave travelled (one inch or twice the channel width) and the measured period of the transverse wave in the streak photographs. It is not certain whether the transverse wave moves at a steady speed across the channel or just oscillates at a steady period. It is interesting to note that the transverse wave maintains a fairly long, 3 to 4 in., and nearly straight shape. This makes one wonder what the mechanism is which keeps the transverse wave straight in the highly turbulent burned gas. A close observation of the laser schlieren photographs, such as those in Fig. 20 and 21, gives the following explanation. The secondary explosion behind the main reaction zone

and transverse wave is a pulsating process which produces a family of weak shock waves moving into the burned products as shown in Fig. 19, 20 and 21. The weak shock waves have a "white" appearance instead of a dark shadow in the photographs because the density gradient is the negative of that of the main shock wave. The weak shock waves, after the initial burst of the secondary explosion, travel fairly steadily as indicated by the traces in Fig. 19a and b. In the stoichiometric mixture (CO/fuel = 97.5%) the weak shock wave velocity is measured from the streak photograph and is 1420 ft/sec relative to the laboratory coordinates and in the -x direction. The burned gas, assuming equilibrium conditions, moves in the +x direction at a velocity of 2630 ft/sec. Thus the weak shock velocity is 4050 ft/sec relative to the burned gas. This velocity is very close to the average transverse wave velocity of 4000 ft/sec in the same mixture. The calculated speed of sound in the burned products is 3230 ft/sec. The steady speed, almost spherical, weak shocks originating from the secondary explosions are always behind the transverse wave. Figure 21 shows this phenomenon clearly. Evidently, then, the weak shocks interacting with the transverse waves cause the latter to be reinforced. These interactions cause a change in slope of the transverse waves and are evident in the circled regions in Fig. 19a and b as well as in Fig. 21.

It must be emphasized that the schlieren photographs show one mode of transverse waves which oscillate in the plane parallel to the test section windows. The other mode of transverse waves, which oscillate in the plane perpendicular to the window glass, do not show up in the schlieren photographs. However, their existence is revealed in the soot track records.

In the previous paragraphs, the influence of H_2 concentration on the wave front structure of a H_2-CO-O_2 detonation in a solid tube was discussed. The effect of side relief on the wave front structure is to be discussed in the following paragraphs wherein the better resolved schlieren photographs reveal some new information.

Typical streak photographs of the detonation wave under the influence of different degrees of confinement are shown in Fig. 22, 23, and 24. As expected, the propagation speed of the side relieved detonation wave decreases, indicated by the slope of the wave front streak. The detonation wave does not slow down immediately upon reaching the thin film because the disturbance due to the side relief takes a finite time to reach the solid side of the channel near which the image slit is located. Generally, the wave speed is less stable and the reaction zone is thicker as the confining gas decreases in density. These phenomena are shown clearly in Fig. 23 and 24. All of these effects resemble those of the addition of CO to the mixture. The wave front structure with side

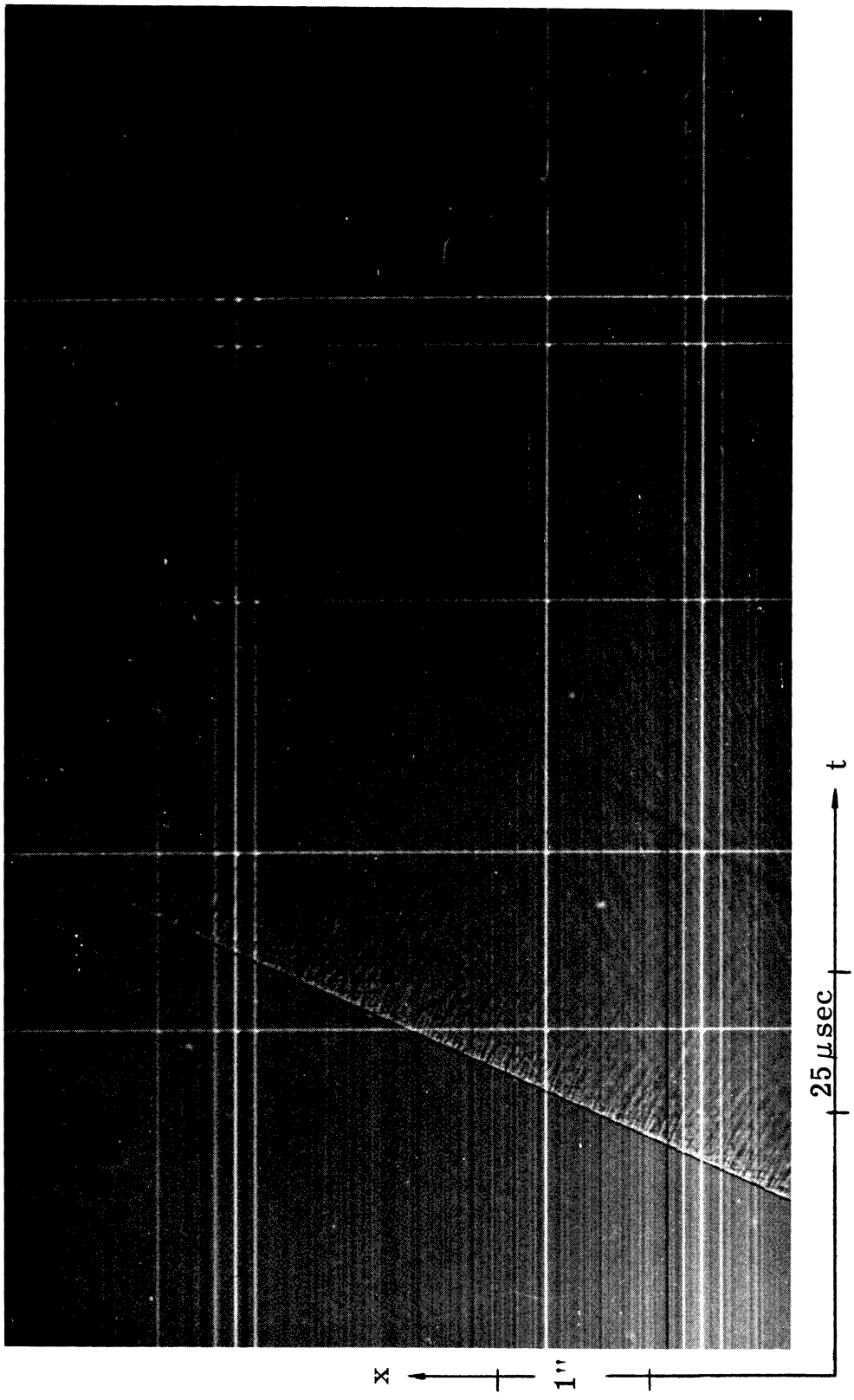

Fig. 22. Streak Schlieren Photograph of a Detonation in Solid Tube.
Mixture 33.3% H_2 + 33.3% CO + 33.3% O_2 Run 1538.

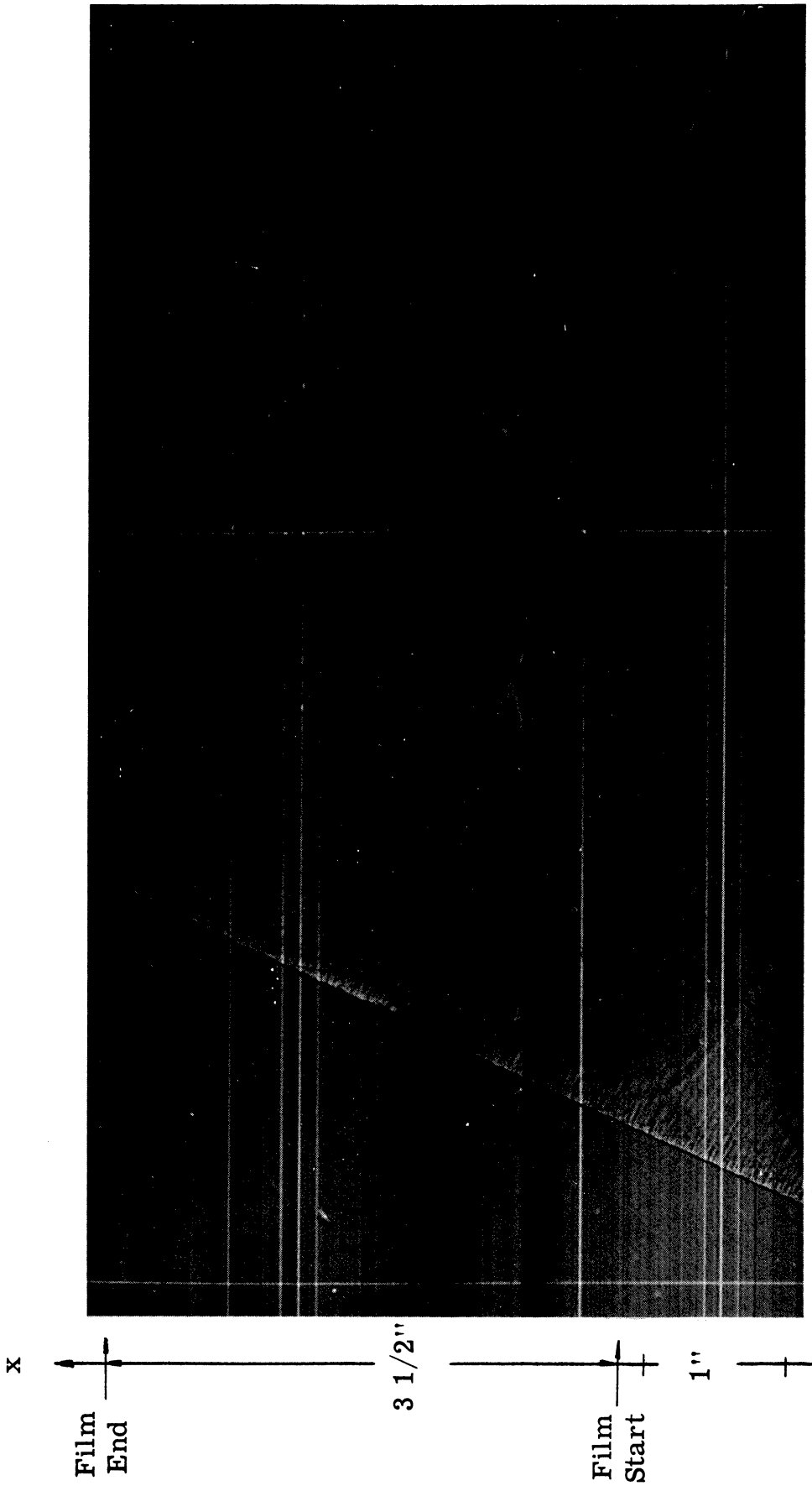

Fig. 23. Streak Schlieren Photograph of a Detonation with Side Relief.

Mixture: 33.3% H_2 + 33.3% CO + 33.3% O_2
Boundary Gas: Argon
Channel Width: 1/2 in.
Run: 1471

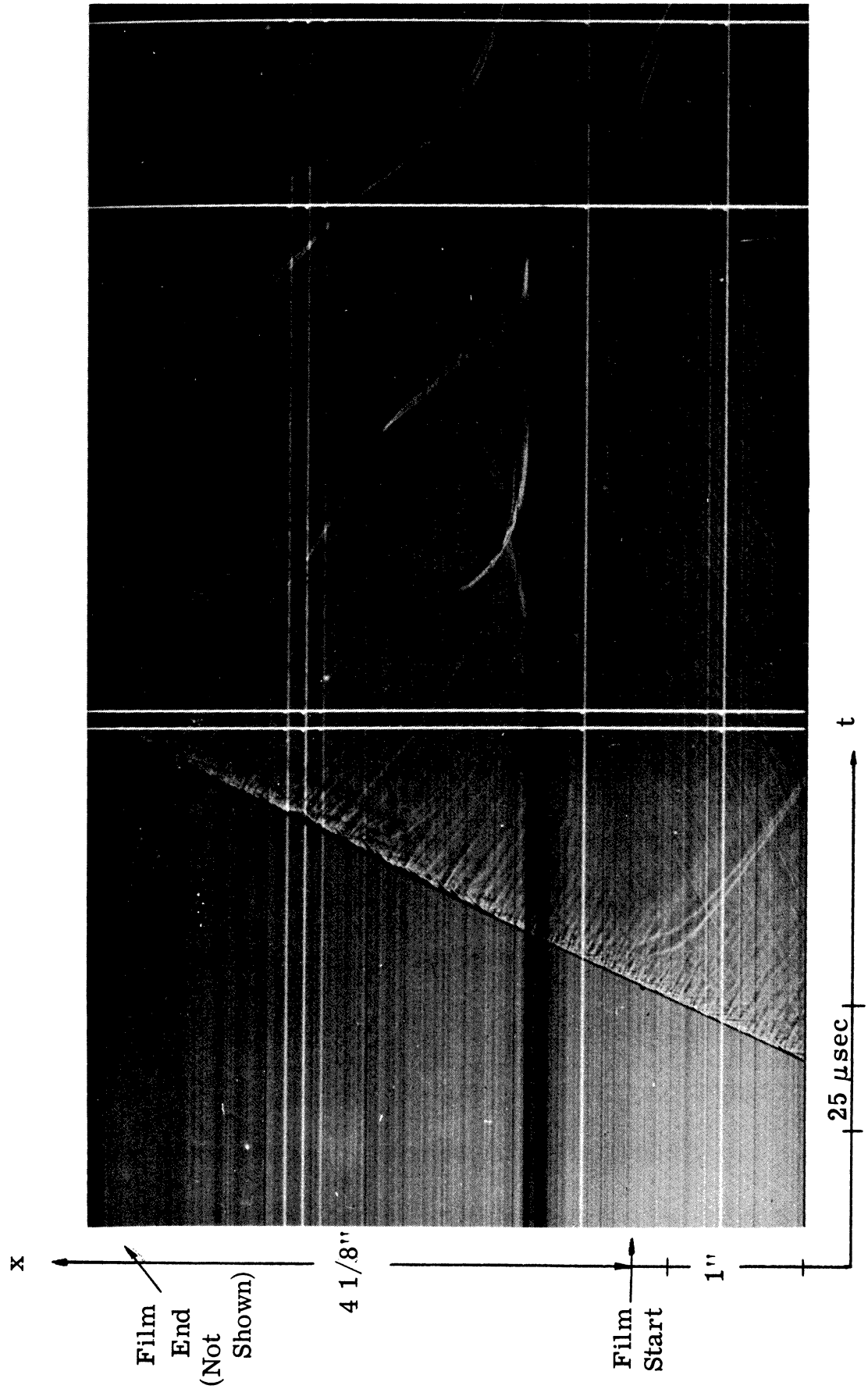

Fig. 24. Streak Schlieren Photograph of a Detonation with Side Relief.
Mixture: 33.3% H_2 + 33.3% CO + 33.3% O_2
Boundary Gas: Nitrogen
Channel Width: 1/2 in.
Run: 1462

relief effect can be best seen in the laser schlieren photographs as shown in Fig. 25. Figure 25a shows the detonation wave in a solid tube and is used as a comparison reference with those side relieved. Grossly speaking the reaction zone is fairly uniform, and the spacing between transverse waves is small in Fig. 25a. In Fig. 25b, the detonation is subjected to a mild degree of side relief. Its reaction zone thickens slightly and becomes uneven. The original straight transverse waves become bent. In Fig. 25c, the detonation is subjected to a severe degree of side relief by using a lighter boundary gas, nitrogen in comparison with the argon used in Fig. 25b. The reaction zone is very uneven. The nonuniformity of the reaction zone, resembling those of spinning detonations, oscillates transversely as shown in the streak schlieren photograph, Fig. 24. The spacing between the transverse waves becomes larger and the straight transverse waves become bent, as shown in Fig. 25b and 25c. A similar phenomenon occurs with the weak shocks as seen in the streak schlieren photographs of Fig. 23 and 24. In the side relieved portion the weak shock trace shows increasing speed at approximately the same location where the transverse waves bend. If these two phenomena are not mere coincidence, then the weak shock supported transverse waves explanation described before can be used to explain these phenomena. The bends in the transverse waves and weak shocks must be attributable to the side relief.

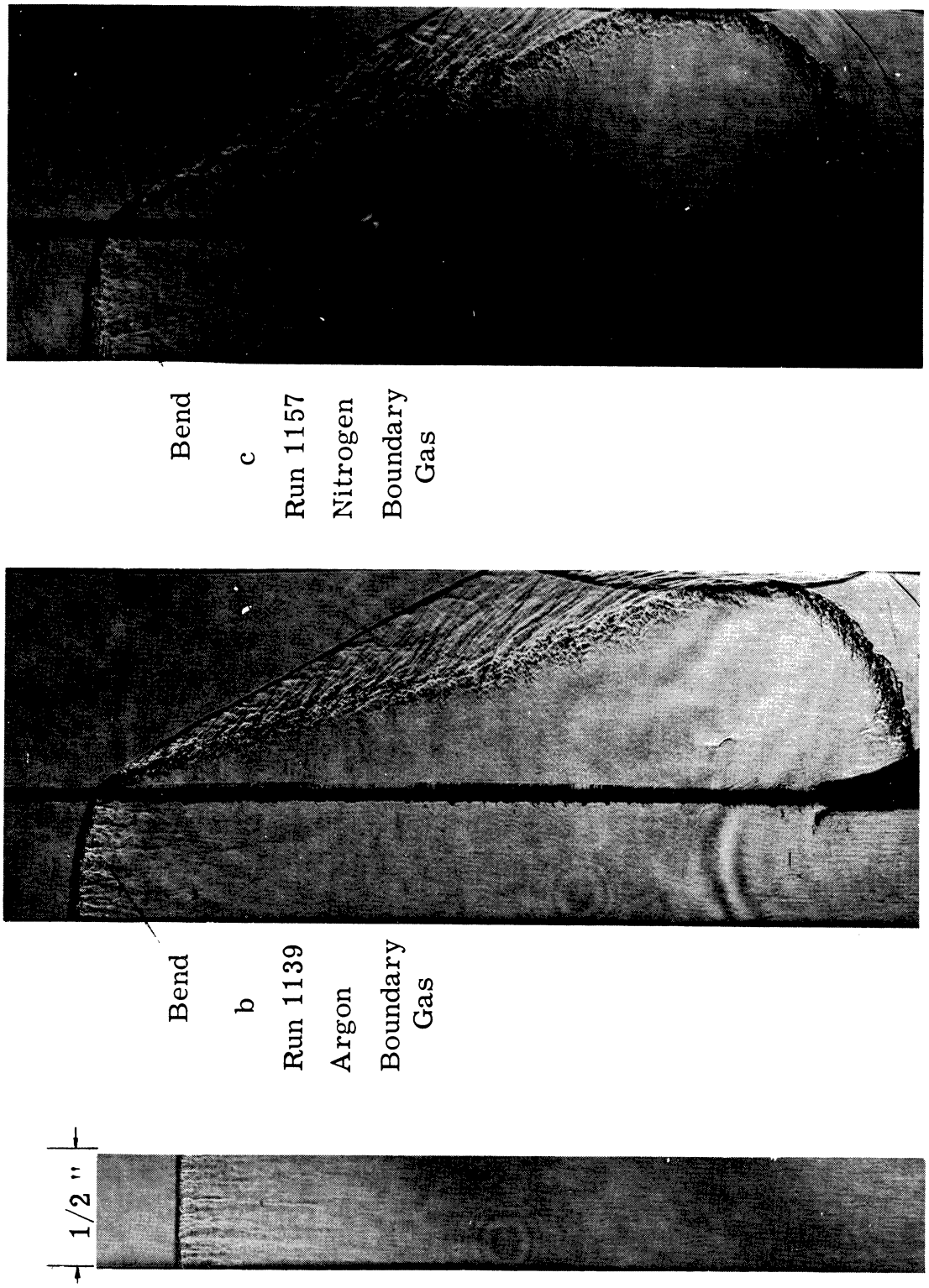

Fig. 25. Laser Schlieren Photographs of Detonation Waves in 33.3% H_2 + 33.3% CO + 33.3% O_2 Without and With Side Relief.

In the inert boundary gas side, a series of wavelets appear periodically behind the oblique shock as shown in Fig. 25b and 25c. These wavelets probably originate from the horizontal detonation wavelets in the reaction zone or the transverse waves. The ripples appearing on the oblique shock are due to the larger spacing between transverse waves in the $H_2 + CO + O_2$ mixtures which cause more severe pulsating interaction. This phenomena is very similar to the one where a detonation is expanded abruptly from a small tube to a large tube as reported by Mitrofanov and Soloukhin[43].

In spite of the detailed wave structure described above, the basic detonation-boundary gas interaction structure still agrees with Dabora's theory fairly well, as indicated by the fairly straight induced oblique shock in the boundary gas and the small curvature of the detonation front as shown in the laser schlieren pictures in Fig. 25b and c.

4.1.2 Velocity Decrement and Inferred Reaction Length.

Four stoichiometric H_2-CO-O_2 mixtures were used in the study. The CO contents were 0%, 10%, 33.3%, and 50% in the mixture by volume. Mixtures with more than 50% of CO were not used due to the unavailability of a suitable dense boundary gas to confine the detonation in the present test section configuration.

The velocity decrement of the wave as it passes from the solid tube to the side relieved portion can be calculated from the change of

slopes of the detonation wave trace in the streak photograph by using the expression

$$\frac{\Delta u_e}{u_e} = \frac{u_e - u_e'}{u_e} = 1 - \frac{\tan(\beta' + \alpha')}{\tan(\beta + \alpha)} \qquad (4.1)$$

The pertinent angles and distances in the streak photographs were measured in a tool maker's microscope. Generally, each streak photograph was measured twice to make sure that no error in measurement was caused by the movement of the photograph during the measuring process. In rich CO mixtures, in which the wave front was less planar and the propagation speed was less steady, the angle β was measured at the tangent of the wavy trace. A summary of the experimental results on the measurements of the velocity decrement of detonation wave propagation velocity in the stoichiometric H_2-CO-O_2 mixtures is shown in Table III.

The results of the measured velocity decrement in all four mixtures with different degrees of side relief are plotted in Fig. 26. The various degrees of side relief as expressed by tan δ/b was achieved by varying the boundary gas and/or the channel width as described before. For a particular mixture, the detonation will quench at a specific value of tan δ/b and this value is also indicated in Fig. 26. No velocity decrement could be measured under such conditions since the wave continues to decelerate. In general, as the CO content in the

Table III. Summary of the Experimental Results Obtained for the Stoichiometric H_2-CO-O_2 Mixtures Bounded by Various Gases.

1	2	3	4	5	6	7	8
CO	u_{eth}	$\overline{u}_{eion}$	B. Gas	b in.	$\frac{\tan \delta}{b}$	$\frac{\overline{\Delta u_e}}{u_e}$	$\frac{\overline{\Delta u_e}}{u_e}$
Percent	m/sec	m/sec			$in.^{-1}$	Percent	Percent
0	2839	2780	N_2	0.3	0.9	4.47- 5.56	5.09
		2770	N_2	0.25	1.08	4.23- 6.65	5.53
		2750	Ar	0.15	1.53	5.62-12.6	7.9
10	2550	2490	Ar	0.3	0.817	1.96- 4.65	3.52
		2530	N_2	0.3	0.968	2.95- 6.4	4.66
		2490	N_2	0.25	1.16	4.13- 7.08	5.43
		2510	Ar	0.15	1.63	7.38-10.9	8.78
33.3	2137	2070	Freon 14	0.5	0.446	2.12- 2.65	2.43
		2090	Ar	0.5	0.56	1.73- 6.85	4.03
		2085	N_2	0.5	0.65	4.78- 6.78	5.84
		2085	Ar	0.4	0.7	2.41- 8.43	5.18
50	1935	1870	Freon C318	0.5	0.36	2.27- 3.7	2.93
		1870	Freon 116	0.5	0.41	3.34- 5.43	4.37

1. CO concentration in the mixture. Note $(xH_2 + yCO/z_{mixture}) = 66.7\%$.
2. Theoretical wave propagation speed taken from Appendix II.
3. Average velocity obtained from ionization probes measurements.
4. Boundary gas used.
5. Explosive channel width.
6. tan δ calculated from Fig. 2.
7. Range of measured velocity decrements for waves with side relief obtained from streak pictures.
8. Average value of 7.

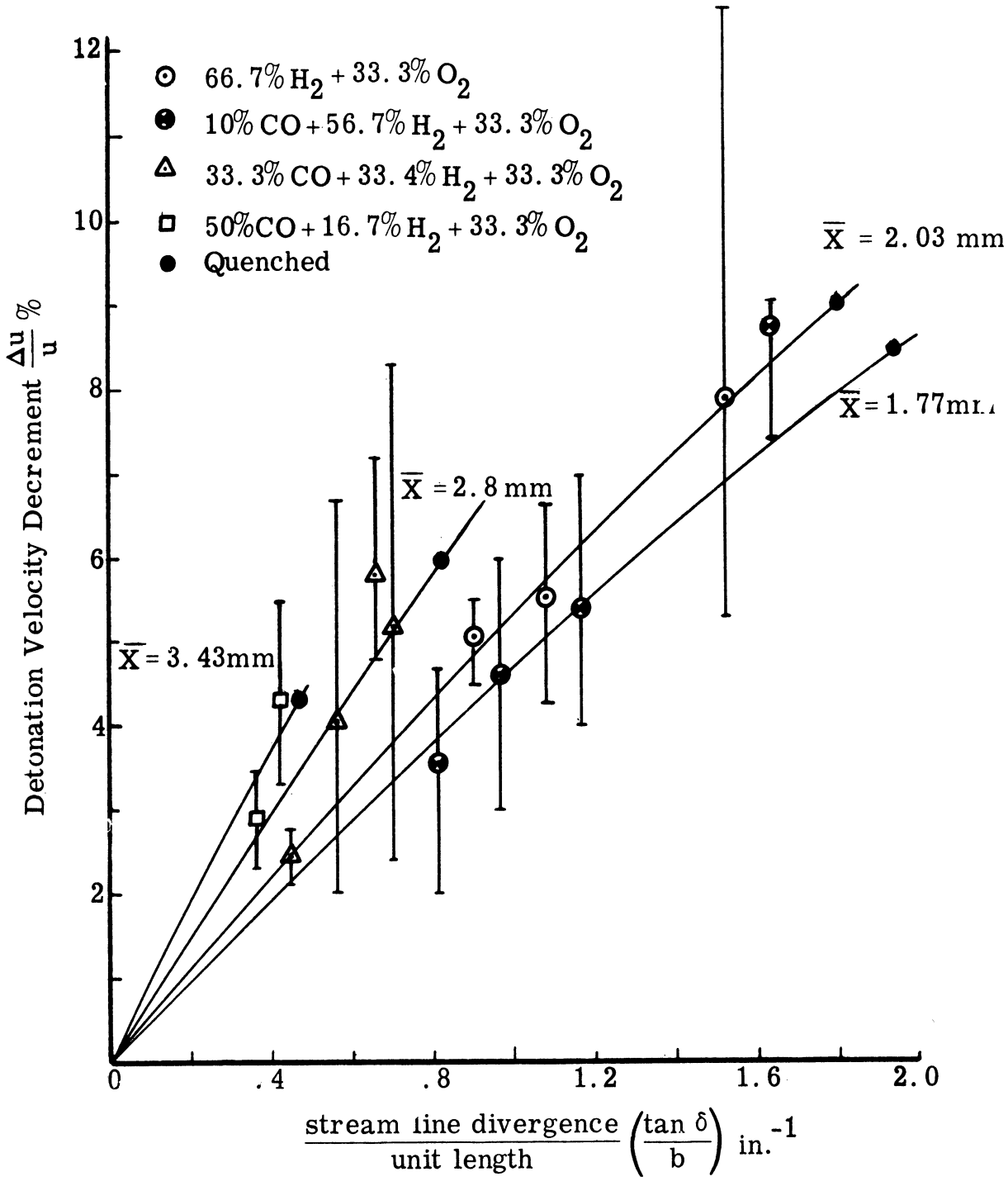

Fig. 26. Variation of Detonation Velocity Decrement with Channel Width b and the Tangent of Interface Angle δ.

mixture increases, the detonation can stand less velocity decrement before it quenches. The range of data scatter is larger in rich CO mixtures, or in the waves closer to the quenching condition. This is due to the difficulty of obtaining an accurate velocity measurement from the wavy detonation trace in the streak photograph.

The inferred reaction length is obtained by finding a reaction length value, $\overline{X}$, calculated according to Eq. (2.9) and Fig. 3, to fit most experimental points of the same explosive mixture. The results are shown in Fig. 26. The calculated best fit reaction lengths $\overline{X}$ in stoichiometric H_2-CO-O_2 mixtures are 2.03 mm (CO = 0), 1.77 mm (CO = 10%), 2.8 mm (CO = 33.3%), and 3.43 mm (CO = 50%). With the exception of the 10% CO mixture, the reaction length increases as the CO content increases. The deviation from the general trend of the 10% mixture may be attributable to the insensitivity of this technique to detect the effect of the presence of a very small amount of CO. It is doubtful that the effect is real.

The reaction length of stoichiometric hydrogen and oxygen has been measured by Dabora using the same technique. The calculated best fit reaction length, $\overline{X}$, to his data is 2.79 mm, in comparison with the $\overline{X}$ = 2.03 mm in this study. The difference could not be traced to any obvious experimental procedure but it may be due to relative data scattering.

4.1.3 Reaction Length Measured from Laser Schlieren Photographs.

The reaction zone is defined as the region in the wave front which has a "turbulent" structure appearance in the schlieren picture. Thus the apparent reaction length is the distance measured from the main shock front to the location where the turbulent structure disappears. Since the wave front thickness is less uniform as the CO content increases, the reaction length was assumed to be the average between the thickest and the smallest zone. The reaction length of one mixture is the average value of the measurements from four to six good pictures. All measurements were made by means of a 6X power comparator on the negative of the Polaroid photograph, which has a higher resolution than the positive. The smallest division on the reticle of the comparator is 0.2 mm.

The reaction lengths of the stoichiometric, lean, and rich fuel mixtures are plotted against the concentration of CO in fuel in Fig. 27, 28, and 29. In the same figures, the range of average values of the thinnest zone and the thickest zone in the reaction zone are also plotted. In all cases, the reaction length at first increases gradually as the CO content increases then increases exponentially as the CO concentration in the fuel exceeds about 75%. The non-stoichiometric mixtures do not show any appreciable change from this general trend as indicated in Fig. 28 and 29. In Fig. 27, Kistiakowsky and Kydd's[8]

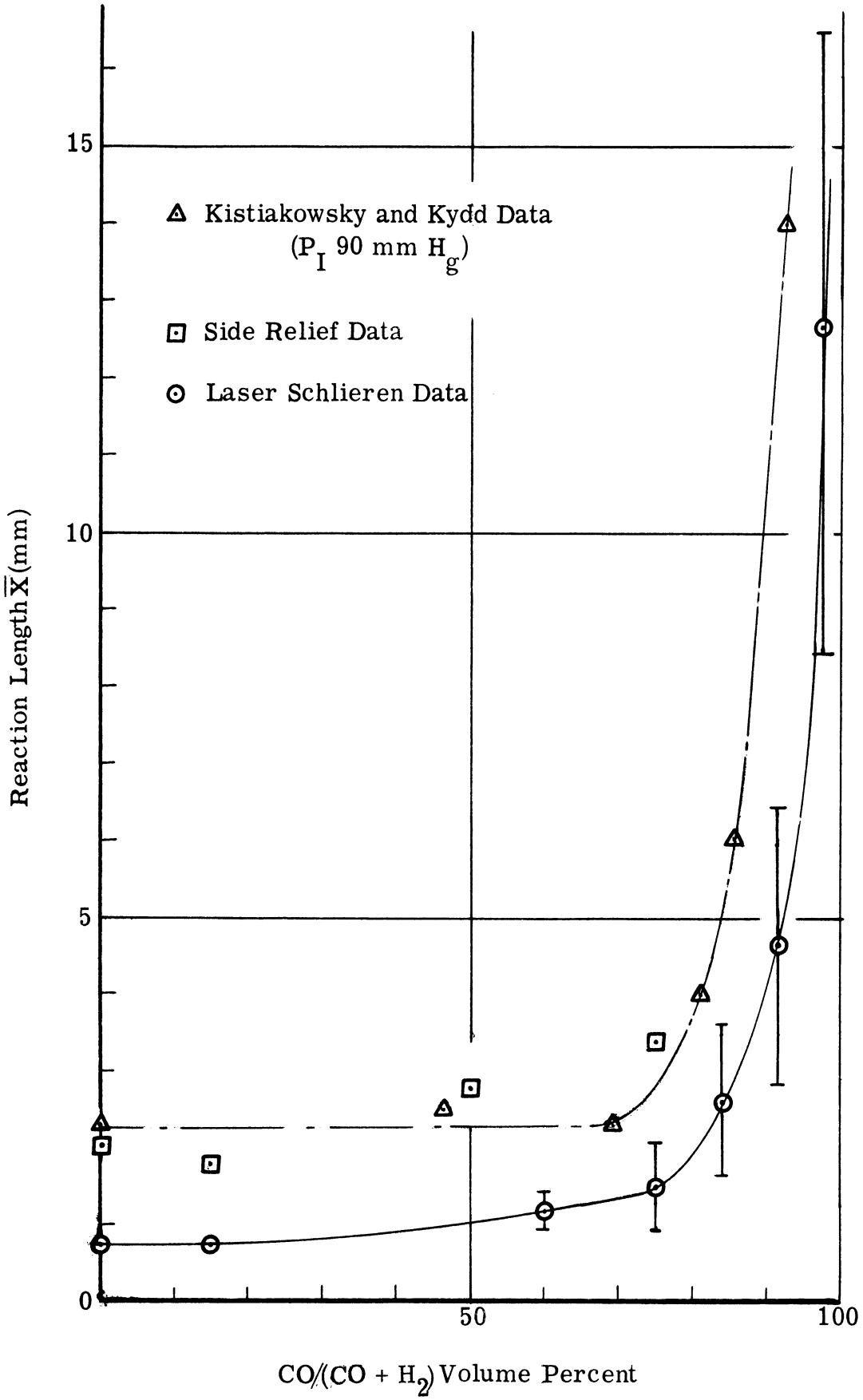

Fig. 27. Reaction Length in Stoichiometric Mixtures by Pulsed Laser Schlieren Pictures.

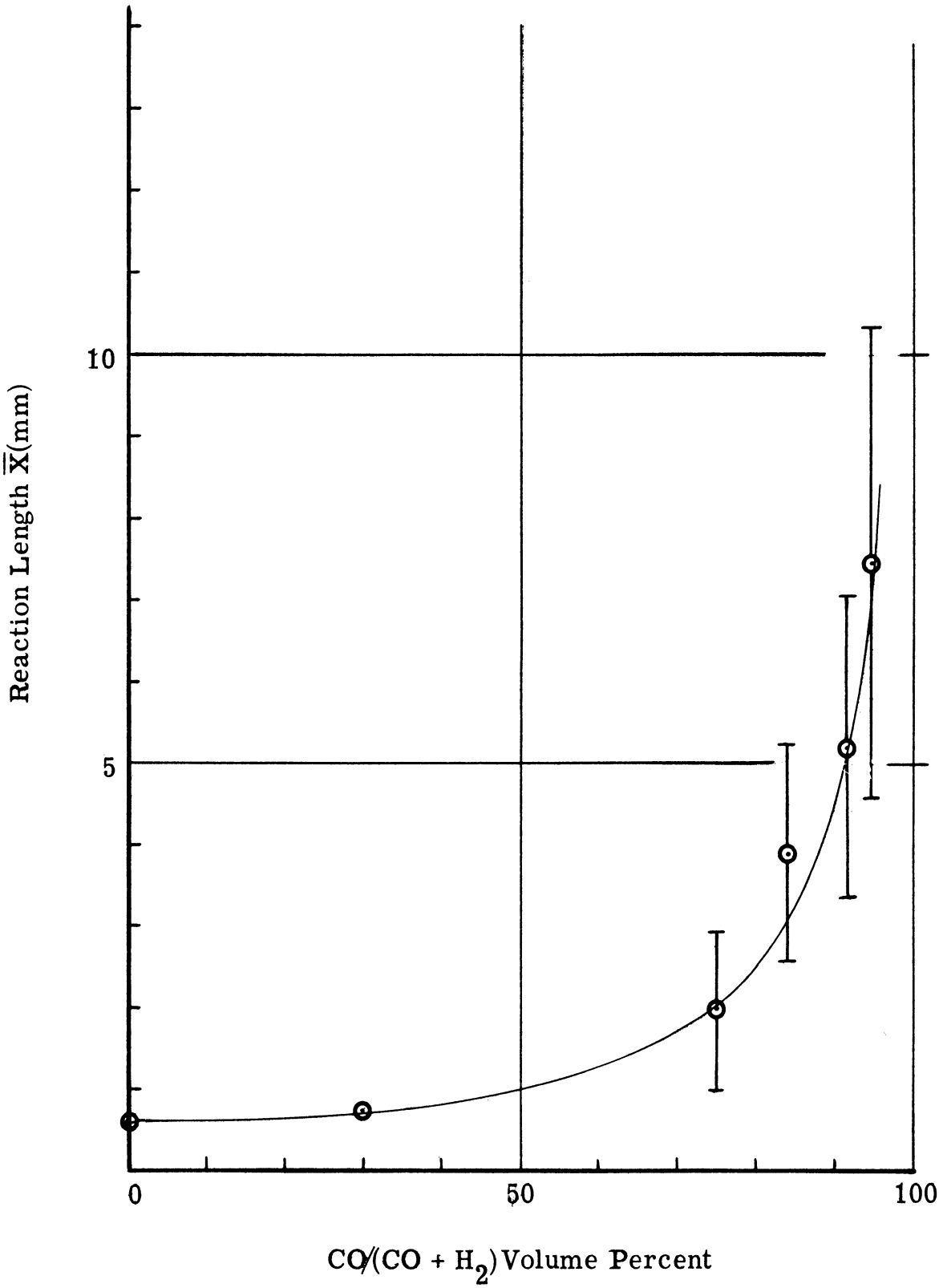

Fig. 28. Reaction Length in 1Fuel + O_2 Mixtures by Pulsed Laser Schlieren Pictures.

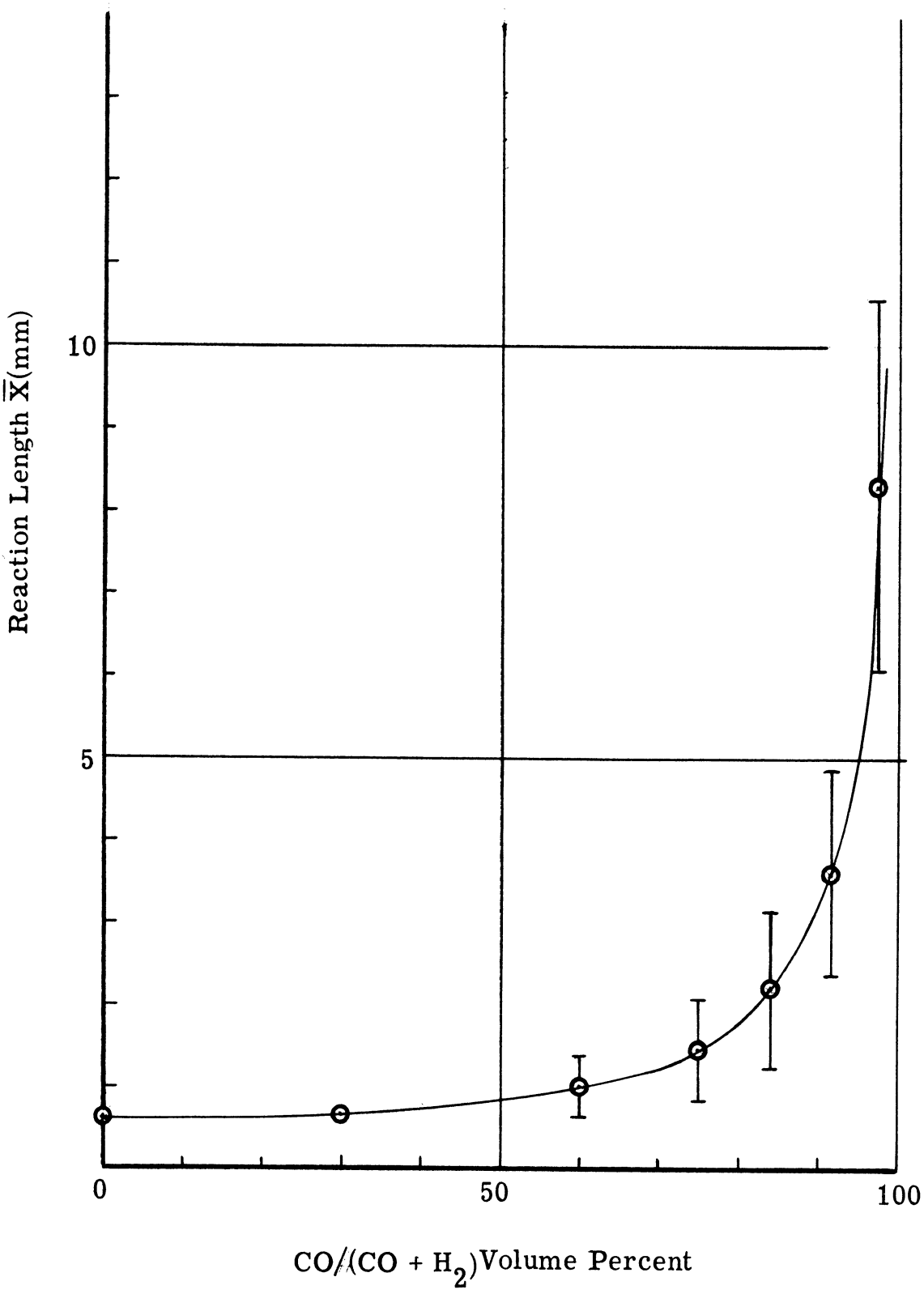

Fig. 29. Reaction Length in 3Fuel + O_2 Mixtures by Pulsed Laser Schlieren Pictures.

reaction time data t_{75}† in the low pressure stoichiometric H_2-CO-O_2-Xe mixtures, suitably transformed into a distance behind the wave front, are also plotted. Their mixture compositions have been corrected for the 5% of hydrogen (water vapor and other gases) which they mentioned but did not correct for in their data. Their absolute values are expectedly larger than the laser schlieren values due to their low initial pressure. However, they indicate a similar trend as the laser schlieren data in that the reaction length increases sharply in mixtures with more than 75% CO in the fuel. It is pertinent to note that in Weston's[44] flame spectra of H_2-CO mixtures in an oxygen atmosphere the characteristic carbon monoxide-oxygen continuum disappeared completely in the mixture of CO/fuel = 53%, but still showed up in the mixture of CO/fuel = 78%. All of these indicate that the CO reactions will be important in the mixture only when the CO concentration in the fuel exceeds an amount of about 75%.

The inferred reaction lengths from the side relief work are also plotted in Fig. 27. The trend of the data is the same as that obtained from the laser schlieren photographs, although the absolute value of the former is always about 2.5 times larger than the latter. This

---

†Kistiakowsky and Kydd defined reaction time t_{75} as the time interval from zero time to the point where the measured density was equal to $(\rho_s + 3\rho_2)/4$. Here ρ_s is the extrapolated shock density and ρ_2 is the observed C-J density.

difference is due to the different definitions of the reaction length used in the two techniques. In the side relief technique the reaction length is defined by the C-J plane location at which chemical equilibrium is supposedly established. In the laser schlieren pictures, the reaction length indicates the region where most of the chemical reactions have taken place. Despite the different definitions, both techniques agree qualitatively on the effect of H_2 concentration on detonation waves in H_2-CO-O_2 mixtures.

If all laser schlieren data on reaction length are plotted against the hydrogen concentration in the mixture as shown in Fig. 30, a linear log-log relationship is obtained. This relationship can be expressed simply as

$$\bar{X} \cdot \left[\frac{P_{H_2}}{P_{H_2\text{-}CO\text{-}O_2}} \right]^{.9} = .332 \qquad (4.2)$$

where $\bar{X}$ is the reaction length in mm and $(P_{H_2}/P_{H_2\text{-}CO\text{-}O_2})$ is the partial pressure of hydrogen in the mixture. This empirical expression fits most data well until the hydrogen concentration in the mixture exceed 50%. The fact that the reaction length is a function of hydrogen concentration in the mixture, suggests that the existence of hydrogen chain carriers is essential to the detonation of H_2-CO-O_2 mixtures. It is interesting to note that Kistiakowsky and Kydd also

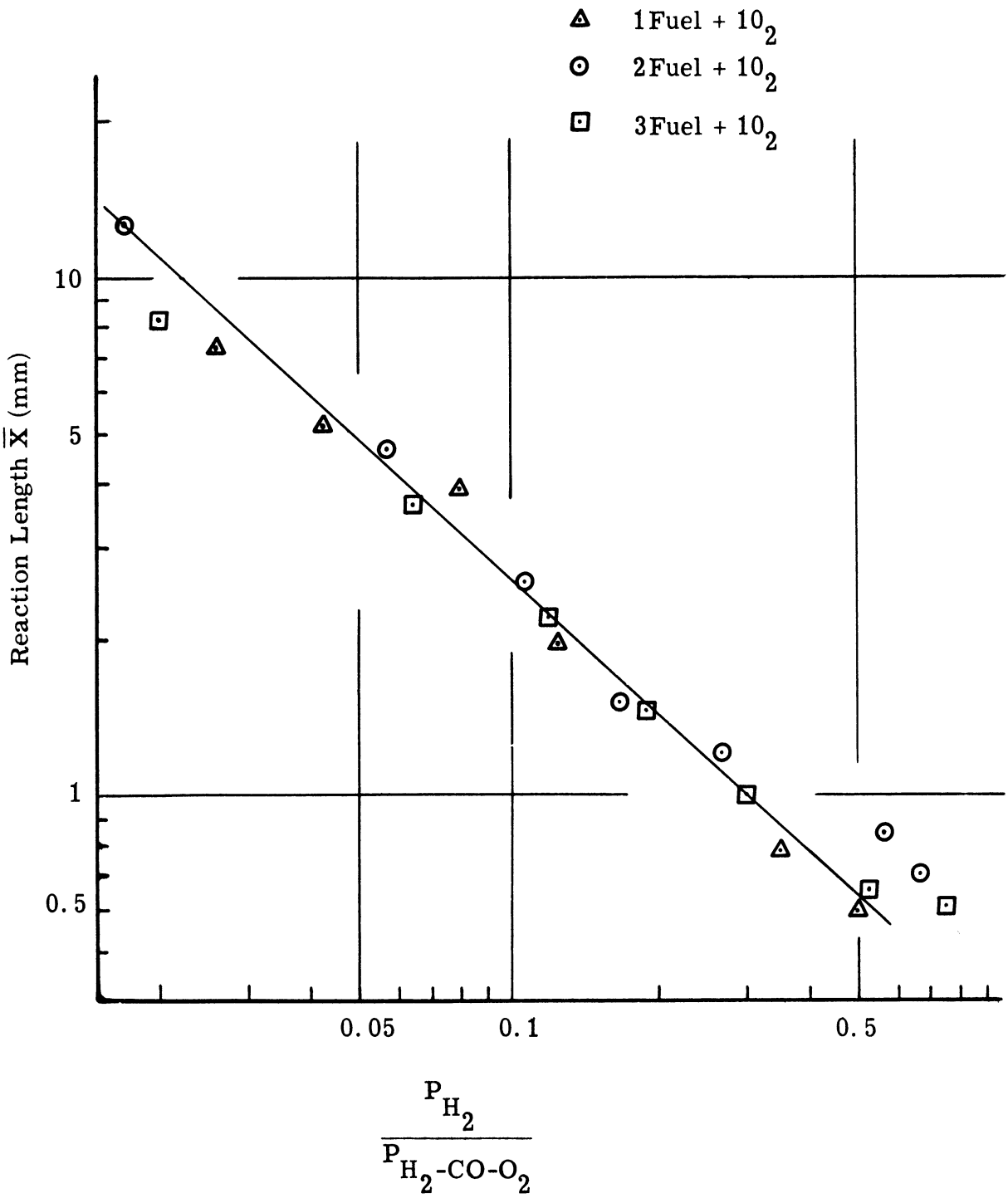

Fig. 30. Effect of Hydrogen Concentration on Reaction Lengths.

proposed an expression to describe the effect of hydrogen on the reaction time. They suggested that the inverse of the reaction time is proportional to the square root of the ratio of H_2 and CO partial pressures. The laser schlieren data was transformed into reaction time to check this expression and it was found that the experimental data did not fit this relation satisfactorily.

Since there is some doubt concerning the sensitivity of the laser schlieren system and the criterion used to define the reaction length from the schlieren pictures, it was decided to compare the stoichiometric hydrogen and oxygen mixture data with the data obtained by other investigators who used different measuring techniques, and different initial pressures. The comparison is shown in Fig. 31. The low pressure data can be extrapolated to higher pressure linearly on a log-log scale due to the overall second order reaction of hydrogen and oxygen. The data by Opel, Kistiakowsky and Kydd, and Just were compiled by Fay[45]. Jost, Just, and Wagner's[46] data are derived by multiplying their reaction time data by the corresponding wave speeds. The laser schlieren data fit into the range of data very well. This adds more confidence to the data described before.

4.1.4 Reaction Zone in Various Channel Sizes.

The effect of channel size on various detonation properties, such as the composition limit and heterogeneities in the wave front, were

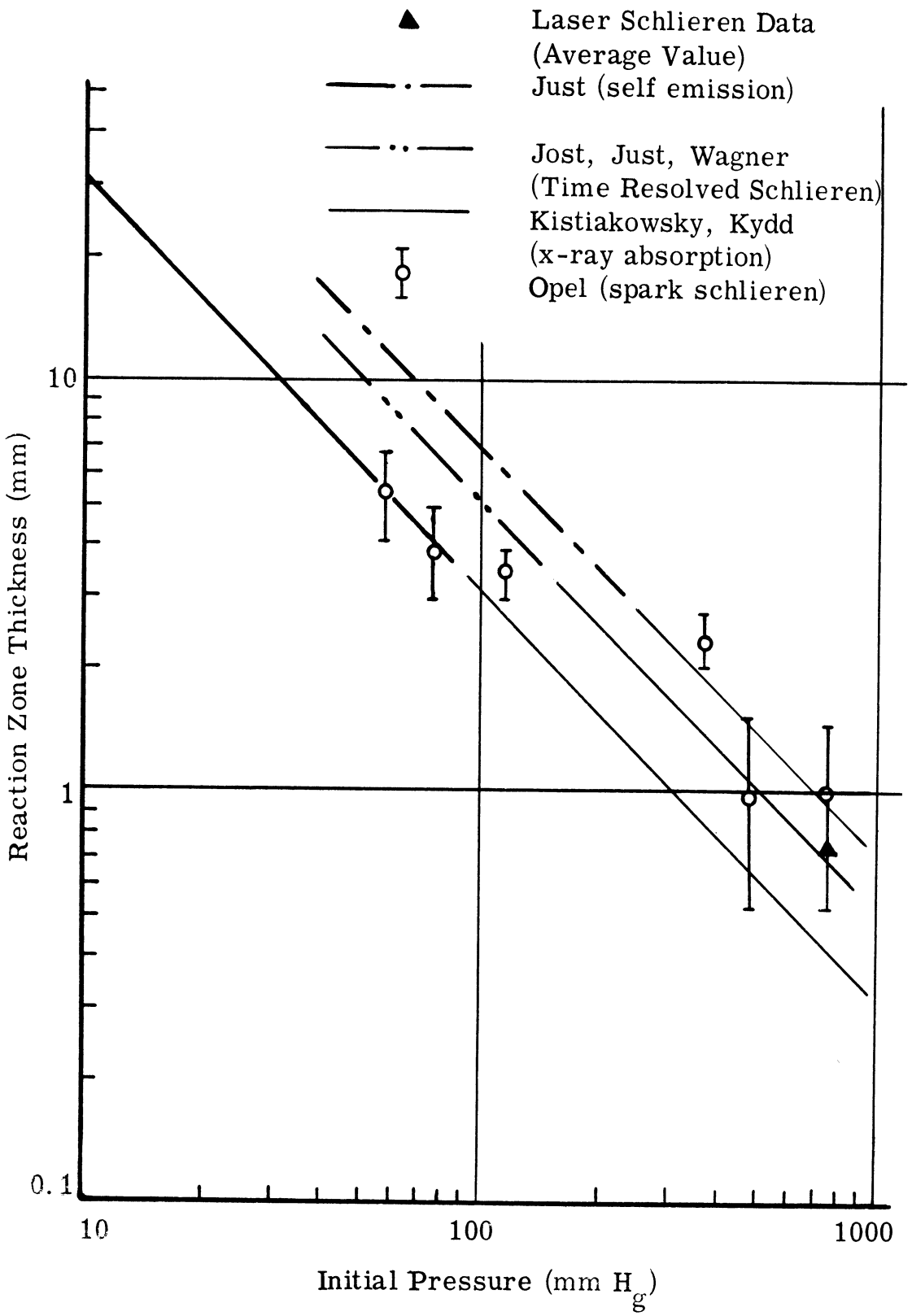

Fig. 31. Reaction Zone Thickness of Detonation Waves in Stoichiometric H_2-O_2 Mixture as a Function of Initial Pressure.

observed by various investigators. Pusch and Wagner[47] reported that the detonability composition limit widened in larger tubes. Voitsekhovsky et al[6] reported that the average size of the heterogeneities in the wave front, as manifested by their photographic technique, increased as the channel size decreased. These two parameters are related to the chemical reactions and so is the reaction length. Because of the success of the pulsed laser schlieren technique in measuring the variation of reaction length with H_2 concentration in H_2-CO-O_2 detonation, a brief experiment was made to see if it could detect the effect of channel size.

The mixture used was 10.7% H_2 + 56% CO + 33.3% O_2. This mixture was chosen because of its relatively thick reaction length and large transverse wave spacing which was comparable to the smallest practical channel width, 0.15 in., in the test section. The channel width was adjusted by means of the wedge piece and spacer arrangement described in Section III. Three channel widths were used, 0.5 in., 0.3 in., and 0.15 in. Typical photographs are shown in Fig. 32.

The reaction length and spacing does not change much when the channel width decreases from 0.5 in. to 0.3 in. When the channel width was reduced to 0.15 in., (a comparable dimension to the transverse wave spacing of about 0.2 in.) the reaction zone length increases by a factor of about 3. It is tempting to suggest that the reaction

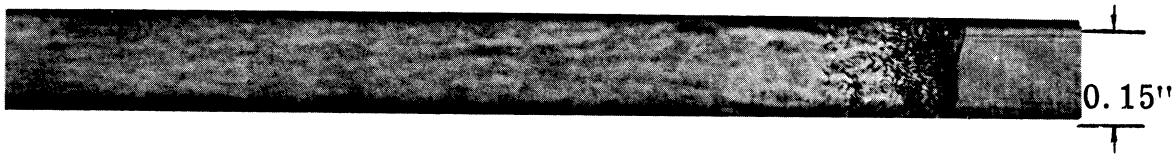

Run 1354

Run 1349

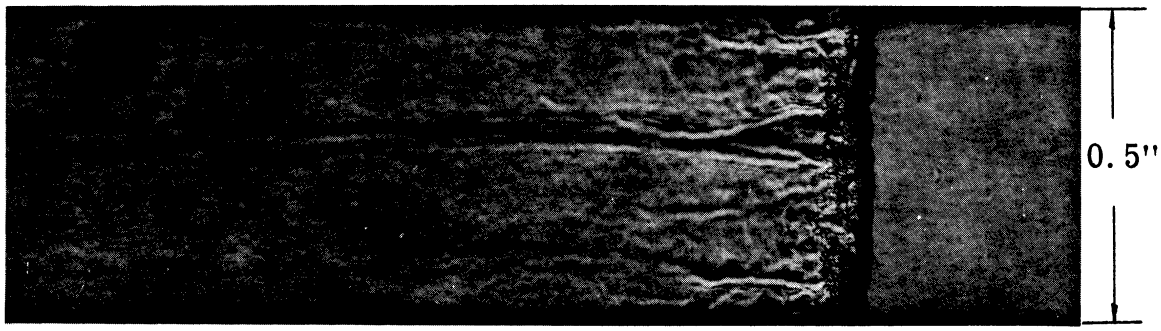

Run 1346

Fig. 32. Laser Schlieren Photographs of Detonation Waves in Various Channel Sizes.

Mixture: 10.7% H_2 + 56% CO + 33.3% O_2

length of a detonation will be increased when the channel dimension is reduced to a size comparable to the average transverse wave spacing in the wave front. This phenomenon may be caused by the lower wave propagation speed due to the relative growth of losses on the wall, which lowers the shocked gas temperature and thus slows down the chemical reaction rates and thickens the reaction zone.

4.1.5 Soot Track Results

The typical soot track records of mixtures with various CO contents are shown in Fig. 33, which was made by using the soot covered glass as a photographic negative. The imprints of the cell structures are not uniform and of poor quality. This is due to the high initial pressure and un-diluted mixtures used, as reported by other investigators[42], [48]. Due to the irregularity of the cell shape, the cell sizes were not measured. However, in general the cell size increases as the CO content increases.

The dominant role of hydrogen concentration in controlling the reaction length, as indicated by the laser schlieren data, is also indicated by the soot track record shown in Fig. 34. In this figure, although the cells are irregular, they do show that the cell sizes are larger in the lean hydrogen concentration mixtures.

Soot track records were taken of the detonation with side relief also and are shown in Fig. 35. Two records were taken simultaneously

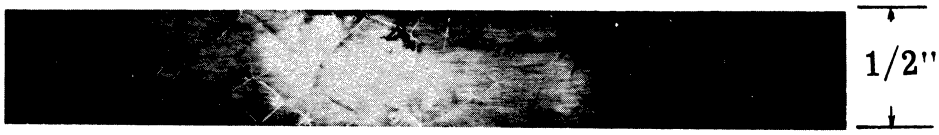

Run 1090 5.7% H_2 + 61% CO + 33.3% O_2

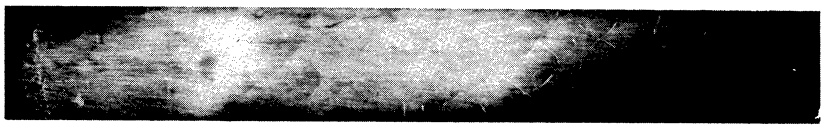

Run 1078 10.7% H_2 + 56% CO + 33.3% O_2

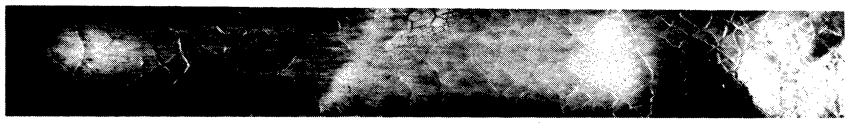

Run 1063 16.7% H_2 + 50% CO + 33.3% O_2

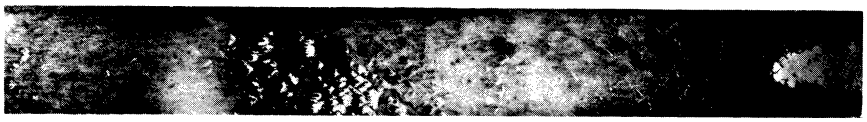

Run 1062 26.7% H_2 + 40% CO + 33.3% O_2

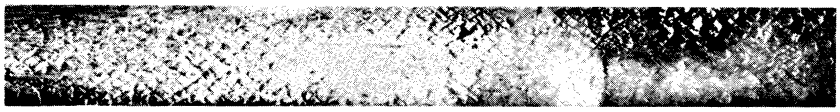

Run 1052 56.7% H_2 + 10% CO + 33.3% O_2

Fig. 33. Soot Track Records of Stoichiometric H_2-CO-O_2 Mixtures.

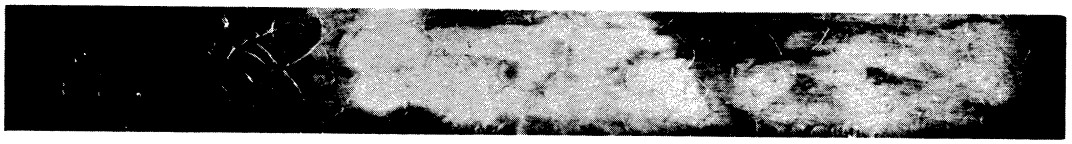

Run 1294 12.5% H_2 + 37.5% CO + 50% O_2

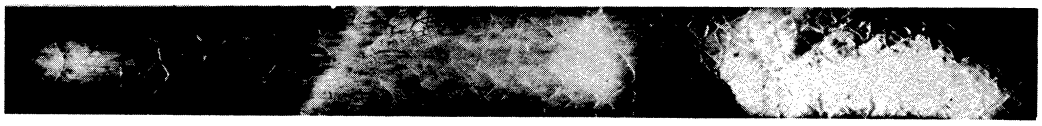

Run 1063 16.7% H_2 + 50% CO + 33.3% O_2

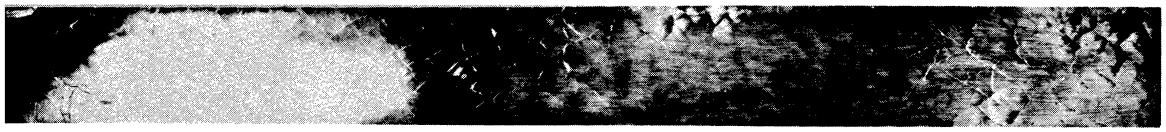

Run 1214 18.8% H_2 + 56.2% CO + 25% O_2

Fig. 34. Soot Track Records of Detonation in H_2-CO-O_2 Mixtures with constant CO – Fuel Ratio.

during each run. One soot coated mylar was attached to the window glass, and the other one was attached to the solid wall side which was opposite to the thin film separating the boundary gas from the explosive gas. The records show clearly the three dimensional effect of the movement of the wave front as indicated by the continuous cell structure at the junction of the two surfaces. The channel width and boundary gas (nitrogen) were kept the same in all cases. The H_2 concentration varied in the three cases. In Fig. 35a, the CO content in the mixture is so low that the effect of side relief is small; the detonation is not quenched and its propagation speed decreases only slightly, about 2.5%. The soot track record shows the effect of side relief well. The cells lose their clear definition after feeling the effect of side relief. It implies that the triple point configuration in the wave front is strongly disturbed by the crossflow due to the side relief as shown by the soot traces. After a short distance the detonation regains a steady speed and the cells appear clearly again with a slightly larger size. In Fig. 35b and 35c, the CO content in the mixture is too rich for the boundary gas, nitrogen, to confine the detonation which is quenched. The diamond shape cells deform and become larger when the detonation reaches the film location. The side relief effect is gradually propagated across the channel as indicated by the gradual deformation of cells. After the side relief effect is felt across the whole channel

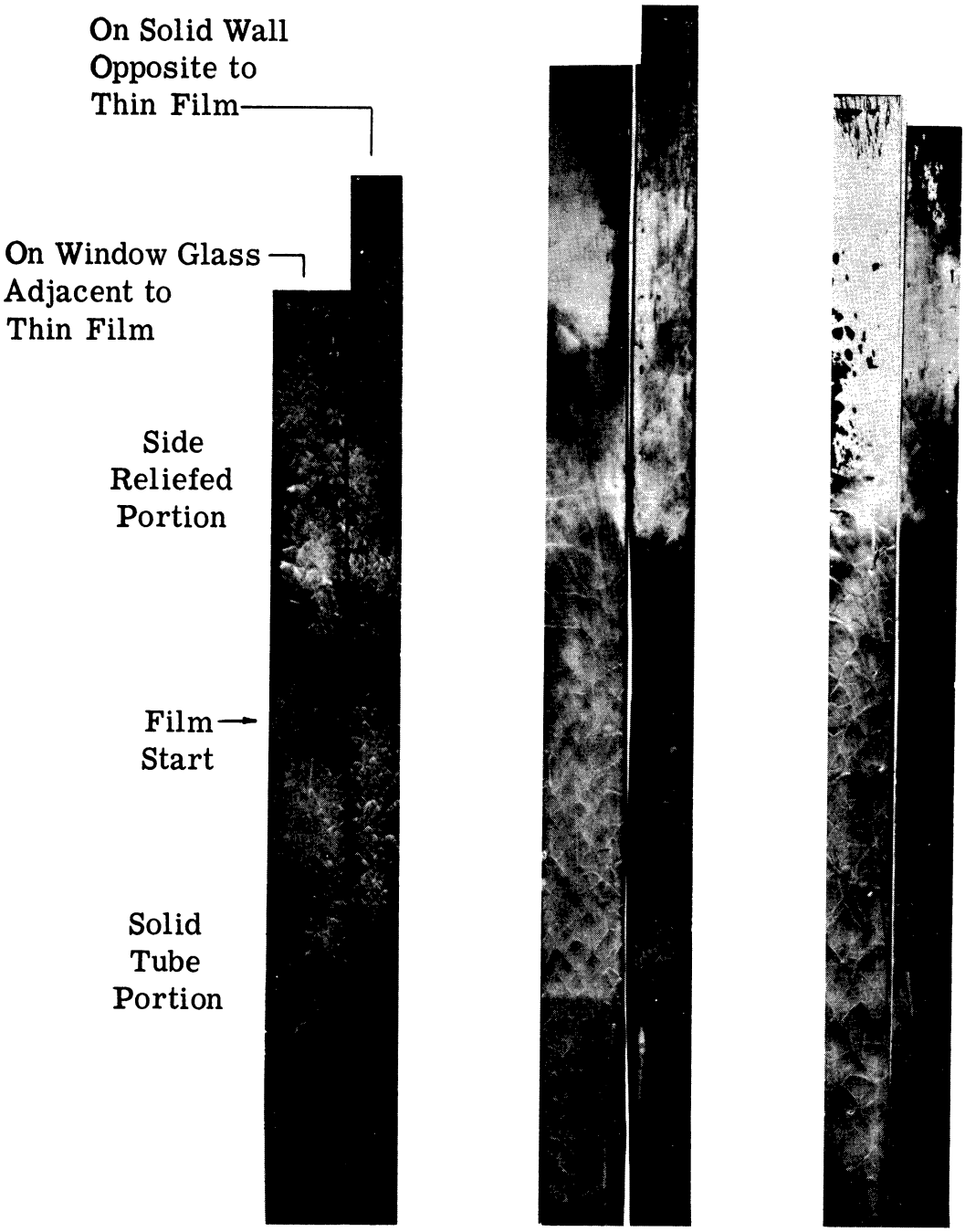

	a	b	c
Run	220	237	244
Mixture H_2%	51.6	21.7	13.4
CO%	15	45	53.3
O_2%	33.3	33.3	33.3

Fig. 35. Soot Track Records of Detonation with Side Relief. (Nitrogen Boundary Gas, 1/2" Channel Width)

width, most cells disappear, and only two "tracks" are shown. This implies that the detonation is a "two-headed" spinning one. Finally, the two tracks disappear also; this indicates that the detonation quenches completely. From these records, it is clear that the quenching process of a detonation wave, unlike the abrupt onset of a detonation shown by Urtiew and Oppenheim[42], is a gradual process. Furthermore, these results indicate that the appearance of cell structure is a necessary part of the existence of a detonation as was also shown in Ref. 42.

4.2 EXPERIMENTAL CRITICAL MACH NUMBERS AND KINETIC SCHEMES IN H_2-CO-O_2 MIXTURES

In order to determine the best of the three proposed chemical schemes describing the reaction in H_2-CO-O_2 mixtures on the basis of Belles' quenching criteria, it is necessary to find the experimental critical Mach number, i.e. that Mach number of propagation below which the detonation quenches. The experimental critical Mach number is found by subtracting from the experimental C-J Mach number the "critical" Mach number decrement (converted from the experimental "critical" velocity decrement). The critical velocity decrement refers to the maximum velocity decrement allowable by side relief before the detonation is quenched. The theoretical C-J Mach number was computed (Appendix II) using the computer program of Zeleznik and Gordon[49]. All of the theoretical and experimental results and

derived quantities therefrom are shown in Table IV. The critical Mach numbers are plotted against CO concentration in the fuel in Fig. 36. The same figure also includes the theoretical critical Mach numbers computed from Eq. (2.6), (2.7), and (2.8). The experimental results indicates rather clearly that the Lewis-vonElbe chemical scheme can be ruled out but it is not so obvious as to the proper choice between the Minkoff-Tipper and Buckler-Norrish model. This requires further consideration and discussion.

There is always the question of the effect of the choice of the kinetic rate constants on the results. In expressions (2.6), (2.7), and (2.8), with the exception of the term $2k_2/k_6[M] = 1$ which is the explosion limit of hydrogen-oxygen mixtures, the terms on the right hand side are due to the carbon monoxide reactions. The effect of these terms on the M_c curve can be seen best by comparing it with that calculated based on $2k_2/k_6[M] = 1$ (in which CO is treated as an inert gas) as shown in Fig. 36. It is clear in Fig. 36 that the CO reaction terms turn the M_c curve upward; and the larger the CO effect the earlier the upward turn starts. In expressions (2.6), (2.7), and (2.8), the only rate constants which are not common are k_{20}, k_7, and $k_{6''}$. Their values should be examined more closely. There is a wide variation in k_7 values obtained by various investigators as compiled by Bahn[50]. The value varies

Table IV. Summary of the Experimental Results Obtained from Side Relieved Stoichiometric H_2-CO-O_2 Mixtures Very Close to Quenched Conditions.

1	2	3	4	5	6	7	8	9	10
CO	u_{eth}	$\bar{u}_{eion}$	$\frac{\Delta u_{eion}}{u_{eth}}$	$\frac{\Delta u_e}{u_e}$	$\frac{\overline{\Delta u}_e}{u_e}$	M_{eth}	M_{eion}	$\overline{M}_{ec}$	Range M_{ec}
Percent	m/sec	m/sec	Percent	Percent	Percent				
0	2839	2750	3.13	5.62-12.6	7.9	5.26	5.095	4.67	4.82 -4.43
10	2550	2510	1.57	7.38-10.9	8.78	5.26	5.177	4.716	4.789-4.60
33.3	2139	2085	2.44	2.41- 8.49	5.18	5.22	5.133	4.81	4.967-4.70
50	1935	1870	3.36	3.34- 5.47	4.37	5.2	5.03	4.798	4.85--4.74

1. CO concentration in the mixture. Note $(x_{H_2} + y_{CO})/z_{mixture} = 66.7\%$.
2. Theoretical wave propagation speed taken from Appendix II.
3. Average velocity obtained from ionization probes measurements.
4. $(u_{eth} - \bar{u}_{eion})/u_{eth}$.
5. Range of measured velocity decrements for wave with side relief obtained from streak pictures.
6. Average value of 5.
7. Theoretical Mach number taken from Appendix II.
8. $= M_{eth}\,[1 - (\overline{\Delta u}_{eion}/u_{eth})]$.
9. $= M_{eion}\,[1 - (\overline{\Delta u}_e/u_e)]$.
10. $= M_{eion}\,[1 - (\Delta u_e/u_e)]$.

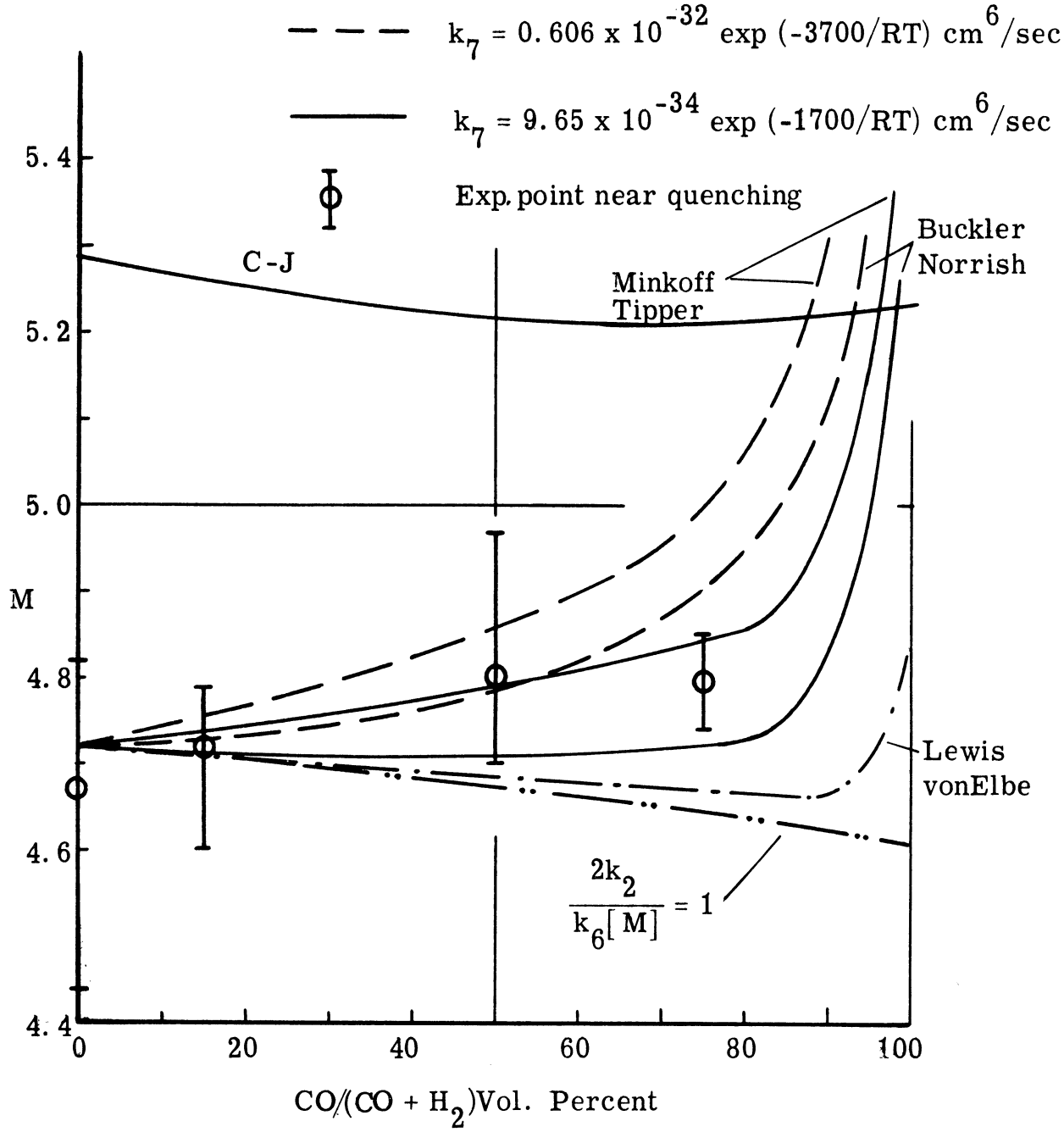

Fig. 36. Theoretical C-J and Critical Mach Numbers of Stoichiometric (H_2 + CO) + O_2 Mixtures.

from the low end of 1.73×10^{-38} cm^6/sec to the high end of 0.83×10^{-30} cm^6/sec at 2500°K. The value $k_7 = 9.65 \times 10^{-34} \exp(-1700/RT)$ cm^6/sec was chosen because it is close to the range where most of the values agree (around 0.276×10^{-32} cm^6/sec at 2500°K). The other reason for using this value is that the calculated critical Mach numbers from expressions (2.7) or (2.8) describe the physical phenomena better than those using larger k_7 values, such as $0.606 \times 10^{-32} \exp(-3700/RT)$ cm^6/sec[9]. In Fig. 36, the calculated critical Mach number curves of expressions (2.7) and (2.8), using $k_7 = 9.65 \times 10^{-34} \exp(-1700/RT)$ cm^6/sec, indicate that the M_c is larger than M_{C-J} when CO/fuel exceeds about 96% and 98% respectively. This implies that a self sustained detonation will not propagate in these mixtures, which agrees with the experimental fact that it is impossible to detonate a stoichiometric mixture with CO/fuel = 98.5% in the present system. On the other hand, the calculated critical Mach number curves using the larger value $k_7 = 0.606 \times 10^{-32} \exp(-3700/RT)$ cm^6/sec indicate that M_c is larger than M_{C-J} when CO/fuel exceeds about 87.5% and 93% respectively. Yet, experimentally, there is no difficulty in detonating the mixtures until CO/fuel = 98.5%. Therefore, the calculated M_c curves, using larger k_7 values, do not explain the mixture limit satisfactorily.

It is possible to argue that the M_c curve based on expression (2.6) may be adjusted to fit the data by using a suitable k_{20} value. The k_{20} values, obtained by various investigators, are very close to each other, around 0.551×10^{-33} cm^6/sec at 300^oK (the k_{20} value used herein, $1.655 \times 10^{-34} \exp(600/RT)$ cm^6/sec is 0.441×10^{-33} cm^6/sec at 300^oK). Therefore it is unlikely that the M_c curve shape will be changed appreciably due to an uncertainty in k_{20}. In other words, the Lewis and von Elbe model cannot describe the experimental data satisfactorily.

In comparing expressions (2.7) and (2.8), it is obvious that the latter has a stronger CO effect by the factor of $1 + (k_{6''}[CO]/k_6[O_2])$ in which the value of $k_{6''}/k_6$ would affect the difference strongly. Unfortunately, no other experimental values for $k_{6''}$ than the one used (18) are available at the present time, therefore the difference between Buckler and Norrish's and Minkoff and Tipper's schemes are not well resolved until more information on the $k_{6''}/k_6$ values are available. However, the experimental results favor Minkoff and Tipper's scheme if the value of $k_{6''}/k_6$ equal to 0.17 is accepted.

V. CONCLUSIONS

The influence of hydrogen concentration on the detonation of gaseous H_2-CO-O_2 mixtures was investigated experimentally. The main aspects of interest were the reaction zone thickness, the detailed structure, and the appropriate chemical kinetics. Two major, but independent, experimental techniques were employed; the side relief and pulsed laser schlieren techniques. Sooted film records of the wave passage were also obtained. Some observations and conclusions based on this study are as follows.

1. The Q-switched pulsed laser schlieren system is much superior to the conventional spark systems. This is particularly true at initial pressure close to atmospheric where the conventional system cannot resolve details of the reaction zone. The development of this technique required a modification to the rotating prism laser for synchronization purposes. The arrangement eliminates the need for an expensive Kerr cell switching device.
2. The side relief technique proved useful in determining reaction zone length and some aspects of structure even when the detonation velocity was mildly pulsating. However, for a fixed maximum channel width as employed in this study, it could not be used on highly pulsating detonation waves due to the lack of a sufficiently

dense inert boundary gas to confine the detonation. Under these conditions relatively small propagation velocity decrements are possible before quenching occurs.

3. The reaction length of the H_2-CO-O_2 detonation waves was measured by using both the side relief and pulsed laser techniques. The results (from both techniques) show that the reaction length increases slowly at first as CO replaces the H_2 in H_2-O_2 mixtures. The laser schlieren data shows that the reaction length increases sharply, as hydrogen is further replaced by CO, when the CO concentration in the fuel exceeds 75%. Kistiakowsky and Kydd's low pressure data has a similar trend. It is found that the reaction length is related directly to the hydrogen concentration in the mixture. An empirical expression is found to describe this relationship.

4. The laser schlieren photographs indicate that the wave front becomes nonplanar as H_2 is replaced by CO in H_2-O_2 mixtures. The wave tilt is very appreciable at high CO contents. The spacing between the transverse waves behind the wave front becomes larger as the CO concentration increases. Based on the laser schlieren pictures, it is suggested that weak shocks, produced from secondary explosions behind the main front, are the propagating mechanism for the trailing portion of the transverse waves.

5. Investigation of the soot track records reveals that the hydrogen concentration in the mixture has the same effect on the cell size as on the reaction zone thickness. In hydrogen rich mixtures, the cell size is smaller.

6. It is demonstrated that the reaction zone thickness is affected by the channel size. It becomes thicker in a small channel. When the channel size is reduced to a size comparable to the spacing of the transverse waves, it thickens drastically.

7. The chemical kinetics of the H_2-CO-O_2 system was investigated by studying the quenching of detonations by the side relief technique with interpretation by Belles' explosion limit criterion. The experimental results rule out the kinetic scheme proposed by Lewis and von Elbe which involves the formation of ozone. The results show slightly better agreement with the scheme proposed by Minkoff and Tipper than with that proposed by Buckler and Norrish, although this cannot be justified as a firm conclusion However, since Minkoff and Tipper's scheme hypothesizes the formation of an HCO radical, the scheme could be checked spectrographically to see whether this radical exists.

Appendix I

SUB-CHAPMAN-JOUGUET WAVE

When Dabora[19] studied the interaction process between a gaseous detonation wave and an inert confining gas, he noticed that the detonation, bounded by an inert gas with a higher sound speed than the explosive, could propagate at velocities much lower than the Chapman-Jouguet velocity. Voitsekhovsky[6] also reported that he was able to maintain a gaseous detonation which travelled at half the C-J velocity in an annular channel. These experiments indicated the possibility of a new mode of detonation wave which has a velocity much less than the classical C-J velocity and which is highly dependent on three dimensional effects.

Some limited efforts were made to investigate this phenomenon. The prime objective was to find out whether the sub-C-J wave observed by Dabora was steady and, if so, what were the details of the propagation mechanism. Several runs were made in the test section described in Section 3.1.2 as well as in a new test section. The new test section had the same construction as the other one except it was longer and used a 10-1/4 in. long separation film. The explosive mixture used 75% H_2 and 25% O_2 by volume and the boundary gases were hydrogen and helium. The explosive channel width was 0.1 and

0.2 in. Streak schlieren photographs were taken with the same setup as described in Section 3.1.3. A typical composite streak schlieren streak picture is shown in Fig. I.1. In the picture, the faint waves ahead of the event are the stress waves in the test section window glass. The transverse wave appearing at the lower portion of the side relieved part is the very steep refracted oblique shock from the boundary gas. The wave speeds measured from the streak pictures were 60-70% of the C-J velocity with hydrogen boundary gas and 50-60% of the C-J velocity with helium boundary gas. These speeds were apparently steady.

Several spark schlieren pictures of the wave were taken at different locations in the test section to obtain the wave structure. Two typical pictures are shown in Fig. I.2; their corresponding locations on the streak picture (Fig. I.1) are indicated by a and b. The wave consisted of a bow shock in the boundary gas side, and a steep oblique shock reflected at the solid wall at the explosive side. Due to the poor quality of the spark schlieren picture, it was not possible to tell whether a reaction zone existed. The angles between the oblique shock and the solid wall were measured and found to vary between 35^{o} to 40^{o} from run to run with hydrogen boundary gas. The temperatures behind the reflected oblique shock waves were calculated based on the propagation wave speed, 60-70% of C-J speed, and the oblique shock angles. In some combinations of the wave speeds and oblique shock angles, the calculated

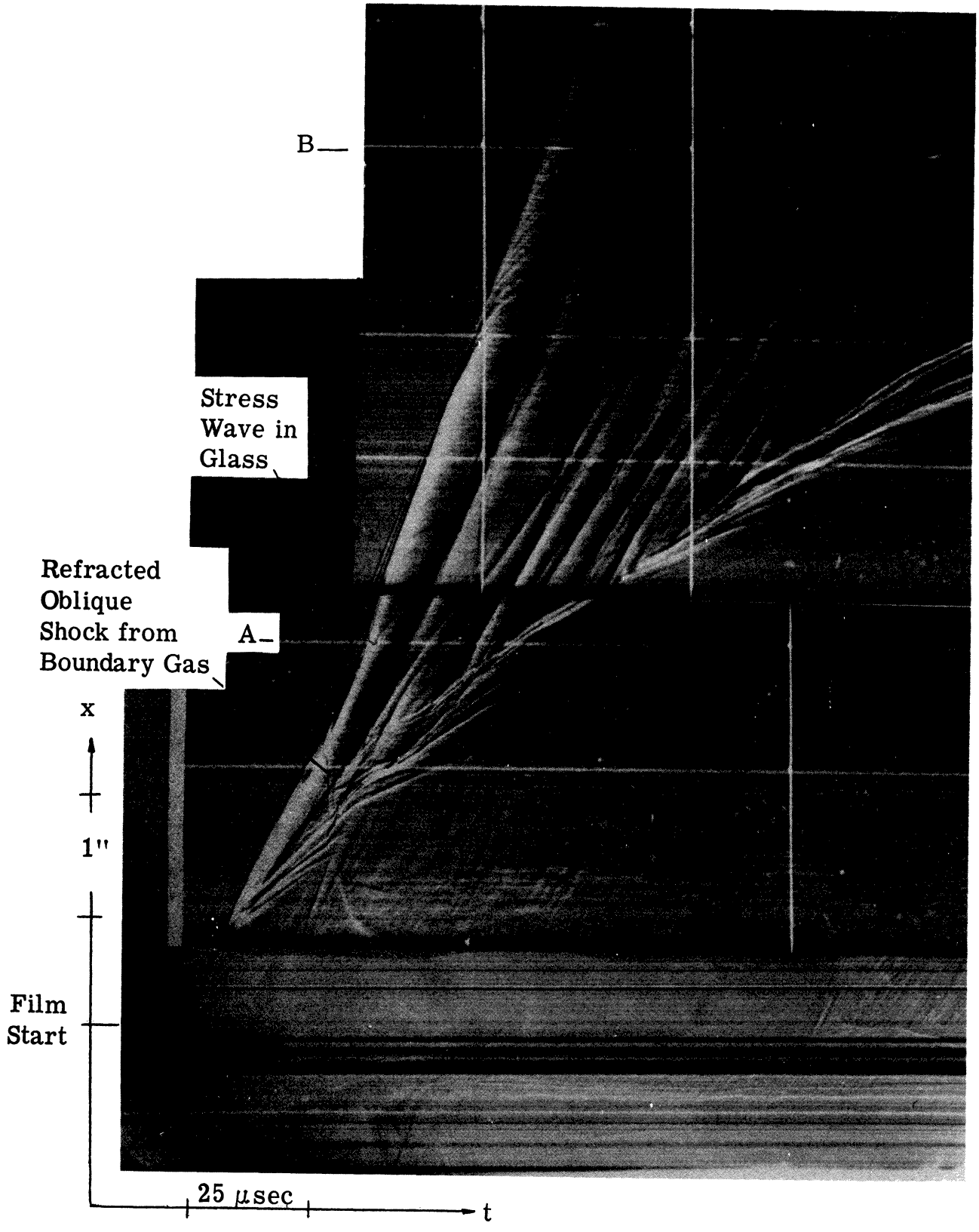

Fig. I.1. Composite Streak Schlieren Picture of Sub-C-J Wave.

Mixture: 75% H_2 + 25% O_2
Boundary Gas: Hydrogen
Channel Width: 0.2"

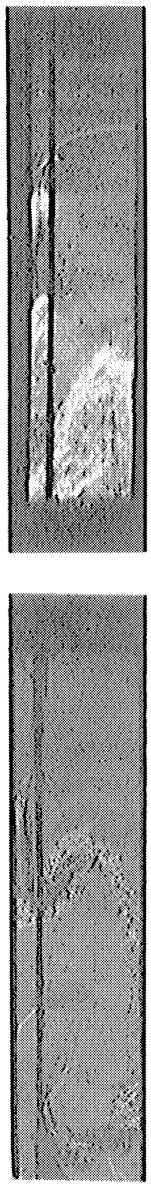

Fig. I.2. Spark Schlieren Photographs of Sub-C-J Wave.

Mixture: 75% H_2 + 25% O_2
Boundary Gas: Hydrogen
Channel Width: 0.2"

temperature behind the reflected shock was lower than the ignition temperature (1600 R^{o}) of the 75% H_2 + 25% O_2 mixture quoted by Jost[51] This raised the question as to whether the observed sub-C-J wave was a true detonation wave. Two techniques were used to clarify this doubt.

One technique used was the combined shadow and luminous wave front streak photographs. A typical picture is shown in Fig. I. 3. In the picture, the luminous combustion zone slowed down drastically when the detonation initially experienced the side relief effect, but there was no indication of a luminous flame following the wave front which can be seen in the shadow portion of the photograph. From this, it might be concluded that there was probably no combustion behind the observed high speed wave. Since there was a possibility that the photographic film was not sensitive enough in the present optical system to be exposed by a very weak or dim flame behind the wave, the soot track technique was also used to check this phenomenon.

It was demonstrated in Section 4. 1. 5, that a quenched detonation loses the diamond shape cell structure imprints on the sooty wall. Urtiew and Oppenheim[42] showed that the cell structure appears immediately at the onset of a detonation. Although a non-reactive Mach stem would imprint a similar soot track structure as demonstrated by Duff[39], the absence of a soot track structure would be

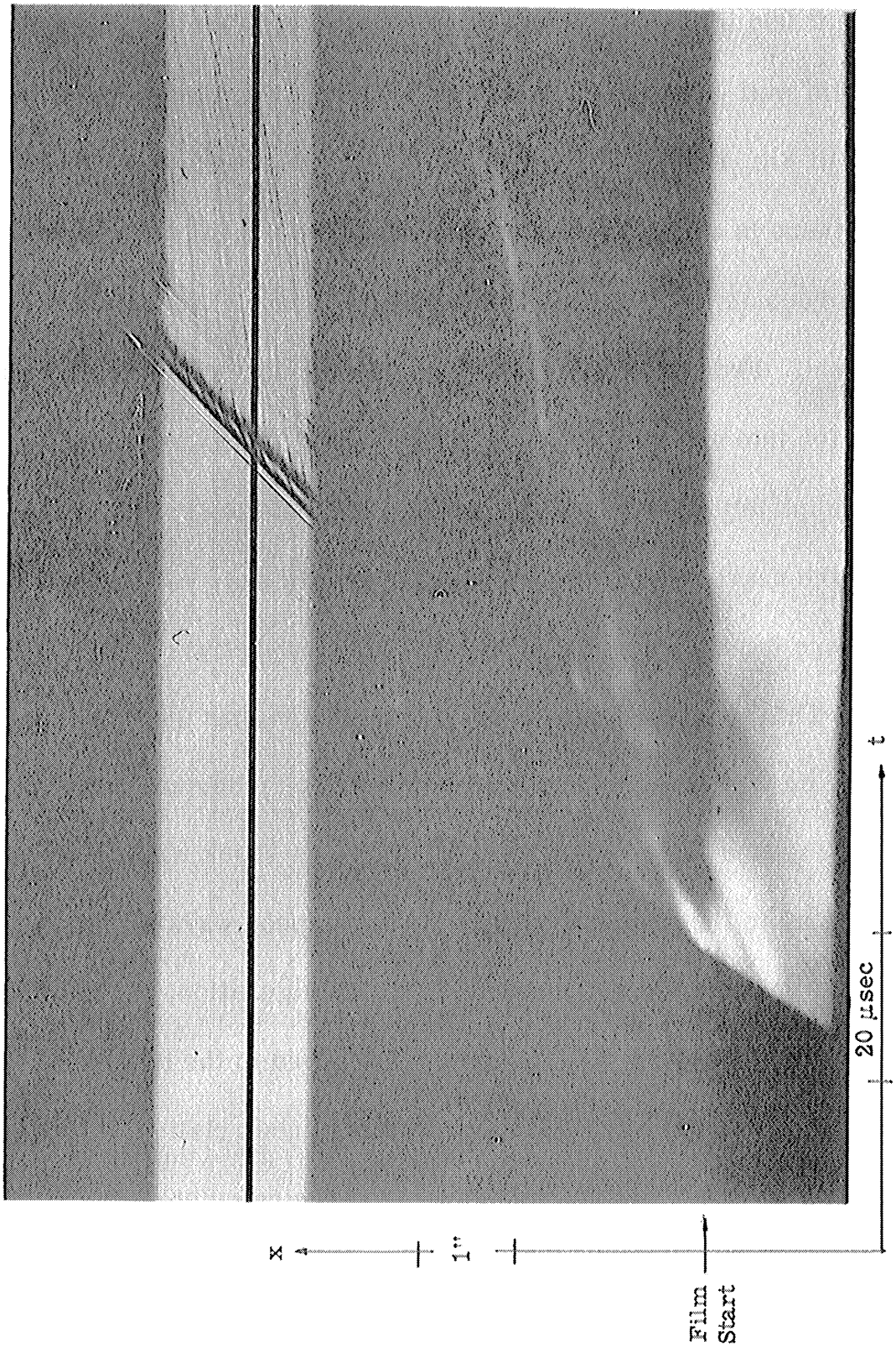

Fig. I.3. Combined Streak Self-Luminous and Shadowgraph Photograph of Sub-C-J Wave.

Mixture: 75% H_2 + 25% O_2 ; Boundary Gas: Hydrogen ; Channel Width: 0.1"

a definite indication of a non-detonation wave. A piece of mylar of thickness 0.006 in. and covered with a thin layer of soot was installed on the solid wall opposite the relief side. A typical soot track record is shown in Fig. I.4. In the solid tube portion, upstream of the film portion, there is a small cell structure which is typical of detonations. The cells become larger as the detonation wave experiences the film relief effect. From the shape of the soot track, the detonation actually deteriorates into a spinning one in this portion. Then the cells disappear completely as soon as the oblique shock in the explosive, induced by the nearly normal shock in the boundary gas, reaches the wall. There is no recognizable cell structure downstream of this location. This is taken to mean that the detonation has quenched.

Based on the observation with the above two techniques, it is suggested that the observed high speed wave is a shock wave. A question arises as to the possibility of such a high speed wave in the boundary gas. Due to the complicated flow configuration, it is not possible to calculate accurately the shock wave speed in the boundary gas. However, by using the detonation driven shock tube relation derived by Morrison[32], an estimate can be made. The calculated shock Mach number in a constant area shock tube with 75% H_2-25% O_2 mixture as driver gas and hydrogen as driven gas is 2.75. Since the explosive channel is smaller than the boundary gas channel, and the

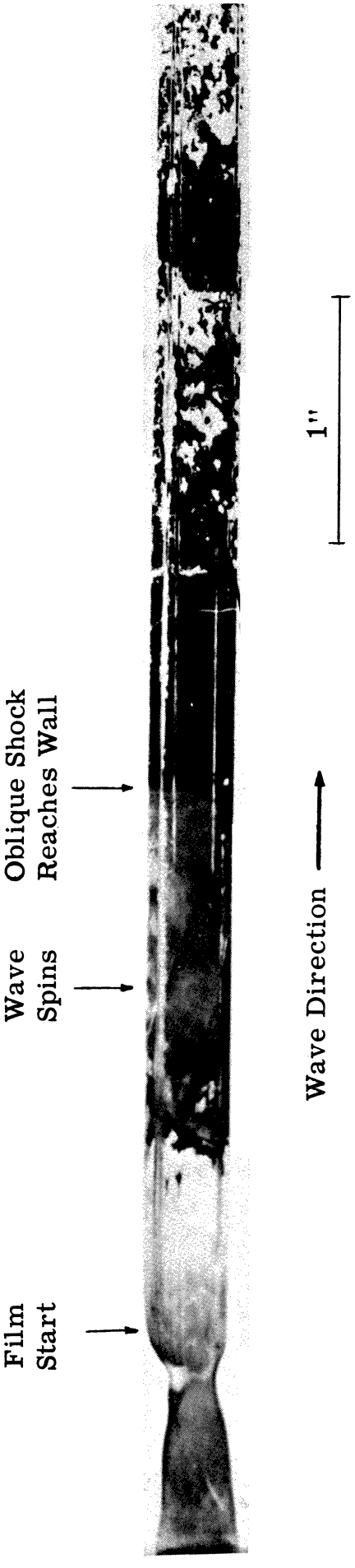

Fig. I. 4. Soot Track Record of Sub-C-J Wave

Mixture: 75% H_2 + 25% O_2
Boundary Gas: Hydrogen
Channel Width: 0.2"

shock wave is not induced normally to the channel axis, it is possible to say that the shock wave should move at a lower Mach number than 2.75. Now, the nearly normal shock velocity in the boundary gas (hydrogen) is about 6000-7000 ft/sec, estimated from the measured sub-C-J wave speed by assuming no change in wave configuration. The corresponding Mach number is 1.4-1.63, which is smaller than 2.75. Therefore, it seems reasonable that a weak shock wave, though its speed is high, can be propagated in the boundary gas and that the attenuation rate may be too low to be detected in the limited length of the test section.

Although the findings from these limited experiments with the detecting techniques used were negative, the possibility of the sub-C-J detonation wave should not be ruled out. It is suggested that this phenomenon be investigated further by manipulating the density ratio between the boundary gas and the explosive so that a larger refraction angle may be obtained and hence form a Mach stem at the reflecting wall. This would provide a high local temperature which might sustain a detonation. It would also be well to investigate other diagnostic techniques for detecting combustion.

Appendix II

THEORETICAL DETONATION PROPAGATION VELOCITIES AND MACH NUMBERS IN H_2-CO-O_2 MIXTURES

The computer program developed by Zeleznik and Gordon[49] has been used to compute the various detonation parameters of H_2-CO-O_2 mixtures. The results show that the detonation Mach number remains nearly the same at a fixed volumetric fuel oxygen ratio regardless of the ratio between CO and H_2, shown in Fig. II-1 and II-2. The results of wave propagation speed of various CO concentrations in fuel are shown in as Fig. II-3.

The comparison of theoretical and experimental wave propagation speeds in 1fuel + $1O_2$, 2fuel + $1O_2$, and 3fuel + $1O_2$ mixtures are as shown in Fig. II-4. Dixon's experimental wave propagation speed is also plotted in Fig. II-4. In general, the experimental wave propagation speed is about 2% lower than the theoretical wave speed.

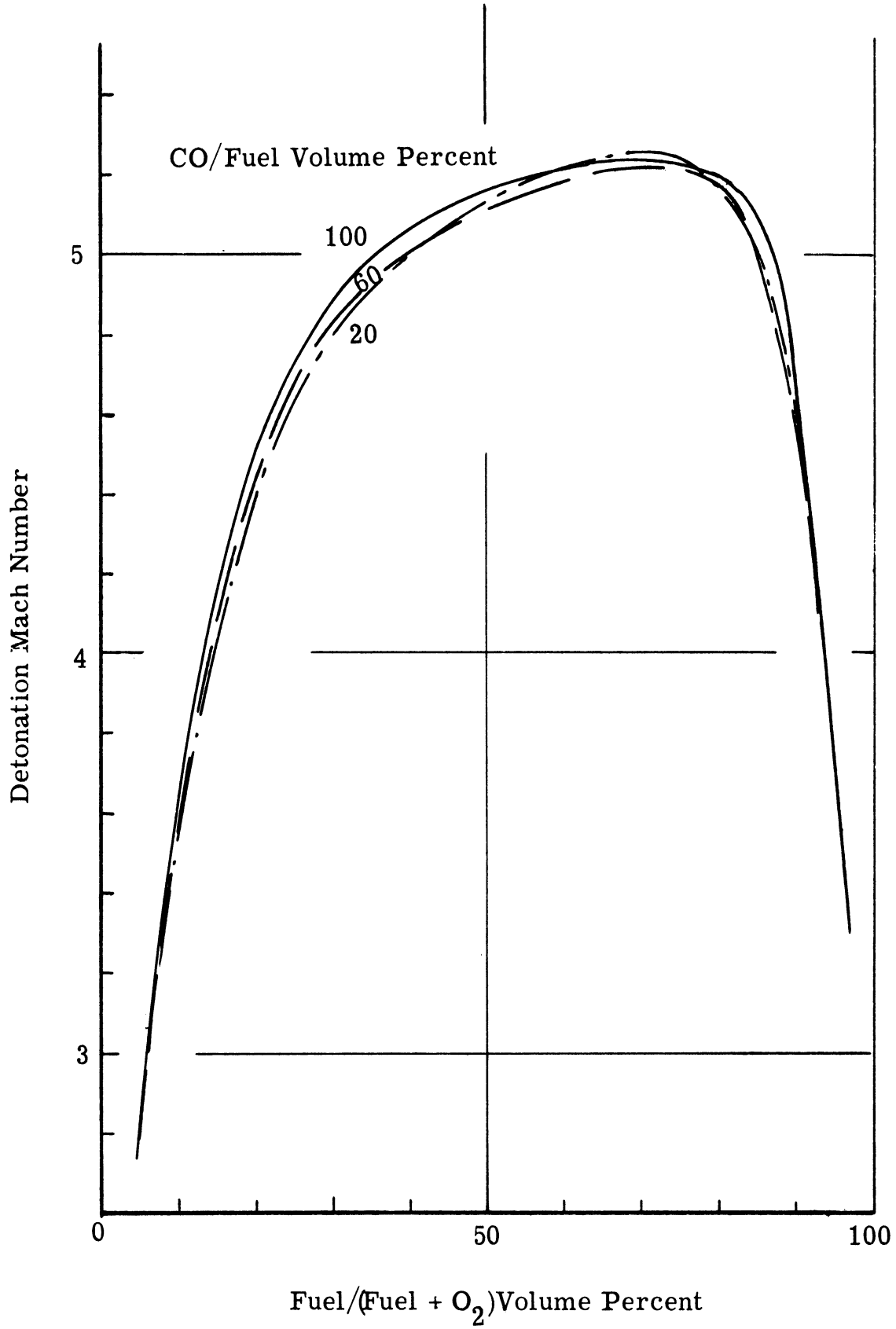

Fig. II. 1. Theoretical Detonation Mach Number in H_2-CO-O_2 Mixtures at One Atmosphere and 298°K.

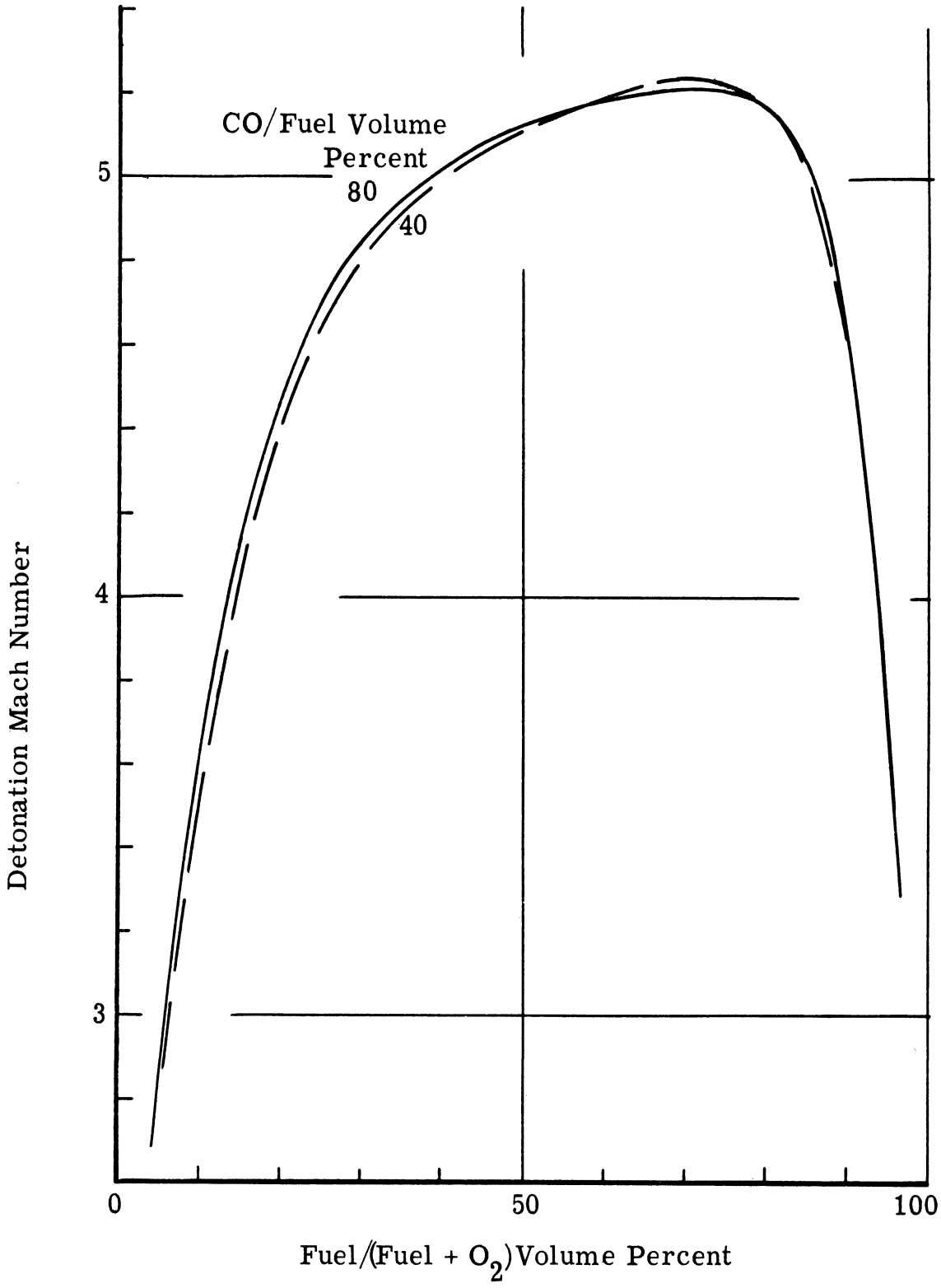

Fig. II. 2. Theoretical Detonation Mach Number in H_2-CO-O_2 Mixtures at One Atmosphere and 298°K.

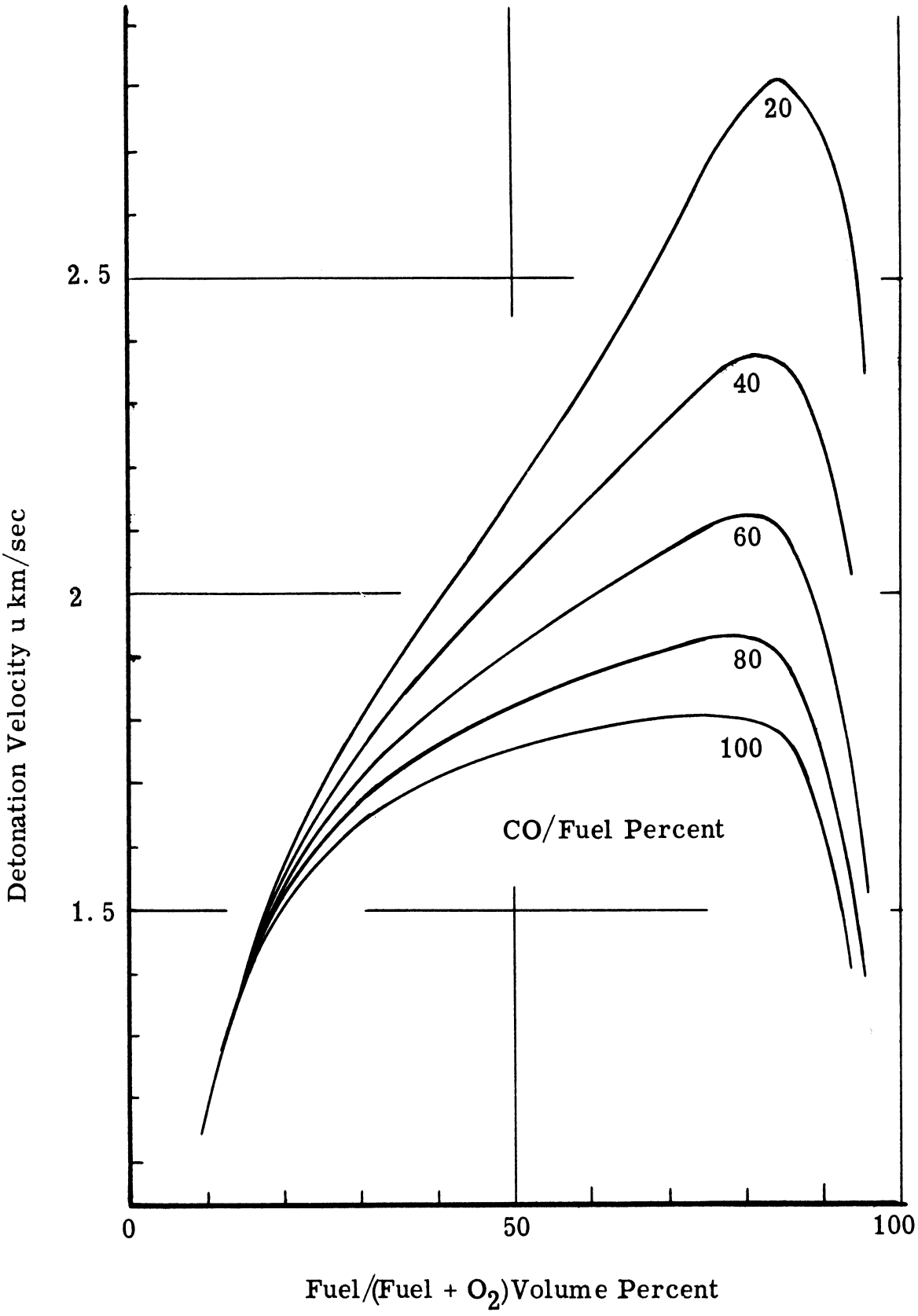

Fig. II. 3. Theoretical Detonation Velocity in H_2-CO-O_2 Mixtures at One Atmosphere and 298°K.

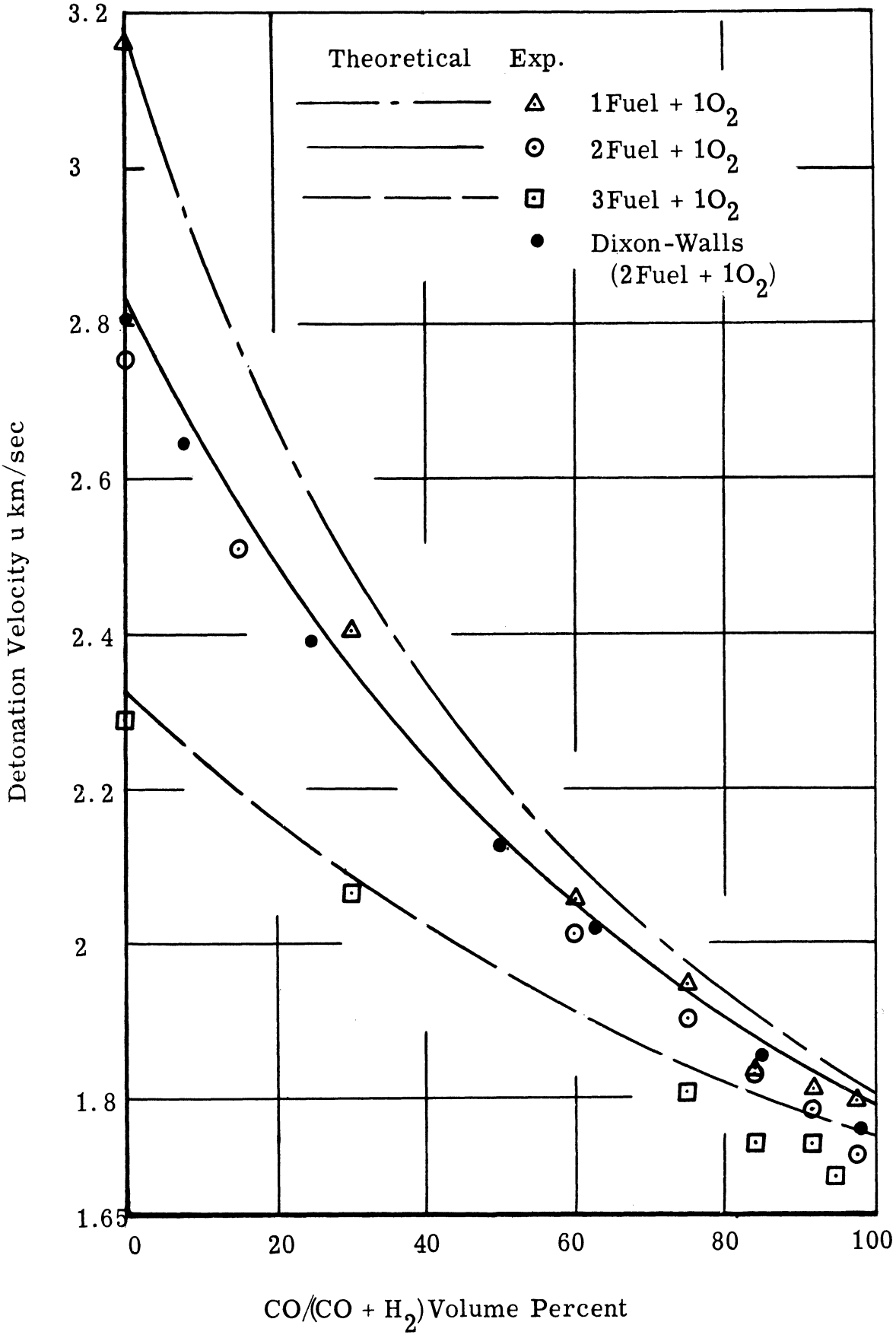

Fig. II. 4. Theoretical and Experimental Detonation Velocity in H_2-CO-O_2 Mixtures at One Atmosphere and 298°K.

Appendix III

PRINCIPLE AND SENSITIVITY OF THE LASER SCHLIEREN SYSTEM

The system uses the optical activity property of crystal quartz to rotate the plane of polarization of a light beam travelling along its optical axis. The angle of rotation depends on the optical thickness of the quartz and the wave length of the light beam. Since the laser light is usually linearly polarized, the light rays, which are deflected by the refractive index gradient in the test section and pass through a different optical thickness of the quartz prism than the undeflected light, rotate their plane of polarization differently. If a polarizer is placed behind the quartz prism, then the cut-off of the transmitted laser light follows Malus' law in optics, i.e.

$$I = I_o \cos^2 \theta$$

Thus, the deflected light intensity behind the polarizer is different from the undeflected one and produces schlieren effects.

The transmittance, for polarized light, of a polarizer is

$$I_\theta = (K_1 - K_2) \cos^2 \theta + K_2 \qquad \text{(III. 1)}$$

where K_1 and K_2 are the principal transmittance which varies with the wave length and type of polarizer, and θ is the angle between the axis of the polarizer used in this system and the polarized light plane

of polarization. The Ednalite polarizer filter, which has similar properties as the Polaroid filter HN 42, has the values $K_1 = 40\%$ and $K_2 = 2\%$ at 5300 Å.

In the schlieren system, if the polaroid filter polarization plane axis is set at 45° with respect to the polarization plane axis of the undisturbed laser light exiting from the quartz prism, then the transmission of laser light is

$$I_{\theta} = (.4 - .02) \cos^2 45^{\circ} + .02 = .21$$

A conventional minimum detectable illumination contrast of 10% at the schlieren image plane between the disturbed and undisturbed light is chosen, i.e. $I_{\theta}' \cong 0.19$. From Eq. (III.1), $\theta' = 48^{\circ}\ 5'$. The change of θ between an undisturbed and disturbed light is then $3^{\circ}\ 5'$. Since the specific rotation of the polarization plane at 5300 Å in crystal quartz is about 27°/mm, the difference of distance travelled in the quartz prism between the undisturbed and disturbed light is $3^{\circ}\ 5'/27^{\circ}/\text{mm} = .114$ mm. This is equivalent to 0.114 mm/tan 30° = 0.199 mm on the longer leg of the prism.

The parabolic mirror focal length is 48", then the minimum deflection angle of a disturbed light that can be detected in the system is 1.63×10^{-4} radians.

REFERENCES

1. Kistiakowsky, G.B., Knight, H.T., and Malin, M.E., "Non-Steady Waves in CO-O_2 Mixtures," J. of Chem. Phys., 20, No. 6, (1952), pp. 994-1000.

2. Dixon, H.B. and Walls, N.S., "On the Propagation of the Explosion Wave. Part I. Hydrogen and Carbon Monoxide Mixture," J. of Chem. Soc. London, 123, Transaction Part 1,(1923), pp. 1025-1037.

3. Campbell, C. and Woodhead, D.W., "The Ignition of Gases by an Explosion Wave. Part I. Carbon Monoxide and Hydrogen Mixtures," J. of Chem. Soc. London, Transaction,(1926), pp. 3010-3021.

4. Bone, W.A., Fraser, R.P., and Wheeler, W.H., "Photographic Investigation of Gaseous Explosions," Philosophical Transaction, 235A,(1935-1936),pp. 29-67.

5. Dove, J.E. and Wagner, H.G., "A Photographic Investigation of the Mechanism of Spinning Detonation," Eighth Symposium (International) on Combustion, William and Wilkins Co., Baltimore, (1962), pp. 589-600.

6. Voitsekhovsky, B.V., Mitrofanov, V.V., and Tropchiyan, M.Ye., The Structure of a Detonation Front in Gases, (1963). Translated Foreign Technology Div., Wright-Patterson AFB, Ohio, AD 633 821, Feb. 1966.

7. Laffitte, P.F., "Flame of High Speed Detonation," Science of Petroleum, 4,(1938), p. 2995.

8. Kistiakowsky, G.B. and Kydd, P.H., "A Study of the Reaction Zone by Gas Density Measurement," J. of Chem. Phys., 25, No. 5, (1956),pp. 824-835.

9. Myers, B.F., Sulzmann, K.G.P., and Bartle, E.R., "Oxidation of CO II.Influence of H_2 on the Induction Period Preceding Rapid CO_2 Formation in Shock Heated CO-O_2-Ar Mixture," J. of Chem. Phys., 43, No. 4,(1965),pp. 1220-1228.

10. Brokaw, R.S., Ignition Kinetics of the Carbon Monoxide-Oxygen Reaction, NASA Report TM X-52196, (1966).

11. Buckler, E.J. and Norrish, R.G.W., "A Study of Sensitized Explosions. III. The Kinetics of Ignition of Carbon-Monoxide and Oxygen Sensitized by Hydrogen," Proc. Royal Soc., A 167, (1938), pp. 318-342.

12. Thompson, H.W. and Hinshelwood, C.N., "The Mechanism of the Homogeneous Combination of Hydrogen and Oxygen," Proc. Royal Soc., A 122, (1924), pp. 610.

13. Lewis, B. and von Elbe, G., Combustion, Flames and Explosions of Gases, Academic Press Inc., Chapter III, New York (1961).

14. Hadman, G., Thompson, H.W., and Hinshelwood, C.N., "The Oxidation of Carbon-Monoxide," Proc. Royal Soc., A 137, (1932), pp. 87-101.

15. Gordon, A.S. and Knipe, R.H., "The Explosive Reaction of Carbon-Monoxide and Oxygen at the Second Explosion Limit in Quartz Vessels," J. Phys. Chem., 59, (1955), pp. 1160-1165.

16. Dickens, P.G., Dove, J.E., and Linnett, J.W., "Explosion Limits of the Dry Carbon-Monoxide + Oxygen Reaction," Trans. Faraday Soc., 60, (1964), pp. 539-552.

17. Dixon-Lewis, G. and Linnett, J.W., "The Oxidation of Mixtures of Hydrogen and Carbon-Monoxide. Part I. The Second Explosion Limits of Mixtures of Hydrogen, Carbon-Monoxide and Oxygen in a Potassium Chloride Coated Silica Vessel," Trans. Faraday Soc., 49, (1953), pp. 756-763.

18. Baldwin, R.R., Jackson, D., Walker, R.W., and Webster, S.J., "The Use of Hydrogen-Oxygen Reaction in Evaluating Velocity Constants," Tenth Symposium (International) on Combustion, The Combustion Institute, Pittsburgh, Penn., (1965), pp. 423-433.

19. Dabora, E.K., The Influence of a Compressible Boundary on the Propagation of Gaseous Detonation, Ph.D. Thesis, University of Michigan, 1963. See also paper in Tenth Symposium (International) on Combustion, The Combustion Institute, Pittsburgh, Penn., (1965), pp. 817-830.

20. Belles, F.E., "Detonability and Chemical Kinetics: Prediction of Limits of Detonability of Hydrogen," Seventh Symposium (International) on Combustion, Butterworths Scientific Publications, London,(1959), p. 745.

21. Patch, R.W., "Prediction of Composition Limits of Hydrogen-Oxygen-Diluent Mixtures," ARS J., (1961), pp. 46-51.

22. Brokaw, R.S., "Analytic Solutions to the Ignition Kinetics of the Hydrogen-Oxygen Reaction," Tenth Symposium (International) on Combustion, The Combustion Institute, Pittsburgh, Penn., (1965), pp. 269-278.

23. Voevodsky, V.V. and Soloukhin, R.I., "On the Mechanism and Explosion Limits of Hydrogen-Oxygen Chain Self-Ignition in Shock Wave," Tenth Symposium (International) on Combustion, The Combustion Institute, Pittsburgh, Penn., (1965), pp. 279-283.

24. Minkoff, G.J. and Tipper, C.F.H., Chemistry of Combustion Reactions, Butterworths and Co. Ltd., London, (1962), Chapter 2.

25. Westenberg, A.A. and Favin, S., Nozzle Flow with Complex Chemical Reaction, John Hopkins Univ., Applied Physics Lab., Report CM-1013, (March 1962).

26. Kondratev, V.N. and Ptichkin, I.I., "Interaction Between CO and O_3 and O_2 Mixtures in Gaseous Phase," Kinetika i Kataliz, 2, (1961), pp. 492.

27. Benson, S.W., The Foundations of Chemical Kinetics, McGraw-Hill Book Co. Ltd., New York, (1960), Chapter XIII.

28. Toennies, J.P. and Greene, E.F., "Dissociation Energies of Carbon-Monoxide and Nitrogen from Reflected Shock Wave Studies," J. of Chem. Phys., 26, No. 3, (1957), pp. 655-662.

29. White, D.R. and Moore, G.E., "Structure of Gaseous Detonation IV. Induction Zone Studies in H_2-O_2 and CO-O_2 Mixtures," Tenth Symposium (International) on Combustion, The Combustion Institute, Pittsburgh, Penn., (1965).

30. Urtiew, P.A. and Oppenheim, A.K., "Detonative Ignition Induced by Shock Merging," Eleventh Symposium (International) on Combustion, The Combustion Institute, Pittsburgh, Penn., (1967), p. 665.

31. Sichel, M., "A Hydrodynamic Theory for the Propagation of Gaseous Detonations Through Charges of Finite Width," AIAA J., 4, No. 2, (1966), pp. 264.

32. Morrison, R.B., A Shock Tube Investigation of Detonative Combustion, University of Michigan Report UMM-97, (Jan. 1952).

33. Wilkerson, T., The Use of the Shock Tube as a Spectroscopic Source with an Application to the Measurement of gf-Values for Lines of Neutral and Singly Ionized Chromium, Ph.D. Thesis, University of Michigan, (June 1961).

34. Opel, G.L., A Study of Gaseous Detonation Waves by Means of Schlieren Photography, M.S. Thesis, Massachusetts Institute of Technology, Cambridge, Mass., (1959).

35. Jost, W., Just, Th., and Wagner, H.Gg., "Investigation of the Reaction Zone of Gaseous Detonations," Eighth Symposium (International) on Combustion, The Williams and Wilkins Co., Baltimore, (1962), p. 582.

36. Murray, D.H. and Paques, H., "Laser Improves Sensitivity of Schlieren Systems," Space and Aeronautics, (Oct. 1966).

37. Oppenheim, A.K., Urtiew, P.A., and Weinberg, F.J., "On the Use of Laser Light Sources in Schlieren Interferometer Systems," Proc. Royal Soc., A 291, (1965), pp. 279-290.

38. Denisov, Yu. N. and Troshin, Ya. K., "Structure of Gaseous Detonation in Tubes," Zhurnal Tekhnicheskoi Fiziki, 30, No. 4, (April 1960).

39. Duff, R.E., "Investigation of Spinning Detonation and Detonation Stability," Phys. of Fluid, 4, No. 11, (1961).

40. Denisov, Yu. N. and Troshin, Ya. K., "On the Mechanism of Detonative Combustion," Eighth Symposium (International) on Combustion, William and Wilkins Co., Baltimore, (1962), pp. 600-610.

41. White, D. R., "Turbulent Structure of Gaseous Detonation," Phys. of Fluids, 4, No. 4, (1961).

42. Urtiew, P. A. and Oppenheim, A. K., "Experimental Observations of the Transition to Detonation in an Explosive Gas," Proc. Royal Soc., A 295, (1966), pp. 13-28.

43. Mitrofanov, V. V. and Soloukhin, R. I., "On Diffraction of a Multifront Detonation Wave," Soviet Physics-Doklady, 9, No. 12, (June 1965), p. 1055. Translated from Doklady Akademii Nauk SSSR, 159, No. 5, (Dec. 1964), p. 1003.

44. Weston, F. R., "The Flame Spectra of Carbon-Monoxide and Water Gas," Proc. Royal Soc., A 109, (1925), pp. 523-526.

45. Fay, J. A., "The Structure of Gaseous Detonation Waves," Eighth Symposium (International) on Combustion, William and Wilkins Co., Baltimore, (1962), pp. 30-40.

46. Jost, W., Just, Th., and Wagner, H. Gg., "Investigation of the Reaction Zone of Gaseous Detonation," Eighth Symposium (International) on Combustion, William and Wilkins Co., Baltimore, (1962), pp. 582-600.

47. Pusch, W. and Wagner, H. Gg., "Investigation of the Dependence of the Limits of Detonability on Tube Diameter," Combustion and Flame, 6, (Sept. 1962).

48. Watson, R. H., A Comparison of Experimental and Theoretical Transverse Wave Spacings in Detonations, University of Illinois Interim Tech. Report 7 for Contract US DA 11-022-AMC-329 (R), (Jan. 1966).

49. Zeleznik, F. J. and Gordon, S., A General IBM 704 and 7090 Computer Program for Computation of Chemical Equilibrium Compositions, Rocket Performance, and Chapman-Jouguet Detonations, NASA TN D-1454, (Oct. 1962). See also NASA TN D-1737, (Oct. 1963) and ARS J., 32, pp. 607-15.

50. Bahn, G.S., "Status Report of Effort on Engineering Selection of Reaction Rate Constants for Gaseous Chemical Species at High Temperature, with a Review of H + CO_2 = OH + CO and CO_2 + M = O + CO + M," Presented 1967 Spring Meeting, Western States Section, The Combustion Institute, University of California, San Diego, Calif.

51. Jost, W. (translated by Croft, H.O.), Explosion and Combustion Processes in Gases, McGraw-Hill Book Co., New York, (1946).